

THEORETICAL STUDIES OF SPIN DYNAMICS IN
PARAMAGNETS.

By
Carlos Calero Borrallo

A dissertation submitted to the Graduate Faculty in Physics in partial fulfillment of
the requirements for the degree of

DOCTOR OF PHILOSOPHY

at

THE CITY UNIVERSITY OF NEW YORK

2007

UMI Number: 3278409



UMI Microform 3278409

Copyright 2007 by ProQuest Information and Learning Company.
All rights reserved. This microform edition is protected against
unauthorized copying under Title 17, United States Code.

ProQuest Information and Learning Company
300 North Zeeb Road
P.O. Box 1346
Ann Arbor, MI 48106-1346

This manuscript has been read and accepted for the Graduate Faculty in Physics in satisfaction of the dissertation requirement for the degree of Doctor of Philosophy.

Date

Dist. Professor Eugene M. Chudnovsky
Chair of Examining Committee

Date

Professor Sultan Catto
Executive Officer

Dist. Professor M. P. Sarachik

Professor A. A. Lisiansky

Professor A. D. Kent

Supervisory Committee

THE CITY UNIVERSITY OF NEW YORK

Abstract

THEORETICAL STUDIES OF SPIN DYNAMICS IN PARAMAGNETS.

by

Carlos Calero Borrallo

Advisor: Eugene M. Chudnovsky, Distinguished Professor of Physics

This thesis deals with problems of spin relaxation in solids, mostly in application to quantum dots and molecular magnets.

Spin-phonon effects are investigated by using a symmetry-based approach that is free of fitting parameters. This approach is developed for molecular magnets and for quantum dots. For both systems, two processes are considered: Direct processes, which involve spin transitions accompanied by the emission or absorption of one phonon, and Raman processes, in which the spin transition is accompanied by the absorption of a phonon and the emission of another phonon of different frequency. Relaxation rates are obtained analytically for both mechanisms and evaluated for various temperature ranges.

The effect of acoustic waves on the magnetization dynamics of crystals built of rigid spin clusters is analyzed. Coupled equations of motion for spins and sound are derived and the possibility of strong resonant magneto-acoustic coupling is demonstrated. Dispersion laws for interacting linear sound and spin excitations are obtained for bulk and surface acoustic waves. It is shown that externally excited surface acoustic waves in the GHz range can generate space-time Rabi oscillations between spin states of molecular magnets.

Spin dynamics of crystals of molecular magnets in a time-dependent magnetic field is analyzed along the lines of the Landau-Zener theory. Quantum dynamics of a molecular magnet in a rotating magnetic field is studied. Analytical expressions for

the probability of spin transition are derived for fast and slow rotation, and the case of a continuous rotation in the presence of the noise is investigated. The dynamics of the magnetization reversal and the electromagnetic radiation emitted due to collective Landau-Zener relaxation in a crystal of molecular magnets is examined.

Acknowledgements

First and foremost, I would like to thank my supervisor, Professor Eugene M. Chudnovsky, for his guidance throughout my Ph. D. studies. For his vast knowledge, talent, and, above all, passion for Physics, he has been an excellent reference to learn from. I also thank him for his complete availability during these four years to discuss Physics with me.

Professor Dmitry A. Garanin has been very important in my Physics education, too. Since the beginning of my Ph. D., when he was still in Germany, Professor Garanin has contributed in almost all the projects that I have been involved in. Thanks a lot. I also need to mention Jaroslav Albert, with whom I have shared not only the office, but also uncountable hours of discussion on Physics that helped me mature many ideas.

I am very grateful to Professor Javier Tejada for putting me in contact with Professor Eugene M. Chudnovsky when I finished my undergraduate studies in Barcelona back in 2003. I also want to thank him for letting me spend the summers working at the University of Barcelona, and his group (especially Alberto Hernández, Marta Jordi and Ferran Macià) for accepting me so kindly.

My thanks to Professor Myriam P. Sarachik and her group (Yoko Suzuki, Sean McHugh, and Reem Jafar) for fruitful discussions and for explaining to me the intricacies of some of the experiments done in the field of nanomagnetism.

Finally, I want to express my gratitude to the members of the committee, Professor

Myriam P. Sarachik, Professor Andrew D. Kent, and Professor Alexander A. Lisyansky
for accepting to be part of it.

To my parents, Rosario Calero and Isabel Borrallo.

To my brother, Joan Calero.

Table of Contents

	v
Table of Contents	viii
List of Figures	xi
I Spin-phonon effects in paramagnets	1
1 Introduction	2
1.1 Systems	4
1.1.1 Molecular magnets	4
1.1.2 Quantum dots	6
1.2 Spin-phonon interaction	7
1.2.1 General approach	7
1.2.2 Rotationally invariant magneto-elastic theories	10
1.2.3 Spin interaction with lattice twists.	15
2 Spin-phonon relaxation in molecular magnets	25
2.1 Direct processes	27
2.1.1 Lattice frame	28
2.1.2 Laboratory frame	29
2.1.3 General expression for the relaxation rate	30
2.1.4 Relaxation between levels of the spin Hamiltonian	31
2.1.5 Spin-phonon relaxation between tunnel-split states	32
2.2 Two-phonon processes [41]	33
2.2.1 Matrix elements of two-phonon processes	34
2.2.2 Raman processes	36
2.2.3 Processes involving emission of two phonons	51

2.2.4	Discussion	55
3	Relaxation of the electron spin in a quantum dot	58
3.1	Direct processes [57]	60
3.2	Raman Processes [61]	67
4	Interaction of spins with ultrasound	71
4.1	Rabi oscillations from ultrasound in spin systems [62]	71
4.1.1	Hamiltonian	73
4.1.2	Rabi oscillations	75
4.1.3	Discussion	79
4.2	Magneto-elastic waves in crystals of magnetic molecules [72]	80
4.2.1	Model of magneto-elastic coupling	83
4.2.2	Linear magneto-elastic waves	88
4.2.3	Non-linear magneto-elastic waves	95
4.2.4	Discussion	98
II	Dynamical Landau-Zener effects in spin systems	101
5	Quantum dynamics of a nanomagnet in a rotating field [80]	102
5.1	Landau-Zener theory in molecular magnets	102
5.2	Hamiltonian	104
5.3	Dynamics without noise	107
5.3.1	A single revolution	107
5.3.2	Continuous rotation	112
5.4	Dynamics with noise.	115
5.4.1	Low-frequency noise, $\gamma \ll \omega/\Gamma \ll 1$	116
5.4.2	High-frequency noise, $\omega/\Gamma \ll \gamma \ll 1$	117
5.5	Conclusions	118
6	Collective electromagnetic relaxation in crystals of molecular magnets [8]	120
6.1	Collective Landau-Zener relaxation	123
6.2	Radiation power	125
6.2.1	Analytical	126
6.2.2	Numerical	129
6.3	Discussion	132
	Papers and presentations by C. Calero	136

List of Figures

1.1	Ferromagnetic rod suspended by a torsion fibre.	12
1.2	Spin transitions cause a local distortion of the lattice in which the spin is embedded, so that the total angular momentum (spin + lattice) is conserved.	16
2.1	Transition between adjacent spin-energy levels of Hamiltonian (2.55) mediated by Raman processes.	39
2.2	Transition between the spin-energy levels of Hamiltonian (2.55) $m \rightarrow m + 2$ due to Raman scattering.	41
2.3	Transition between tunnel-split states due to Raman scattering.	44
4.1	Geometry of the problem.	74
4.2	Time dependence ($t' \equiv t\Delta/\hbar$) of the probability to find the spin in the state $ \phi_+\rangle$ at $x = 0$, $S = 10$, $\omega_R = 0.1\omega$, and $\omega = 0.9(\Delta/\hbar)$. Dotted line (red): Numerical result for the laboratory-frame Hamiltonian (4.18). Dash line (blue): Numerical result for the lattice-frame Hamiltonian (4.10). Solid line (black): Analytical result given by Eq. (4.13).	77

4.3	Time dependence ($t' \equiv t\Delta/\hbar$) of the expectation value of the projection of the spin on the anisotropy axis at $x = 0$, $S = 10$, $\omega_R = 0.1\omega$ and $\omega = 0.9(\Delta/\hbar)$. Dotted line (red): Numerical result for the laboratory-frame Hamiltonian (4.18). Dash line (blue): Numerical result for the lattice-frame Hamiltonian (4.10). Solid line (black): Analytical result given by Eq. (4.15).	78
4.4	Interacting sound and spin modes. Notice the gap below spin resonance ω_0	90
4.5	Geometry of the problem with surface acoustic waves.	92
4.6	Magnetization inside the soliton as a function of ξ for $W = 0$	97
5.1	Time dependence of the energy levels (normalized by D) of the Hamiltonian (5.6) (solid line) at $S = 4$ and $g\mu_B H/D = 3.1$. Dash line shows the distance between the energy levels if they were unperturbed by the second term in Eq. (5.6).	106
5.2	Probability of staying at $ -S\rangle$, P , as a function of parameter $\tilde{\epsilon}$ at $\gamma = 0.1$ and $S = 5$. The solid line represents the numerical data, the short-dash line is the analytical result, Eq. (5.19), and the long-dash line is the LZS result (see explanation in the text).	110
5.3	Probability of staying at the initial state, P , as a function of γ at $\tilde{\epsilon} = 0.1$ and $S = 5$. The solid line represents numerical data, the short-dash line is the analytical result Eq.(5.19), and the long-dash line is the LZS result.	110
5.4	Probability of staying at the initial state, P , as a function of the parameter $\tilde{\epsilon}$ at $\gamma = 0.1$ and $S = 5$. The solid line represents the numerical data, the short-dash line is the analytical result, Eq. (5.29), and the long-dash line is the LZS result	113

5.5	Time dependence of the probability of finding a continuously rotating system in the initial state $ -S \rangle$ for $\tilde{\epsilon} = 0.04, \gamma = 0.06$ and $S = 5$. The solid line represents numerical data. The dash line shows analytical result obtained by successive application of M, M^T and G_n	114
5.6	Time dependence of the probability of finding a particle in the state $ -S \rangle$ in the presence of a low-frequency noise for $\tilde{\epsilon} = 1/3, S = 10$, and $\gamma = 0.01$. The plotted probability is the average over an ensemble of 20 two-state dissipative systems.	115
5.7	Time dependence of the probability of finding a particle in the state $ -S \rangle$ in the presence of a high-frequency noise for $S = 10, \tilde{\epsilon} = 1/3$ and $(\Gamma/h_0) = 0.01$	118
6.1	Approximate energy levels of a spin-10 molecule in a zero magnetic field. The tunnel splitting of the degenerate levels is not shown. Arrows show the relaxation path from $m = -10$ to $m = 10$ through thermally assisted quantum tunneling.	121
6.2	A pair of tunnel-split levels vs. energy bias W . The Landau-Zener (LZ) transition is followed by the emission of the coherent light via superradiance.	122
6.3	Time dependence of the magnetization reversal for two values of ϵ due to pure Landau-Zener relaxation of individual molecules ($\alpha = 0$) and due to collective relaxation via superradiance ($\alpha = 0.01$).	125
6.4	Approximate analytical solution for $n_z(t')$ averaged over oscillations, Eq. (6.20), for two values of ϵ and $\alpha = 0.01$ (solid line). The numerical solution of Eq. (6.11) is shown by the dash line.	128
6.5	Time dependence of the reduced radiation power, $P' = (d^2n_z/dt'^2)^2$ at $\epsilon = 0.3$ and $\alpha = 0.05$. Solid line represents numerical results. Dash line corresponds to Eq. (6.22) at $\phi_0 = 2.576$	129
6.6	The ϵ dependence of the total emitted energy at two values of α . Points represent numerical results. Solid line corresponds to Eq. (6.23). . . .	130

6.7	The α dependence of E' at two values of ϵ . Points represent numerical results. Solid line corresponds to Eq. (6.23).	130
6.8	Spectral function $I'(\omega')$ for three values of alpha at $\epsilon = 0.1$	131
6.9	Dependence of f of Eq. (6.27) on ϵ	132

Part I

Spin-phonon effects in paramagnets

Chapter 1

Introduction

Understanding spin-phonon interaction is of fundamental interest, and it is also important for applications of spin physics such as magnetic recording, spintronics and the development of the spin-based solid-state qubit. In spite of being an old subject studied since the inception of the quantum theory of solids, the interaction of spins with the distortions of the lattice is still poorly understood. While it is clear that the dominant spin-phonon coupling has its origin in the modulation of the crystal field surrounding the spin [12], no simple treatment has been yet provided. Tackling the problem from a microscopic perspective in terms of fundamental spin-orbit couplings at the atomic level is a very difficult and extremely cumbersome task [10, 11, 12], even for the current numerical capacities. Other methods are based on the use of phenomenological Hamiltonians containing all spin-lattice terms permitted by symmetry [13]. Comparison of such theory with experiment is hampered by the presence of many fitting parameters. An alternative approach to handle the interaction of rigid spins with transverse phonons has been recently developed [33, 36] based on the imposition of rotational invariance that is required by the local conservation of the angular momentum. This results in a parameter-free magneto-elastic coupling which

effects can be easily tested in experiment.

Comprehension of the mechanism of spin-phonon interaction is crucial to explain the spin-relaxation towards thermal equilibrium in paramagnetic solids. In contrast to other kind of interactions, like, e.g. interaction with nuclear spins, impurities, dipolar fields, etc. the interaction of the spin with the electromagnetic field or the vibrations of the lattice cannot be eliminated. Thermal equilibrium of the spin-system with reservoirs such as the electromagnetic radiation field or the lattice vibrations within the paramagnet can be attained by emission or absorption of photons or phonons. The relaxation process towards equilibrium is characterized by the *relaxation rate* Γ , which is a measure of the time taken by the system to reach thermal equilibrium from a non-equilibrium state. From general considerations of the magneto-elastic coupling and the coupling of spins with the electromagnetic field, and with the help Fermi golden rule (see below), one obtains the following ratio for the phonon-induced and photon-induced relaxation rates

$$\frac{\Gamma_{phonon}}{\Gamma_{photon}} = \frac{A_{phonon}}{A_{photon}} \left(\frac{c}{v_s} \right)^3. \quad (1.1)$$

Here, c is the speed of light, v_s is the velocity of sound, and A_{phonon}, A_{photon} are the coupling constants of the spin with the phonon and photon fields, respectively. This expression is dominated by the last factor, of order 10^{15} . Hence, unless collective electromagnetic effects take place [7, 8], the spin-lattice relaxation process will dominate over the electromagnetic one. Consequently, spin-phonon interactions provide the most fundamental upper bound on the relaxation time of spin states in paramagnetic solids.

Research on spin-lattice relaxation has been recently revived by the needs of spintronics and by the hope of achieving spin-based solid state qubits. The ability to

confine a single electron in all three spatial directions by using quantum dots and the scalability of such dots made them good candidates for a spin-based qubit. Molecular magnets, which exhibit quantum spin transitions in macroscopic experiments (see section 1.1), were also proposed as candidates for the basic unit of the quantum computer [14]. In both cases, understanding of the spin-lattice relaxation is of great importance.

Magneto-elastic coupling is also needed to describe the dynamics of the magnetization when externally driven elastic waves are present in a paramagnetic solid. Conversely, one can also study how the coupling with the magnetization affects the structure of such waves. For a comprehensive review on this subject, see Ref.[15].

A brief description of the paramagnetic systems of interest is provided in Section 1.1. In Section 1.2 we present an overview to the subject of spin-phonon interaction in paramagnetic systems. First, we present the conventional treatment that historically has been given to such a coupling. Second, we introduce the idea of rotationally invariant magneto-elastic interaction and derive its main effects for paramagnets. Finally, a universal magneto-elastic coupling for paramagnets based on the local conservation of the angular momentum is derived and justified from different perspectives. This interaction is the basis of the studies on magneto-elastic effects presented in Chapters 2, 3, and 4.

1.1 Systems

1.1.1 Molecular magnets

Crystals of molecular magnets consist of a large number of weakly interacting, chemically identical spin clusters. In contrast to most ensembles of small magnetic clusters,

which are composed of particles with various sizes and magnetic properties, molecular magnets are characterized by a unique set of parameters. This allows a precise and rigorous description of them by theoretical models, thus making molecular magnets good candidates to test fundamental theories. Each of the magnetic clusters typically consists of several magnetic ions strongly coupled through exchange interaction. The cluster's energy levels caused by such interaction belong to various multiplets labeled by the value of the total spin S . In most cases, at low temperatures one can assume that only the lowest energy multiplet, with a definite value of S , is involved in the dynamics of the system. In the absence of an external magnetic field, the S -multiplet is partially split by the (weak) coupling with the crystal field through spin-orbit interaction. Exact calculation of this effect from fundamental theories is an extremely difficult and involved task. Nevertheless, one can use an alternative approach and describe the interaction with the crystal field by a phenomenological spin-Hamiltonian containing all terms permitted by symmetry. As the Hamiltonian must be invariant under time-reversal, the crystal field Hamiltonian \mathcal{H}_A must contain only even powers of \mathbf{S} . Thus, in the first approximation, the magnetic clusters can be treated as independent entities of spin S described by a phenomenological spin-Hamiltonian like, e.g.,

$$\mathcal{H} = -DS_z^2 + E(S_x^2 - S_y^2) - g\mu_B \mathbf{H} \cdot \mathbf{S}. \quad (1.2)$$

The first two terms (with $D, E > 0$) account for the magnetic anisotropy caused by the internal crystal field. The specific form of this term depends on the symmetry of the cluster and symmetry of the crystal lattice. The biaxial case used here is the most general expression for such coupling to second order in spin operators. The last term is the Zeeman Hamiltonian of the spin \mathbf{S} in the external magnetic field \mathbf{H} , with

g and μ_B being the gyromagnetic factor and the Bohr magneton, respectively. Other interactions like, e.g., dipolar coupling with other nanomagnets, interactions with nuclear spins, etc. are often considered as perturbations of the above Hamiltonian.

As a result of this structure, high-anisotropy crystals that are composed of high-spin molecular magnets can preserve uniform magnetization opposite to the direction of the external field for a very long time [1] at low temperatures. The latter is due to the high energy barrier between spin-up and spin-down states of such molecular magnets. This feature and the uniformity of the ensembles are responsible for the unusual magnetic properties of these paramagnetic crystals. In particular, that allows the observation of macroscopic quantum effects such as quantum tunneling of the magnetization [2, 3] and the periodic quenching of the tunneling rates due to the interference of tunneling paths with different geometrical phase [4]. The symmetry of the magnetic quantum tunneling and the exact form of the spin-Hamiltonian for the molecular magnet Mn_{12} -acetate were recently determined in Ref. [5].

1.1.2 Quantum dots

A quantum dot is a semiconductor nanostructure that confines the motion of conduction band electrons (or valence band holes) to a limited region in all three dimensions. In that region, electrons have a discrete quantized energy spectrum determined by the geometry of such nanostructure. The number of trapped electrons can be set to zero, one, two, etc. Quantum dots have been widely studied recently in relation to the development of a quantum computer. Their simplicity and versatility make them perfect candidates to implement Shor's algorithm [6], the quantum-mechanics based algorithm which can factorize large numbers exponentially faster than any available classical algorithm. Many proposals have been made that use quantum dots as the

basic units, the so-called qubits, of the quantum computer. Indeed, one of the earliest and most successful proposed solid state quantum computer schemes uses the spin of a single electron trapped in a GaAs quantum dot as its qubit. Local magnetic fields are used to manipulate single spins creating local Zeeman splittings that can be accessed by a resonant RF pulse. The Hamiltonian of such a system is

$$\hat{\mathcal{H}}_Z = -\mu_B g_{\alpha\beta} s_\alpha B_\beta, \quad (1.3)$$

where μ_B is the Bohr magneton, $g_{\alpha\beta}$ is the gyromagnetic tensor, and $\mathbf{s} = \sigma/2$ is the dimensionless electron spin with σ_α being Pauli matrices. In general, $g_{\alpha\beta}$ differs from its free-electron value $g_0 = 2.0023$ due to the spin-orbit coupling in semiconductors [55] (see also Ref. [56]).

To use the spin of a single-electron quantum dot as a qubit, it should possess very long coherence time (the criteria to determine the lower bound in the coherence time is the need of successfully performing quantum error correction, which requires $10^4 - 10^6$ operations). Therefore, for such applications, a thorough understanding of the mechanisms of electron-spin relaxation is crucial. The uniqueness of the spin-lattice interaction is that, while sources of decoherence like the interaction with nuclear spins, impurities, etc. can be eliminated, the spin-phonon relaxation cannot. Thus, spin-phonon interactions provide the most fundamental upper bound on the lifetime of the spin states.

1.2 Spin-phonon interaction

1.2.1 General approach

Historically, a distinction can be made between two kinds of magneto-elastic coupling: the two ion coupling arising from the modulation of the distance between the ions

and the single ion coupling where the strain wave modulates the surrounding of the ion under consideration.

Two-ion coupling.

The two main effects originating from the variation of the distance between magnetic particles are the modulation of the exchange interaction (between the particles that constitute the magnetic ion) and the modulation of the dipolar interaction between magnetic ions, both strongly dependent on the distance. We will show that the modulation of the isotropic exchange interaction cannot provide a mechanism for spin-lattice interaction. An estimate for the relaxation rate produced by the modulation of dipolar interactions will be given; this rate turns out to be too small compared with the rate produced by the single ion coupling treated in the next section.

The isotropic exchange interaction between the particles constituting a magnetic ion is described by

$$\mathcal{H}_{ex} = \sum_{i < j} J_{ij} \mathbf{s}_i \cdot \mathbf{s}_j, \quad (1.4)$$

where J_{ij} are the exchange integrals between the particles i, j , strongly dependent on the distances between them. In spite of the modulation of J_{ij} caused by the distortions of the lattice, \mathcal{H}_{ex} commutes with the total spin of the magnetic ion $\mathbf{S} = \sum_i \mathbf{s}_i$. Therefore, this term cannot produce transitions between states of the magnetic ion that change its total spin quantum numbers S or M . The allowed transitions are the ones to excited exchange multiplets with the same S , which are typically at such high energies that no phonons can provide such transitions.

The modulation of the dipolar interactions between magnetic ions by the sound waves is a source of spin-phonon relaxation, the so-called Waller processes [9]. As a result of a lattice strain of amplitude ϵ fluctuating at frequency ω , the distance

between two ions is $r = r_0(1 + \epsilon \cos \omega t)$. Thus the dipolar field between magnetic ions will have an oscillating part given by

$$H_{dipolar}^{osc}(t) \simeq -\frac{3\mu}{r_0^3} \cos \omega t. \quad (1.5)$$

By working out the matrix elements of spin transitions caused by this magnetic field and using the Fermi golden rule, one obtains that the relaxation rate is

$$\Gamma = \alpha \frac{\gamma^2 n^2 \mu^2 \hbar}{\rho v_s^5} \omega^3 \coth \left(\frac{\hbar \omega}{2k_B T} \right), \quad (1.6)$$

where α is a numerical factor of order 1, γ is the gyromagnetic ratio, n is the concentration of magnetic particles, ρ is the mass density, and v_s is the sound velocity. For $\rho = 2g/cm^3$, $n \sim 10^{21}cm^{-3}$, $\mu \sim \mu_B$, $\omega = 30GHz$, and $T = 1K$, one obtains $\Gamma \sim 10^{-4}s^{-1}$. This value is too small compared to the relaxation rates observed in experiment.

Single-ion coupling

A more potent spin-phonon relaxation mechanism was suggested by Heitler and Teller [10] and developed by Kronig [11] and Van Vleck [12]. This mechanism consists of the modulation of the crystal electric field through motion of the electrically charged ions under the action of the lattice vibrations. This fluctuating electric field influences the spin-states, defined by the static crystal field through spin-orbit interaction, inducing transitions between them.

Tackling the problem directly, that is, considering the influence of the fluctuating electric field on the spin-states, is a task of great difficulty. An alternative approach was proposed by Orbach [13]. It was based on the use of phenomenological spin-phonon interaction Hamiltonians containing all spin-lattice terms permitted by

symmetry. To first order in the strain, all terms must be quadratic in the spin operators since the Hamiltonian must be invariant under time-reversal transformations for vanishing magnetic fields. According to this procedure, the general expression for the spin-phonon Hamiltonian of a spin located at \mathbf{r} , to first order in the displacement field, is given by

$$\mathcal{H}_{s-ph} = \sum_{\alpha\beta\gamma\eta} \Lambda_{\alpha\beta\gamma\eta} \epsilon_{\alpha\beta}(\mathbf{r}) S_\gamma S_\eta, \quad (1.7)$$

where $\epsilon_{\alpha\beta}$ are the components of the strain tensor. The number of independent coefficients $\Lambda_{\alpha\beta\gamma\eta}$ depends on the symmetry of the crystal under consideration. For instance, using symmetry strains of an irreducible representation for cubic symmetry and combining them with the corresponding quadrupolar operators, one obtains to first order in the displacement field that \mathcal{H}_{s-ph} must be given by

$$\mathcal{H}_{s-ph} = g_1 \epsilon_v + g_2 \left(\sqrt{3} \epsilon_2 O_2^2 + \epsilon_3 O_2^0 \right) + g_3 \epsilon_{xy} O_{xy}. \quad (1.8)$$

Here, $\epsilon_v = \epsilon_{xx} + \epsilon_{yy} + \epsilon_{zz}$, $\epsilon_2 = \frac{1}{\sqrt{2}}(\epsilon_{xx} - \epsilon_{yy})$, $\epsilon_3 = 2\epsilon_{zz} - \epsilon_{xx} - \epsilon_{yy}$ and $O_2^0 = 2S_z^2 - S_x^2 - S_y^2$, $O_2^2 = S_x^2 - S_y^2$, and $O_{xy} = \frac{1}{2}(S_x S_y + S_y S_x)$. The coupling constants g_i are phenomenological coefficients that must be determined from experiment.

This form of the spin-phonon interaction Hamiltonian provides qualitative description of several phenomena in relation to magneto-elastic effects (like, e.g., magnetostriction, Jahn-Teller effect, deviation of the elastic constants of the solid from the non-magnetic solid's values... see Ref.[15]). It can also account for the temperature dependence of spin-phonon relaxation rates for diluted paramagnetic solids [16].

1.2.2 Rotationally invariant magneto-elastic theories

In the magneto-elastic theory presented above, the displacement field and the spins are coupled through a linear term between the symmetric strain and the quadrupole

operators of the magnetic ions. This theory successfully explains magnetostriction experiments for different materials and also the temperature dependence of elastic constants in the paramagnetic phase for many rare-earth compounds.

However, qualitative and quantitative inconsistencies of these theories with respect to experimental results were found in ferromagnets [17], antiferromagnets [18] and paramagnets [27]. Besides, several authors noted that such magneto-elastic theories violated the principle of rotational invariance required by the conservation of the total angular momentum of the system [18, 19, 20]. The requirement for the total Hamiltonian of the coupled spin-lattice system to be rotationally invariant led to new magneto-elastic theories for ferromagnetic crystals [17, 19, 20, 21] and antiferromagnets [18]. Such theories contained additional contributions to the spin-phonon interaction which had been previously ignored. This work was followed by a number of theoretical papers that extended the theory to paramagnetic systems [22, 23, 24, 25, 26], as well as by experimental works that, with the help of the new terms in the total Hamiltonian, successfully interpreted the discrepancies with the previous magneto-elastic theories [24, 27, 28].

Einstein-de Haas effect and Barnett effect

Conservation of the total angular momentum in a magneto-mechanical system was elucidated for the first time in the Einstein-de Haas experiment [29, 30]. The experiment consists of the measurement of the rotation of a freely suspended ferromagnetic cylindrical rod due to the reversal of the direction of its magnetization initially directed along its axis (see Fig. 1.1). The conservation of the total angular momentum $\mathbf{J} = \mathbf{L} + \mathbf{S}$, with \mathbf{L} being the angular momentum of the rod and \mathbf{S} being the total spin, requires that the body begins to rotate if its total magnetization changes. The reverse

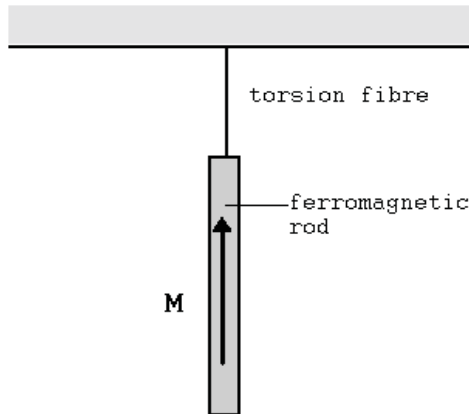


Figure 1.1: Ferromagnetic rod suspended by a torsion fibre.

effect was proposed by Barnett [31]: the rotation of a magnetic material induces its magnetization along the axis of rotation. It was predicted and verified experimentally that a body of any magnetic substance, initially not magnetized, when set into rotation develops a magnetic moment parallel to the axis of rotation and proportional to the angular velocity.

Rotationally invariant magneto-elastic theories in paramagnets

In previous studies of magneto-elastic interaction in paramagnets, it was assumed that the spins were coupled to the lattice only via deformations of the latter that could be described by the symmetrical elastic strain tensor. These theories, as pointed out by R. L. Melcher [22], are not rotationally invariant, so that, he argues, they are not consistent with the conservation of total angular momentum. In his work [22], Melcher postulates the form that the microscopic Hamiltonian describing a paramagnet in a diamagnetic medium must have to account for the conservation of the angular momentum. Expanding this Hamiltonian to first order in phonon amplitudes, one obtains some extra magneto-elastic terms in the Hamiltonian. Following the work by Melcher, V. Dohm and P. Fulde [23] derived the results given by Melcher and

applied the rotationally invariance principle to develop a magneto-elastic theory for paramagnets.

Dohm and Fulde restrict their discussion to rare earth ions, in which localized 4f-electrons of total angular momentum \mathbf{J} interact with the electrostatic crystal field. They argue, however, that the treatment employed should not be restricted to this kind of paramagnets and should apply to magnetically ordered phases as well. The Hamiltonian of the crystal is then

$$\mathcal{H} = \mathcal{H}_{Lattice} + \sum_{m=1}^N \mathcal{H}_{cf}^m, \quad (1.9)$$

$$\mathcal{H}_{Lattice} = \frac{1}{2M} \sum_{m=1}^N (\mathbf{p}^m)^2 + \phi(\mathbf{r}^1, \dots, \mathbf{r}^N), \quad (1.10)$$

$$\mathcal{H}_{cf}^m = V \{ \mathbf{J}^m; \mathbf{r}^m - \mathbf{r}^1, \dots, \mathbf{r}^m - \mathbf{r}^N \}. \quad (1.11)$$

Here, $\mathcal{H}_{Lattice}$ is the kinetic and potential energy of a Bravais lattice of N ions of mass M , momentum \mathbf{p}^m , and instantaneous position \mathbf{r}^m , while \mathcal{H}_{cf}^m describes the interaction of the spin \mathbf{J}^m of the m -th ion with the crystal field caused by other ions.

As it is usually done, the crystal field Hamiltonian (1.11) can be expressed phenomenologically as a polynomial in J_x^m, J_y^m, J_z^m containing all terms permitted by symmetry. To account for the invariance of this Hamiltonian under time reversal, it can contain only even-degree terms. We can rewrite (1.11) in terms of the displacements $\mathbf{u}^n = \mathbf{r}^n - \mathbf{R}^n$ from the rest positions \mathbf{R}^n of the lattice

$$\mathcal{H}_{cf}^m = V \{ \mathbf{J}^m; \mathbf{R}^{m1} + \mathbf{u}^{m1}, \dots, \mathbf{R}^{mN} + \mathbf{u}^{mN} \}, \quad (1.12)$$

with $\mathbf{R}^{mn} \equiv \mathbf{R}^m - \mathbf{R}^n, \mathbf{u}^{mn} \equiv \mathbf{u}^m - \mathbf{u}^n$. The displacement relative to the rest positions can be replaced by the displacement field $\mathbf{u}(\mathbf{R})$, such that $\mathbf{u}(\mathbf{R}^n) = \mathbf{u}^n$. One assumes also that the characteristic length of variation of the displacement field $\mathbf{u}(\mathbf{R})$ is much

larger than the range of the crystal field, which is of the order of the interatomic distance. Thus, one can approximate

$$u_{\alpha}^{mn} \approx (R_{\beta}^m - R_{\beta}^n)v_{\alpha\beta}^m, \quad v_{\alpha\beta}^m \equiv \left. \frac{\partial u_{\alpha}(\mathbf{R})}{\partial R_{\beta}} \right|_{\mathbf{R}=\mathbf{R}^m}, \quad (1.13)$$

so that the crystal field becomes

$$\mathcal{H}_{cf}^m \simeq V \{ \mathbf{J}^m; (1 + \mathbf{v}^m)\mathbf{R}^{m1}, \dots, (1 + \mathbf{v}^m)\mathbf{R}^{mN} \}, \quad (1.14)$$

Taking into account that the rotation matrix produced by the deformation \mathbf{v}^m is given by [32]

$$\mathcal{R}(\mathbf{v}^m) \equiv (1 + \mathbf{v}^m)(1 + \eta^m)^{-1/2}, \quad (1.15)$$

the spatial arguments of V can be rewritten as

$$(1 + \mathbf{v}^m)\mathbf{R}^{mn} = \mathcal{R}(\mathbf{v}^m)(1 + 2\eta^m)^{1/2}\mathbf{R}^{mn}, \quad (1.16)$$

where

$$\eta_{\alpha\beta}^m = \frac{1}{2} (v_{\alpha\beta}^m + v_{\beta\alpha}^m + v_{\gamma\alpha}^m v_{\gamma\beta}^m). \quad (1.17)$$

Therefore, Eq. (1.14) can be interpreted as the interaction of the spin \mathbf{J}^m with the strained and successively rotated lattice. One now makes use of the rotational invariance that the crystal field Hamiltonian must possess to account for the conservation of total angular momentum. According to this principle, this interaction must be equivalent to the interaction of the reversely rotated spin $\mathcal{R}^{-1}(\mathbf{v}^m)\mathbf{J}^m$ with the purely strained lattice. Thus Eq. (1.14) becomes

$$\mathcal{H}_{cf}^m = V \{ \mathcal{R}^{-1}(\mathbf{v}^m)\mathbf{J}^m; (1 + 2\eta^m)^{1/2}\mathbf{R}^{m1}, \dots, (1 + 2\eta^m)^{1/2}\mathbf{R}^{mN} \}. \quad (1.18)$$

It is apparent from the previous expression for the crystal field that due to rotational invariance there exists a coupling of the spin \mathbf{J}^m with the local rotations of the lattice.

This can be understood as follows: local deformations of the lattice produce rotations of the crystal field that affect the angular dependence of the wave functions of the ions, dependent on \mathbf{J}^m . One now expands the crystal field Hamiltonian in powers of the deformation tensor \mathbf{v}^m and obtains

$$\mathcal{H}_{cf}^m = \mathcal{H}_{cf}^0(\mathbf{J}^m) + \mathcal{H}_{Rotation}(\mathbf{J}^m) + \mathcal{H}_{Strain}(\mathbf{J}^m), \quad (1.19)$$

where $\mathcal{H}_{cf}^0(\mathbf{J}^m)$ is the crystal field Hamiltonian in the absence of lattice deformations, and $\mathcal{H}_{Rotation}(\mathbf{J}^m)$ and $\mathcal{H}_{Strain}(\mathbf{J}^m)$ are (smaller) terms caused by pure rotations and pure strain, respectively. Here, $\mathcal{H}_{Rotation}(\mathbf{J}^m)$ and $\mathcal{H}_{Strain}(\mathbf{J}^m)$ are expressions of the function $V\{\mathbf{J}^m; \mathbf{r}^{m1}, \dots, \mathbf{r}^{mN}\}$ and its derivatives contracted with the infinitesimal rotation and strain tensors. Notice that having expressed the crystal field Hamiltonian as in Eq. (1.18) allowed us to obtain in the expansion given by Eq. (1.19) the effects of the pure strain and the pure rotation separately. Remarkably, to first order in the linear strain tensor, $\mathcal{H}_{Strain}(\mathbf{J}^m)$ derived in this way coincides with the strain term used in conventional theory of magneto-elastic interactions. Finally, the total Hamiltonian of the system in the presence of a magnetic field \mathbf{H} is given by

$$\mathcal{H} = \sum_{m=1}^N \{ \mathcal{H}_{cf}^0(\mathbf{J}^m) - g\mu_B \mathbf{H} \cdot \mathbf{J}^m + \mathcal{H}_{Strain}(\mathbf{J}^m) + \mathcal{H}_{Rotation}(\mathbf{J}^m) \} + \mathcal{H}_{Lattice}, \quad (1.20)$$

with g being the gyromagnetic factor and μ_B the Bohr magneton. This theory illustrates that the spin-phonon interactions caused by strain and pure rotation can be separated into different terms in the Hamiltonian.

1.2.3 Spin interaction with lattice twists.

The conservation of the total angular momentum and its consequences for the problem of tunneling of the magnetic moment were first analyzed in 1994 by E. M. Chudnovsky

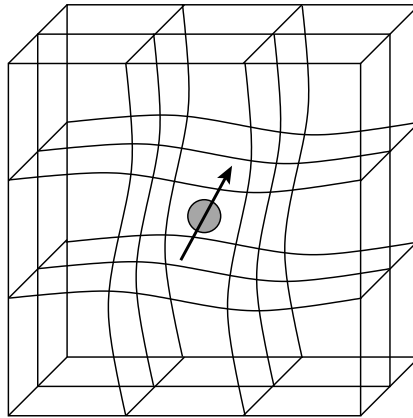


Figure 1.2: Spin transitions cause a local distortion of the lattice in which the spin is embedded, so that the total angular momentum (spin + lattice) is conserved.

[33]. From the requirement of the conservation of the total angular momentum, a model-independent magneto-elastic interaction term in the Lagrangian was derived and its contribution to the tunneling rate was calculated. With the help of this spin-phonon interaction term, transition rates between adjacent spin levels in molecular magnets were calculated [34] and collective effects in the relaxation of the spin-states of molecular magnets were predicted [35]. An expanded approach to the subject was developed in Ref. [36] based on the principle of rotational invariance of the crystal field Hamiltonian of magnetic molecules. In this work, spin-phonon relaxation rates between spin states of molecular magnets were computed for several cases.

The main steps of the development of the theory are specified in the following sections.

Conservation of angular momentum in the problem of tunneling of the magnetic moment

Let us consider a magnetic particle embedded in a large stationary solid matrix with finite elastic modulus. Its macroscopic magnetic moment, \mathbf{M} , can be due to the ordering of electron spins, to orbital momenta or a combination of the two. Consequently, it has an angular momentum associated with it given by $\gamma^{-1}\mathbf{M}$, with γ being the gyromagnetic ratio. Any spontaneous transition of \mathbf{M} between magnetic states is only possible if the system finds the way to compensate the corresponding change of the total angular momentum. That is,

$$\mathbf{L} + \gamma^{-1}\mathbf{M} = \text{constant} , \quad (1.21)$$

where \mathbf{L} is the mechanical angular momentum of the particle. Let us assume that, initially, the particle has $\mathbf{L} = 0$. Then, any transition $\mathbf{M}_i \rightarrow \mathbf{M}_f$ between degenerate magnetization states of the particle will need to be compensated by a mechanical rotation of the solid matrix with mechanical angular momentum $\mathbf{L} = -\gamma^{-1}(\mathbf{M}_f - \mathbf{M}_i)$ (see Fig.1.2). Note that the energy associated with this rotation, $E_{Rotation} = L^2/2I_m$, with I_m being the moment of inertia of the solid matrix, must be negligible compared to the tunneling splitting of the considered degenerate transition. The magnetic particle under consideration will be treated as a point particle, so that its magnetization is given by

$$\mathbf{m}(\mathbf{r}, t) = \mathbf{M}(t)\delta(\mathbf{r}) . \quad (1.22)$$

The Lagrangian of the system consists of three parts,

$$\mathcal{L} = \mathcal{L}_m + \mathcal{L}_e + \mathcal{L}_{s-ph} , \quad (1.23)$$

where \mathcal{L}_m gives the dynamics of the magnetic moment, \mathcal{L}_e accounts for the elastic

matrix and \mathcal{L}_{s-ph} describes the magneto-elastic interaction.

To obtain the Lagrangian of magneto-elastic interactions, we will apply the conservation of the total angular momentum. According to Eq. (1.21), the change of \mathbf{M} in the small particle must produce a mechanical torque in the solid matrix given by

$$\mathbf{T}(\mathbf{r}, t) = -\gamma^{-1}\dot{\mathbf{M}}(t)\delta(\mathbf{r}). \quad (1.24)$$

The local twist in the lattice produced by such a torque can be expressed in terms of the displacement vector $\mathbf{u}(\mathbf{r})$ [37],

$$\mathbf{\Phi}(\mathbf{r}, t) = \frac{1}{2}\nabla \times \mathbf{u}. \quad (1.25)$$

Therefore, the Lagrangian of the interaction must be

$$\mathcal{L}_{s-ph} = \int d^3r \mathbf{T} \cdot \mathbf{\Phi} = -\frac{1}{2\gamma} \int d^3r \dot{\mathbf{m}} \cdot (\nabla \times \mathbf{u}), \quad (1.26)$$

which is equivalent to

$$\mathcal{L}_{s-ph} = \gamma^{-1} \int d^3r \mathbf{m} \cdot \dot{\mathbf{\Phi}}, \quad (1.27)$$

since they differ by the total time derivative of a function. Note that Eq. (1.27) reflects the fact that a rotation is equivalent to the magnetic field $\mathbf{h} = \gamma^{-1}\dot{\mathbf{\Phi}}$. In a formulation in terms of the Hamiltonian, the interaction of the magnetic particle at \mathbf{r} with the solid matrix is given by

$$\mathcal{H}_{s-ph} = -\gamma^{-1} \int d^3r \mathbf{m} \cdot \dot{\mathbf{\Phi}} = -\frac{1}{2\gamma} \mathbf{M} \cdot \nabla \times \dot{\mathbf{u}}(\mathbf{r}). \quad (1.28)$$

With the help of this interaction term, one can compute the contribution of such magneto-elastic interaction to the tunnel-splitting of the degenerate ground state of a magnetic particle with biaxial anisotropy by using the method of imaginary-time path integrals [33].

Spin-lattice coupling in rotating frames of reference

Another approach based on fundamental principles can be taken to obtain the spin-phonon interaction Hamiltonian $\mathcal{H}_{s-ph} = -\frac{1}{2}\mathbf{S} \cdot \nabla \times \dot{\mathbf{u}}(\mathbf{r})$. Provided that lattice distortions $\mathbf{u}(\mathbf{r})$ produce local rotations of angular velocity $\boldsymbol{\Omega} = \frac{1}{2}\nabla \times \dot{\mathbf{u}}(\mathbf{r})$, the question is what the effect of the rotation is on the molecular spin at the point \mathbf{r} . For a similar problem involving an orbital moment, \mathbf{L} , it is well known from classical mechanics that in the reference frame rotating at an angular velocity $\boldsymbol{\Omega}$ the Hamiltonian acquires a term $-\hbar\mathbf{L} \cdot \boldsymbol{\Omega}$ (we use dimensionless L and S). The same rule is expressed by the Larmor theorem in classical electrodynamics: Rotation is equivalent to the magnetic field, leading to the effective Zeeman term, $-\mathbf{M} \cdot \mathbf{B}_{eff}$, in the rotating-frame Hamiltonian, with $\mathbf{M} = \hbar\gamma\mathbf{L}$, $\mathbf{B}_{eff} = \boldsymbol{\Omega}/\gamma$, where γ is the gyromagnetic ratio. The extension of the Larmor theorem to a spin is a consequence of the fact that in relativistic quantum theory the generator of rotations is $\mathbf{J} = \mathbf{L} + \mathbf{S}$. Rigorous derivation of the term $-(\hat{\mathbf{L}} + \hat{\mathbf{S}}) \cdot \boldsymbol{\Omega}$ in the Hamiltonian can be obtained from the study of the non-relativistic limit of the Dirac equation in the rotating frame [38].

Universal mechanism of spin-lattice coupling in paramagnets

Let us consider a magnetic particle (like, e.g. a molecular magnet) whose spin-state can be described, in the absence of magnetic field, by a fixed- S anisotropy Hamiltonian produced by the internal crystal field. Such crystal field is locally generated by the environment of the spin under consideration. Hence crystal-field Hamiltonians must

have the rotationally invariant form

$$\mathcal{H}_A = -D(\mathbf{S} \cdot \mathbf{e}^{(3)})^2 \quad (1.29)$$

$$\mathcal{H}_A = -D(\mathbf{S} \cdot \mathbf{e}^{(3)})^2 + E [(\mathbf{S} \cdot \mathbf{e}^{(1)})^2 - (\mathbf{S} \cdot \mathbf{e}^{(2)})^2] , \quad (1.30)$$

$$\mathcal{H}_A = C \sum_{\alpha \neq \beta} (\mathbf{S} \cdot \mathbf{e}^{(\alpha)})^2 (\mathbf{S} \cdot \mathbf{e}^{(\beta)})^2 , \quad (1.31)$$

where $\mathbf{e}^{(\alpha)}$ with $\alpha = 1, 2, 3$ are local unit vectors of a coordinate system rigidly coupled with the symmetry axes of the magnetic cluster (and which determine the direction of the crystal field).

Laboratory frame

In the absence of deformations of the lattice, one can choose the coordinate system in which in Eqs. (1.29)-(1.31) $e_\beta^\alpha = \delta_{\alpha\beta}$, so that the crystal-field Hamiltonians acquire the usual form $\mathcal{H}_A = -DS_z^2$, etc. Consider now the presence of transverse deformations of the crystal described by the displacement field $\mathbf{u}(\mathbf{r})$. This causes a rotation of the axes of the local crystal field, $(\mathbf{e}^{(1)}, \mathbf{e}^{(2)}, \mathbf{e}^{(3)})$ by an angle

$$\delta\boldsymbol{\phi}(\mathbf{r}) = \frac{1}{2} \nabla \times \mathbf{u}(\mathbf{r}) , \quad (1.32)$$

so that they become

$$\mathbf{e}^{(\alpha)} \rightarrow \mathbb{R} \mathbf{e}^{(\alpha)} , \quad (1.33)$$

where \mathbb{R} is the rotation matrix. Because of the rotational invariance of \mathcal{H}_A , the rotation of the crystal-field is equivalent to the rotation of the vector \mathbf{S} in the opposite direction, $\mathbf{S} \rightarrow \mathbb{R}^{-1} \mathbf{S}$. Such rotation can be performed by the $(2S + 1) \times (2S + 1)$ matrix in the spin space,

$$\mathbf{S} \rightarrow e^{-i\mathbf{S} \cdot \delta\boldsymbol{\phi}} \mathbf{S} e^{i\mathbf{S} \cdot \delta\boldsymbol{\phi}} . \quad (1.34)$$

Then, in the presence of lattice deformations, the Hamiltonian of the cluster in a magnetic field \mathbf{H} is

$$\mathcal{H} = e^{-i\mathbf{S}\cdot\delta\phi}\mathcal{H}_A e^{i\mathbf{S}\cdot\delta\phi} + \mathcal{H}_Z + \mathcal{H}_{ph}, \quad (1.35)$$

where \mathcal{H}_A is the crystal-field Hamiltonian in the absence of deformations, \mathcal{H}_Z is the Zeeman Hamiltonian, and \mathcal{H}_{ph} is the Hamiltonian of harmonic phonons. In this formulas, \mathbf{u} and $\delta\phi$ must be treated as operators. Indeed, according to canonical quantization of phonons and Eq. (1.32)

$$\delta\phi = \frac{1}{2}\sqrt{\frac{\hbar}{2MN}} \sum_{\mathbf{k},\lambda} \frac{[i\mathbf{k} \times \mathbf{e}_{\mathbf{k}\lambda}]e^{i\mathbf{k}\cdot\mathbf{r}}}{\sqrt{\omega_{\mathbf{k}\lambda}}} (a_{\mathbf{k}\lambda} + a_{-\mathbf{k}\lambda}^\dagger), \quad (1.36)$$

where M is the mass of the unit cell, N is the number of cells in the crystal, $\mathbf{e}_{\mathbf{k}\lambda}$ are unit polarization vectors, $\lambda = t_1, t_2, l$ denotes polarization, and $\omega_{\mathbf{k}\lambda} = v_k k$ is the phonon frequency. To first order in the angle of deformation, Eq. (1.35) becomes

$$\hat{\mathcal{H}} \simeq \hat{\mathcal{H}}_0 + \hat{\mathcal{H}}_{s-ph}, \quad (1.37)$$

where $\hat{\mathcal{H}}_0$ is the Hamiltonian of non-interacting spins and phonons

$$\hat{\mathcal{H}}_0 = \hat{\mathcal{H}}_S + \hat{\mathcal{H}}_{ph}, \quad \hat{\mathcal{H}}_S = \hat{\mathcal{H}}_A + \hat{\mathcal{H}}_Z, \quad (1.38)$$

and $\hat{\mathcal{H}}_{s-ph}$ is the spin-phonon interaction term, given by

$$\hat{\mathcal{H}}_{s-ph} = i \left[\hat{\mathcal{H}}_A, \hat{\mathbf{S}} \right] \cdot \delta\phi. \quad (1.39)$$

This is a new interaction term describing the magneto-elastic coupling between the spin and the elastic twists caused by transverse long-wave phonons. It is a consequence of the locality of the crystal field and the requirement of the crystal-field Hamiltonian to be rotationally invariant. This interaction corresponds to the most

significant spin-lattice coupling for clusters in which the spin is formed inside a relatively rigid magnetic core that can rotate in the presence of the deformation field due to transverse phonons but is more resistant to distortions of the core itself.

Lattice frame

One can study the same problem in the coordinate system that is rigidly coupled to the cluster under consideration, the so-called lattice frame. In this frame of reference, Hamiltonian (1.35) becomes

$$\mathcal{H}^{(lat)} = e^{i\mathbf{S}\cdot\delta\phi}\mathcal{H}e^{-i\mathbf{S}\cdot\delta\phi} = \mathcal{H}_A + \mathcal{H}_Z^{(lat)} + \mathcal{H}_{ph}^{(lat)}. \quad (1.40)$$

To first order in $\delta\phi$,

$$\mathcal{H}_{ph}^{(lat)} \simeq \mathcal{H}_{ph} - i[\mathcal{H}_{ph}, \delta\phi] \cdot \mathbf{S}, \quad (1.41)$$

and

$$\mathcal{H}_Z^{(lat)} \simeq \mathcal{H}_Z - i[\mathcal{H}_Z, \mathbf{S}] \cdot \delta\phi = \mathcal{H}_Z - g\mu_B[\mathbf{H} \times \delta\phi] \cdot \mathbf{S}. \quad (1.42)$$

The total Hamiltonian is, then

$$\mathcal{H}^{(lat)} = \mathcal{H}_0 + \mathcal{H}_{s-ph}^{(lat)}, \quad (1.43)$$

where \mathcal{H}_0 is specified in Eq. (1.38) and

$$\mathcal{H}_{s-ph}^{(lat)} = -i[\mathcal{H}_{ph}, \delta\phi] \cdot \mathbf{S} - g\mu_B[\mathbf{H} \times \delta\phi] \cdot \mathbf{S}. \quad (1.44)$$

For $\delta\phi$ in the Heisenberg picture,

$$\delta\dot{\phi} = \frac{i}{\hbar}[\mathcal{H}_{ph}, \delta\phi], \quad (1.45)$$

so that the spin-phonon interaction term can be expressed as

$$\mathcal{H}_{s-ph}^{(lat)} = -\hbar\boldsymbol{\Omega} \cdot \mathbf{S}, \quad \boldsymbol{\Omega} = \delta\dot{\boldsymbol{\phi}} + \gamma[\mathbf{H} \times \delta\boldsymbol{\phi}], \quad (1.46)$$

where $\gamma = g\mu_B/\hbar$ is the gyromagnetic ratio for \mathbf{S} . The first term in Eq. (1.46), $\hbar\delta\dot{\boldsymbol{\phi}}$, is of kinematic origin: in the rotating frame, the rotation is equivalent to the magnetic field $\mathbf{H}_{eff} = \delta\dot{\boldsymbol{\phi}}/\gamma$ acting on the spin. The second term in Eq. (1.46) describes the fact that the external magnetic field, which is constant in the laboratory frame, is rotated in the lattice frame. Note that in the absence of magnetic field we recover the same expression for the spin-phonon interaction term deduced in the previous two sections.

Spin-phonon superradiance and laser effect in crystals of molecular magnets

Recently, E. M. Chudnovsky and D. A. Garanin suggested that coherent generation of phonons in crystals of molecular magnets could enhance the spin-lattice relaxation rates due to acoustic superradiance and acoustic laser effect [35]. The spin-lattice interaction term $\hat{\mathcal{H}}_{s-ph} = -\frac{1}{2}\hbar\mathbf{S} \cdot (\nabla \times \dot{\mathbf{u}})$ has the same form as the interaction with an electromagnetic field having effective vector potential $\mathbf{A}_{eff} = \dot{\mathbf{u}}/(2\hbar\gamma)$. Consequently, if one prepares a crystal of molecular magnets in a state with inverse population of spin levels, then one expects such a system to behave like an atomic laser. Using Heisenberg representation, E. M. Chudnovsky and D. A. Garanin derived the equations for spin and phonon operators that govern the collective dynamics of spins coupled through acoustic radiation of wavelength that exceeds the distance between individual molecular magnets. Two different results were obtained depending on the size of the sample. For samples smaller or comparable to the phonon wavelength, the spin-lattice relaxation rate is seen to be enhanced by a large factor, $\Upsilon/(v_0k_0)$,

where v_0 is the volume per spin, k_0 is the phonon wave-vector and Υ is a geometrical factor. This is an extension of the idea of Dicke superradiance [39]. If the sample is significantly smaller than the wavelength, this enhancement factor turns out to be the total number of nanomagnets in the sample. In the other limit of a macroscopic crystal, a laser-type expression for the spin-lattice relaxation rate was obtained, $\Gamma = S^2 \Delta^2 \omega_0 / (8\hbar \rho v_0 v_t^2 \gamma_{k_0})$, where γ_{k_0} is the decay rate of a phonon of wave vector k_0 . This laser rate can exceed the rate of the spin-lattice relaxation of a single spin by many orders of magnitude.

Chapter 2

Spin-phonon relaxation in molecular magnets

The spin relaxation due to interaction with the lattice can occur by various mechanisms. The most studied and often the dominant ones are direct processes, in which a single quantum is exchanged between the spin system and the lattice. It was pointed out by Waller in studying the modulation of the spin-spin interaction by the lattice waves that, unlike in electromagnetic phenomena, the inelastic scattering of a phonon combined with a transition in the spin system could be also very important [9]. This is a two-phonon process consisting of the absorption of one phonon and the emission of another phonon with different frequency. Although it is a second order process, it can be significant, since the phase space of the phonons triggering the transition is not limited to the distance between the levels as in the direct case. The mechanism is analogous to the Raman effect in optical spectroscopy and it is often referred to as a Raman process. As was explained in Section 1.2.1, spin-lattice relaxation mechanisms based on dipolar interactions (Waller) are, though, insufficient to account for the transition rates measured in experiment. Consideration of Raman processes based on the modulation of the crystal field, as done by Heitler and Teller [10], Kroning [11]

and Van Vleck [12], permitted calculation of relaxation rates that were of the same order of magnitude as the experimental ones.

Recently, this problem has received new attention in connection with spin relaxation of molecular clusters. The spin of many such clusters is formed inside a relatively rigid magnetic core that can rotate in the presence of the deformation field due to transverse phonons but is more resistant to distortions of the core itself. As was explained in Section 1.2.3 the spin relaxation of such a cluster can be obtained within a model that is parameter free, that is, it gives the relaxation rates in terms of the known crystal field Hamiltonian of the magnetic core $\hat{\mathcal{H}}_A$.

Even for non-rigid clusters, calculation of the effect of rotations is meaningful. It has been theoretically established that spin-phonon relaxation rates due to both, one-phonon and multi-phonon processes, are inversely proportional to some high powers of the sound velocity [16]. Since longitudinal phonons have a larger sound velocity than the transverse phonons, processes involving longitudinal phonons can be safely neglected. The effects of the transverse phonons can be split into shear deformations of the lattice cell and local rotations of the lattice that preserve the symmetry of the crystal field. To describe deformations of the first kind one needs to employ terms in the Hamiltonian containing phenomenological coupling constants, whereas the local rotations can be described by a parameter-free spin-phonon Hamiltonian that is defined solely by the form of $\hat{\mathcal{H}}_A$. In general, processes due to the shear distortion of the lattice and those due to the local rotation of the lattice should result in comparable relaxation rates. Even in this case, the latter are of a fundamental importance because they provide a parameter-free lower bound on the decoherence of any spin-based qubit.

For rigid spin clusters, interaction of the spin with rotations of the crystal field is the only source of spin-lattice relaxation.

2.1 Direct processes

Direct processes involve spin transitions accompanied by the emission or absorption of one phonon. To describe such processes, one needs to take into account terms in the Hamiltonian linear in phonon amplitudes. As has been derived in Section 1.2.3, the Hamiltonian of a molecular magnet in the presence of lattice distortions, to the first order in phonon amplitudes, is given by

$$\hat{\mathcal{H}} = \hat{\mathcal{H}}_0 + \hat{\mathcal{H}}_{s-ph}, \quad (2.1)$$

where $\hat{\mathcal{H}}_0$ is the Hamiltonian of non-interacting spins and phonons

$$\hat{\mathcal{H}}_0 = \hat{\mathcal{H}}_S + \hat{\mathcal{H}}_{ph}, \quad \hat{\mathcal{H}}_S = \hat{\mathcal{H}}_A + \hat{\mathcal{H}}_Z. \quad (2.2)$$

The spin-phonon interaction term is given by

$$\hat{\mathcal{H}}_{s-ph} = i \left[\hat{\mathcal{H}}_A, \hat{\mathbf{S}} \right] \cdot \delta\boldsymbol{\phi}. \quad (2.3)$$

As stated in Section 1.2.3, one can also pose the problem in the frame of reference that is rigidly coupled to the magnetic cluster. In this case, the Hamiltonian of the system becomes

$$\hat{\mathcal{H}}^{(lat)} = \hat{\mathcal{H}}_0 + \hat{\mathcal{H}}_{s-ph}^{(lat)}, \quad (2.4)$$

with

$$\hat{\mathcal{H}}_{s-ph}^{(lat)} = -\hbar\boldsymbol{\Omega} \cdot \mathbf{S}, \quad \boldsymbol{\Omega} = \delta\dot{\boldsymbol{\phi}} + \gamma[\mathbf{H} \times \delta\boldsymbol{\phi}]. \quad (2.5)$$

The spin-phonon transitions under consideration are between the eigenstates of the Hamiltonian \mathcal{H}_0 defined in Eq. (2.2), which are direct products of the spin and

phonon states,

$$|\Psi_{\pm}\rangle = |\psi_{\pm}\rangle \otimes |\phi_{\pm}\rangle. \quad (2.6)$$

Here $|\psi_{\pm}\rangle$ are the eigenstates of \mathcal{H}_S with eigenvalues E_{\pm} ($E_+ > E_-$) and $|\phi_{\pm}\rangle$ are the eigenstates of \mathcal{H}_{ph} with energies $E_{ph,\pm}$. Direct transitions involve the emission or absorption of one phonon with wave vector \mathbf{k} and polarization λ , so that it is convenient to use the following designations

$$|\psi_+\rangle \equiv |n_{\mathbf{k}\lambda}\rangle \quad |\psi_-\rangle \equiv |n_{\mathbf{k}\lambda} + 1\rangle. \quad (2.7)$$

The probability per unit time for the system (spin + phonons) to transit from an initial state $|\psi_+\rangle$ with $n_{\mathbf{k}\lambda}$ phonons in the state (\mathbf{k}, λ) to a final state $|\psi_-\rangle$ by the absorption or emission of one phonon in the state (\mathbf{k}, λ) (direct process) is given by the Fermi golden rule [40]

$$p(+, n_{\mathbf{k}\lambda} \rightarrow -, n_{\mathbf{k}\lambda} \pm 1) = \frac{2\pi}{\hbar} |\langle \psi_+, n_{\mathbf{k}\lambda} | \mathcal{H}_{s-ph} | \psi_-, n_{\mathbf{k}\lambda} \pm 1 \rangle|^2 \delta(E_+ - E_- \pm \hbar\omega_{\mathbf{k}\lambda}). \quad (2.8)$$

Thus, the decay rate Γ_{+-} of the state $|\psi_+\rangle$ into the state $|\psi_-\rangle$ accompanied by the emission of a phonon, and the rate Γ_{-+} of the inverse process are given by

$$\Gamma_{\pm\mp} = \frac{2\pi}{\hbar} \sum_{\mathbf{k}\lambda} |\langle \psi_+, n_{\mathbf{k}\lambda} | \mathcal{H}_{s-ph} | \psi_-, n_{\mathbf{k}\lambda} \pm 1 \rangle|^2 \delta(E_+ - E_- \pm \hbar\omega_{\mathbf{k}\lambda}). \quad (2.9)$$

Therefore, to evaluate the decay rate of the transition $|\psi_+\rangle \rightarrow |\psi_-\rangle$ one needs to compute the matrix element corresponding to such transition (see Eq. (2.9)). It will be shown that the matrix elements coincide in both frames, so that the same decay rates are obtained for both the lattice frame and the laboratory frame.

2.1.1 Lattice frame

From Eq. (2.5) one obtains

$$\langle \Psi_- | \mathcal{H}_{s-ph}^{(lat)} | \Psi_+ \rangle = -\hbar\boldsymbol{\Omega}_{-+} \cdot \langle \psi_- | \mathbf{S} | \psi_+ \rangle, \quad (2.10)$$

where

$$\mathbf{\Omega}_{+-} \equiv \langle \phi_- | \mathbf{\Omega} | \phi_+ \rangle = \langle n_\lambda + 1 | \delta \dot{\boldsymbol{\phi}} + \gamma [\mathbf{H} \times \delta \boldsymbol{\phi}] | n_{\mathbf{k}\lambda} \rangle \equiv \mathbf{\Omega}_{\mathbf{k}\lambda}. \quad (2.11)$$

Using Eq. (1.45) one realizes that the first term of $\mathbf{\Omega}_{+-}$ is

$$\langle \phi_- | [\mathcal{H}_{ph}, \delta \boldsymbol{\phi}] | \phi_+ \rangle = (E_{ph,-} - E_{ph,+}) \delta \boldsymbol{\phi}_{-+}, \quad (2.12)$$

with

$$\delta \phi_{+-} \equiv \langle \phi_- | \delta \boldsymbol{\phi} | \phi_+ \rangle = \langle n_{\mathbf{k}\lambda} + 1 | \delta \boldsymbol{\phi} | n_{\mathbf{k}\lambda} \rangle \equiv \delta \boldsymbol{\phi}_{\mathbf{k}\lambda}. \quad (2.13)$$

Spin-phonon transitions conserve energy, so that

$$E_+ + E_{ph,+} = E_- + E_{ph,-} \quad \rightarrow \quad E_{ph,-} - E_{ph,+} = E_+ - E_- \equiv \hbar\omega_0. \quad (2.14)$$

Thus one finally obtains

$$\mathbf{\Omega}_{\mathbf{k}\lambda} = i\omega_0 \delta \boldsymbol{\phi}_{\mathbf{k}\lambda} + \gamma [\mathbf{H} \times \delta \boldsymbol{\phi}_{\mathbf{k}\lambda}]. \quad (2.15)$$

2.1.2 Laboratory frame

The matrix element of the transition in the laboratory frame is given by

$$\langle \Psi_- | \mathcal{H}_{s-ph} | \Psi_+ \rangle = i \langle \psi_- | [\mathcal{H}_A, \mathbf{S}] | \psi_+ \rangle \cdot \delta \boldsymbol{\phi}_{\mathbf{k}\lambda}, \quad (2.16)$$

where Eq. (2.3) has been used. It is convenient to add and subtract \mathcal{H}_Z from \mathcal{H}_A in the previous commutator

$$\langle \psi_- | [\mathcal{H}_A, \mathbf{S}] | \psi_+ \rangle = \langle \psi_- | [\mathcal{H}_S, \mathbf{S}] | \psi_+ \rangle - \langle \psi_- | [\mathcal{H}_Z, \mathbf{S}] | \psi_+ \rangle \quad (2.17)$$

On one hand, the states $|\psi_\pm\rangle$ are exact eigenstates of the spin-Hamiltonian \mathcal{H}_S with energies E_\pm , so that

$$\langle \psi_- | [\mathcal{H}_S, \mathbf{S}] | \psi_+ \rangle = -\hbar\omega_0 \langle \psi_- | \mathbf{S} | \psi_+ \rangle. \quad (2.18)$$

On the other hand,

$$i\langle\psi_-|[\mathcal{H}_Z, \mathbf{S}]|\psi_+\rangle \cdot \delta\boldsymbol{\phi}_{\mathbf{k}\lambda} = g\mu_B(\mathbf{H} \times \delta\boldsymbol{\phi}_{\mathbf{k}\lambda}) \cdot \langle\psi_-|\mathbf{S}|\psi_+\rangle. \quad (2.19)$$

Therefore, the matrix element in the laboratory frame is

$$\langle\Psi_-|\mathcal{H}_{s-ph}|\Psi_+\rangle = -\hbar\boldsymbol{\Omega}_{\mathbf{k}\lambda} \cdot \langle\psi_-|\mathbf{S}|\psi_+\rangle, \quad (2.20)$$

which coincides with the expression obtained in the lattice frame of reference, Eq. (2.15).

2.1.3 General expression for the relaxation rate

Working out Eq. (2.20) by using the quantization of phonons, Eq. (1.36), one can rewrite the spin-phonon matrix element in the form

$$\langle\Psi_-|\mathcal{H}_{s-ph}|\Psi_+\rangle = \frac{\hbar}{\sqrt{N}} V_{\mathbf{k}\lambda} \langle n_{\mathbf{k}\lambda} + 1 | (a_{\mathbf{k}\lambda} + a_{-\mathbf{k}\lambda}^\dagger) | n_{\mathbf{k}\lambda} \rangle \quad (2.21)$$

where

$$V_{\mathbf{k}\lambda} \equiv \frac{e^{i\mathbf{k}\cdot\mathbf{r}}}{\sqrt{8M\hbar\omega_{\mathbf{k}\lambda}}} \boldsymbol{\Lambda} \cdot [\mathbf{k} \times \mathbf{e}_{\mathbf{k}\lambda}], \quad (2.22)$$

with $\boldsymbol{\Lambda}$ being the spin matrix element given by

$$\boldsymbol{\Lambda} = -i\hbar\omega_0 \langle\psi_-|\mathbf{S}|\psi_+\rangle - \langle\psi_-|\mathbf{S}|\psi_+\rangle \times g\mu_B\mathbf{H}. \quad (2.23)$$

According to Eq. (2.9), the decay rates Γ_{+-} and Γ_{-+} are

$$\begin{Bmatrix} \Gamma_{+-} \\ \Gamma_{-+} \end{Bmatrix} = \Gamma_0 \begin{Bmatrix} n_{\omega_0} + 1 \\ n_{\omega_0} \end{Bmatrix}, \quad (2.24)$$

where $n_{\omega_0} = (e^{\hbar\omega_0/(k_B T)} - 1)^{-1}$ is the phonon occupation number at equilibrium and

$$\Gamma_0 = \frac{1}{N} \sum_{\mathbf{k}\lambda} |V_{\mathbf{k}\lambda}|^2 2\pi\delta(\omega_{\mathbf{k}\lambda} - \omega_0). \quad (2.25)$$

By using the continuum limit $\sum_{\mathbf{k}} \dots \rightarrow V/(2\pi^3) \int d^3k \dots$ and the dispersion relation $\omega_{\mathbf{k}} = v_t k$ for transverse phonons one obtains

$$\Gamma_0 = \frac{1}{12\pi\hbar} \frac{|\mathbf{\Lambda}|^2 \omega_0^3}{\rho v_t^5}, \quad (2.26)$$

where ρ is the mass density. Note that this expression depends only on the matrix elements of the spin operator \mathbf{S} .

The master equation for the populations of the spin states n_+ and n_- , satisfying $n_+ + n_- = 1$,

$$\dot{n}_+ = -\Gamma_{+-}n_+ + \Gamma_{-+}n_- = -\Gamma n_+ + W_{+-} \quad (2.27)$$

defines the relaxation rate

$$\Gamma = \Gamma_{+-} + \Gamma_{-+} = \Gamma_0 \coth\left(\frac{\hbar\omega_0}{2k_B T}\right). \quad (2.28)$$

2.1.4 Relaxation between levels of the spin Hamiltonian

Here we shall study the spin Hamiltonian

$$\mathcal{H}_S = -DS_z^2 - g\mu_B H_z S_z. \quad (2.29)$$

The eigenstates of this Hamiltonian are the eigenstates of the S_z operator, $S_z|m\rangle = m|m\rangle$, with energies $E_m = -Dm^2 - g\mu_B H_z m$. It is clear from the expression for the matrix element of the direct transition, Eq. (2.20), that only transitions between adjacent levels of \mathcal{H}_S (with, say, m and $m' = m+1$) are allowed. The energy difference between these levels is

$$\hbar\omega_0 \equiv E_m - E_{m+1} = D(2m+1) + g\mu_B H_z. \quad (2.30)$$

The transition occurs between the states $|\Psi_+\rangle = |m\rangle \otimes |n_{\mathbf{k}\lambda}\rangle$ and $|\Psi_-\rangle = |m+1\rangle \otimes |n_{\mathbf{k}\lambda}+1\rangle$. The transition matrix element can be calculated with the help of Eq. (2.20),

and results

$$\langle \Psi_- | \mathcal{H}_{s-ph} | \Psi_+ \rangle = \frac{iD}{2} l_{m,m+1} (2m+1) \delta\phi_{\mathbf{k}\lambda,-}, \quad (2.31)$$

where $l_{m,m+1} = \sqrt{S(S+1) - m(m+1)}$, $\delta\phi_{\mathbf{k}\lambda,-} \equiv \delta\phi_{\mathbf{k}\lambda,x} - i\delta\phi_{\mathbf{k}\lambda,y}$, and $\delta\phi_{\mathbf{k}\lambda}$ is defined by Eq. (2.13). The relaxation rate at $T = 0$ is

$$\Gamma_0 = \frac{(2m+1)^2 l_{m,m+1}^2 D^2 \omega_{m,m+1}^3}{24\pi\hbar \rho v_t^5}. \quad (2.32)$$

2.1.5 Spin-phonon relaxation between tunnel-split states

Here we will consider a molecular magnet with spin-Hamiltonian given by

$$\mathcal{H}_S = -DS_z^2 + V - g\mu_B S_z H, \quad (2.33)$$

where V is a small perturbation that does not commute with the S_z -operator responsible for the tunnel splitting, Δ , of spin-up and spin-down states. The unperturbed energy states are the eigenstates of the S_z -operator, $S_z|m\rangle = m|m\rangle$. In the vicinity of a resonance between the unperturbed states $|m\rangle$ and $|m'\rangle$, the system can be described by the two-state effective Hamiltonian

$$h_{eff} = \frac{1}{2}W(|m\rangle\langle m| - |m'\rangle\langle m'|) + \frac{1}{2}\Delta(|m'\rangle\langle m| + |m\rangle\langle m'|), \quad (2.34)$$

where W is the energy difference between the unperturbed states. Note that this is an approximate description. More precisely, because of the presence of V , one should consider states $|\phi_m\rangle = \sum_m' c_{mm'}|m'\rangle$ instead of $|m\rangle$ in the previous two-state Hamiltonian. It can be proved, though, that the contribution to the decay rate of this extra terms originated by V are negligible.

The tunnel-split states are the eigenstates of Hamiltonian (2.34), which are given by

$$|\phi_{\pm}\rangle = \frac{1}{\sqrt{2}}(C_{\pm}|m\rangle \pm C_{\mp}|m'\rangle), \quad C_{\pm} = \sqrt{1 \pm \frac{W}{\sqrt{W^2 + \Delta^2}}}. \quad (2.35)$$

According to Eqs. (2.26) and (2.23), we only need to compute the matrix elements of the spin operator between the states involved in the transition. From Eq. (2.35) one realizes the only non-zero matrix element of the spin operator is

$$\langle \phi_- | S_z | \phi_+ \rangle = -\frac{\Delta}{\sqrt{W^2 + \Delta^2}} \frac{m' - m}{2}. \quad (2.36)$$

With the help of Eqs. (2.26) and (2.23) one finally obtains

$$\Gamma_0 = \frac{(m' - m)^2 \Delta^5}{48\pi\hbar^4 \rho v_t^5}. \quad (2.37)$$

2.2 Two-phonon processes [41]

Direct processes dominate spin-phonon relaxation at zero temperature when no thermal phonons are present in the system. At finite temperature, however, two-phonon processes may take over. In this Section we study two kinds of two-phonon processes. The first kind consists of an inelastic scattering of phonons by the spin-system, or spin-phonon Raman processes. It corresponds to the annihilation of an incoming phonon of frequency $\omega_{\mathbf{k}}$ and the creation of an outgoing phonon of frequency $\omega_{\mathbf{q}}$, with \mathbf{k} and \mathbf{q} being the corresponding wave vectors. The second kind involves emission of two phonons. Note that the conservation of the energy in spin-phonon interactions requires

$$\hbar\omega_{\mathbf{q}} \pm \hbar\omega_{\mathbf{k}} = \Delta E > 0, \quad (2.38)$$

where ΔE is the energy difference between the spin-states and $\omega_{\mathbf{k}}, \omega_{\mathbf{q}}$ are the frequencies of the phonons involved in the transition. The plus sign applies to processes involving the emission of two phonons and the minus sign applies to Raman processes. When $\Delta E \ll \hbar\omega_D$ (with ω_D being the Debye frequency), Eq. (2.38) causes the phase space of phonons to be much greater for Raman processes than for processes involving

the emission of two phonons. Consequently, the spin-phonon Raman scattering usually dominates over the processes involving the emission of two phonons. However, the same condition (2.38) implies that the energy of the phonon emitted in the Raman scattering process, $\hbar\omega_{\mathbf{q}}$, must satisfy $\hbar\omega_{\mathbf{q}} > \Delta E$, whereas in the process involving the creation of two phonons their energy must be smaller than ΔE . Therefore, if $k_B T \ll \Delta E$, the total number of phonons available to carry out the spin transition may be much greater in the two-phonon emission case than in the Raman case, so that the former case can become dominant. In both cases the matrix element of the transition is a sum of two terms. The first term, $M^{(2)}$, comes from the first order of the perturbation theory on the spin-phonon coupling containing a product of two phonon displacement fields. The second term, $M^{(1+1)}$, comes from the second order of the perturbation theory on the spin-phonon coupling that is linear in the phonon displacement field. In some cases these two terms interfere, so that the resulting transition rate, based upon $|M^{(2)} + M^{(1+1)}|^2$, is different from the one obtained by adding up the rates, $|M^{(2)}|^2$ and $|M^{(1+1)}|^2$, that each term would produce by itself, as was incorrectly done in the past [16]. Note that in the conventional approach to spin-phonon relaxation it is customary to distinguish between cases of Kramers and non-Kramers ions. We consider only the non-Kramers case when the spin-phonon transitions occur between spin levels that are split by the crystal field even in the absence of the magnetic field.

2.2.1 Matrix elements of two-phonon processes

The treatment of two-phonon processes requires consideration of terms up to second order in phonon amplitudes in the Hamiltonian of the molecular magnet in the presence of lattice distortions. From the general Hamiltonian of a rigid nanomagnet in

the presence of lattice distortions, Eq. (1.35), one obtains

$$\hat{R}\hat{\mathcal{H}}_A\hat{R}^{-1} \simeq \hat{\mathcal{H}}_A + \hat{\mathcal{H}}_{s\text{-ph}} \quad \hat{\mathcal{H}}_{s\text{-ph}} = \hat{\mathcal{H}}_{s\text{-ph}}^{(1)} + \hat{\mathcal{H}}_{s\text{-ph}}^{(2)}, \quad (2.39)$$

with

$$\begin{aligned} \hat{\mathcal{H}}_{s\text{-ph}}^{(1)} &= i \left[\hat{\mathcal{H}}_A, S_\alpha \right] \delta\phi_\alpha \\ \hat{\mathcal{H}}_{s\text{-ph}}^{(2)} &= \frac{i^2}{2!} \left[\left[\hat{\mathcal{H}}_A, S_\alpha \right], S_\beta \right] \delta\phi_\alpha \delta\phi_\beta. \end{aligned} \quad (2.40)$$

The total Hamiltonian can then be written as

$$\hat{\mathcal{H}} = \hat{\mathcal{H}}_0 + \hat{\mathcal{H}}_{s\text{-ph}}, \quad (2.41)$$

where $\hat{\mathcal{H}}_0$ is the Hamiltonian of non-interacting spin and phonons,

$$\hat{\mathcal{H}}_0 = \hat{\mathcal{H}}_S + \hat{\mathcal{H}}_{\text{ph}}, \quad \hat{\mathcal{H}}_S = \hat{\mathcal{H}}_A + \hat{\mathcal{H}}_Z. \quad (2.42)$$

We will study spin-phonon transitions between the eigenstates of $\hat{\mathcal{H}}_0$, which are direct products of the spin and phonon states,

$$|\Psi_\pm\rangle = |\psi_\pm\rangle \otimes |\phi_\pm\rangle. \quad (2.43)$$

Here $|\psi_\pm\rangle$ are the eigenstates of $\hat{\mathcal{H}}_S$ with eigenvalues E_\pm ($E_+ > E_-$) and $|\phi_\pm\rangle$ are the eigenstates of $\hat{\mathcal{H}}_{\text{ph}}$ with energies $E_{\text{ph},\pm}$. Spin-phonon transitions conserve energy

$$E_+ + E_{\text{ph},+} = E_- + E_{\text{ph},-}. \quad (2.44)$$

To obtain the relaxation rate of the transition $|\Psi_+\rangle \rightarrow |\Psi_-\rangle$ one needs to evaluate the matrix element of the process. This matrix element is the sum of the matrix element with $\hat{\mathcal{H}}_{s\text{-ph}}^{(2)}$ and that with $\hat{\mathcal{H}}_{s\text{-ph}}^{(1)}$ in the second order [40]:

$$M = M^{(2)} + M^{(1+1)}, \quad (2.45)$$

where

$$M^{(2)} = \langle \Psi_- | \hat{\mathcal{H}}_{\text{s-ph}}^{(2)} | \Psi_+ \rangle \quad (2.46)$$

and

$$M^{(1+1)} = \sum_{\xi} \frac{\langle \Psi_- | \hat{\mathcal{H}}_{\text{s-ph}}^{(1)} | \Psi_{\xi} \rangle \langle \Psi_{\xi} | \hat{\mathcal{H}}_{\text{s-ph}}^{(1)} | \Psi_+ \rangle}{E_+ - E_{\xi}}. \quad (2.47)$$

Here ξ labels intermediate spin-phonon states.

2.2.2 Raman processes

For the Raman processes of interest, a phonon with the wave vector \mathbf{k} is absorbed and a phonon with the wave vector \mathbf{q} is emitted. We will use the following designations for the phonon states

$$|\phi_+\rangle \equiv |n_{\mathbf{k}}, n_{\mathbf{q}}\rangle, \quad |\phi_-\rangle \equiv |n_{\mathbf{k}} - 1, n_{\mathbf{q}} + 1\rangle \quad (2.48)$$

In this case, the conservation of the energy reads:

$$\Delta E = E_+ - E_- = \hbar\omega_{\mathbf{q}} - \hbar\omega_{\mathbf{k}}. \quad (2.49)$$

The matrix element of the Raman process can be written as $M_R = M_R^{(2)} + M_R^{(1+1)}$.

According to equations (2.40) and (2.46)

$$M_R^{(2)} = - \frac{1}{2} \langle \psi_- | \left[\left[\hat{\mathcal{H}}_A, S_{\alpha} \right], S_{\beta} \right] | \psi_+ \rangle \times \langle n_{\mathbf{k}} - 1, n_{\mathbf{q}} + 1 | \delta\phi_{\alpha} \delta\phi_{\beta} | n_{\mathbf{k}}, n_{\mathbf{q}} \rangle. \quad (2.50)$$

It is convenient to express the phonon matrix element as

$$\langle n_{\mathbf{k}} - 1, n_{\mathbf{q}} + 1 | \delta\phi_{\alpha} \delta\phi_{\beta} | n_{\mathbf{k}}, n_{\mathbf{q}} \rangle = M_{\text{ph-R}}^{\alpha\beta} + M_{\text{ph-R}}^{\beta\alpha}, \quad (2.51)$$

where

$$M_{\text{ph-R}}^{\alpha\beta} = \langle n_{\mathbf{q}} + 1 | \delta\phi_{\alpha} | n_{\mathbf{q}} \rangle \langle n_{\mathbf{k}} - 1 | \delta\phi_{\beta} | n_{\mathbf{k}} \rangle. \quad (2.52)$$

With the help of Eq. (1.36) one obtains

$$M_{\text{ph-R}}^{\alpha\beta} = \frac{\hbar^2}{8\rho V} \frac{[\mathbf{k} \times \mathbf{e}_{\mathbf{k}\lambda_{\mathbf{k}}}]_{\alpha} [\mathbf{q} \times \mathbf{e}_{\mathbf{q}\lambda_{\mathbf{q}}}]_{\beta}}{\sqrt{\hbar\omega_{\mathbf{k}\lambda_{\mathbf{k}}} \hbar\omega_{\mathbf{q}\lambda_{\mathbf{q}}}}} \sqrt{(n_{\mathbf{q}} + 1) n_{\mathbf{k}}}. \quad (2.53)$$

On the other hand, using the definition (2.52), one obtains from Eq. (2.47)

$$\begin{aligned} M_R^{(1+1)} = & - \sum_{\xi} \frac{\langle \psi_- | [\hat{\mathcal{H}}_A, S_{\alpha}] | \psi_{\xi} \rangle \langle \psi_{\xi} | [\hat{\mathcal{H}}_A, S_{\beta}] | \psi_+ \rangle}{E_+ + \hbar\omega_{\mathbf{k}} - E_{\xi}} M_{\text{ph-R}}^{\alpha\beta} \\ & - \sum_{\xi} \frac{\langle \psi_- | [\hat{\mathcal{H}}_A, S_{\alpha}] | \psi_{\xi} \rangle \langle \psi_{\xi} | [\hat{\mathcal{H}}_A, S_{\beta}] | \psi_+ \rangle}{E_+ - E_{\xi} - \hbar\omega_{\mathbf{q}}} M_{\text{ph-R}}^{\beta\alpha}, \end{aligned} \quad (2.54)$$

where ξ now labels intermediate states of the spin only. The intermediate phonon states are $|n_{\mathbf{k}} - 1, n_{\mathbf{q}}\rangle$ in the first term and $|n_{\mathbf{k}}, n_{\mathbf{q}} + 1\rangle$ in the second term.

Transition between eigenstates of S_z

Consider for example the spin Hamiltonian

$$\hat{\mathcal{H}}_S = \hat{\mathcal{H}}_A + \hat{\mathcal{H}}_Z = -DS_z^2 - g\mu_B H_z S_z \quad (2.55)$$

that commutes with S_z . The exact energy states of this Hamiltonian are the eigenstates of the S_z operator, $S_z|m\rangle = m|m\rangle$, with energies given by

$$E_m = -Dm^2 - g\mu_B H_z m. \quad (2.56)$$

Let us study the general case of the spin transition $m_+ \rightarrow m_-$ chosen so that $E_{m_+} > E_{m_-}$. From equations (2.50), (2.51) and (2.55) one obtains

$$M_R^{(2)} = D \sum_{\alpha\beta} \tilde{M}_{\text{ph-R}}^{\alpha\beta} \sum_{m_{\xi}} (m_+^2 + m_-^2 - 2m_{\xi}^2) \langle m_- | S_{\alpha} | m_{\xi} \rangle \langle m_{\xi} | S_{\beta} | m_+ \rangle, \quad (2.57)$$

with $\tilde{M}_{\text{ph-R}}^{\alpha\beta} = \frac{1}{2} (M_{\text{ph-R}}^{\alpha\beta} + M_{\text{ph-R}}^{\beta\alpha})$. The summation on m_ξ runs over all the spin states. On the other hand, Eq. (2.54) results in

$$\begin{aligned}
M_R^{(1+1)} &= \sum_{m_\xi} \frac{D^2(m_-^2 - m_\xi^2)(m_+^2 - m_\xi^2)}{D(m_\xi^2 - m_+^2) + g\mu_B H(m_\xi - m_+) + \hbar\omega_{\mathbf{k}}} \\
&\quad \times \langle m_- | S_\alpha | m_\xi \rangle \langle m_\xi | S_\beta | m_+ \rangle M_{\text{ph-R}}^{\alpha\beta} \\
&+ \sum_{m_\xi} \frac{D^2(m_-^2 - m_\xi^2)(m_+^2 - m_\xi^2)}{D(m_\xi^2 - m_+^2) + g\mu_B H(m_\xi - m_+) - \hbar\omega_{\mathbf{q}}} \\
&\quad \times \langle m_- | S_\alpha | m_\xi \rangle \langle m_\xi | S_\beta | m_+ \rangle M_{\text{ph-R}}^{\beta\alpha}, \tag{2.58}
\end{aligned}$$

where summation over α and β is assumed.

Adjacent spin levels, $m \rightarrow m \pm 1$

We will first treat the Raman processes involving transitions between adjacent levels of the spin-Hamiltonian (2.55) (see Fig. 2.1). Therefore, the spin-states in this case will be

$$|m_+\rangle = |m\rangle, \quad |m_-\rangle = |m \pm 1\rangle, \tag{2.59}$$

where the plus sign applies to positive m and the minus sign applies to negative m , so that $E_{m_+} > E_{m_-}$. A straightforward calculation of the matrix elements in equations (2.57) and (2.58) leads to

$$\begin{aligned}
M_R^{(2)} &= D(-2m \mp 1) l_{m, m \pm 1} \tilde{M}_{\text{ph-R}}^{\pm z} \\
M_R^{(1+1)} &= 0, \tag{2.60}
\end{aligned}$$

where

$$\tilde{M}_{\text{ph-R}}^{z\pm} = \frac{1}{2} (\tilde{M}_{\text{ph-R}}^{zx} \mp i \tilde{M}_{\text{ph-R}}^{zy}) \tag{2.61}$$

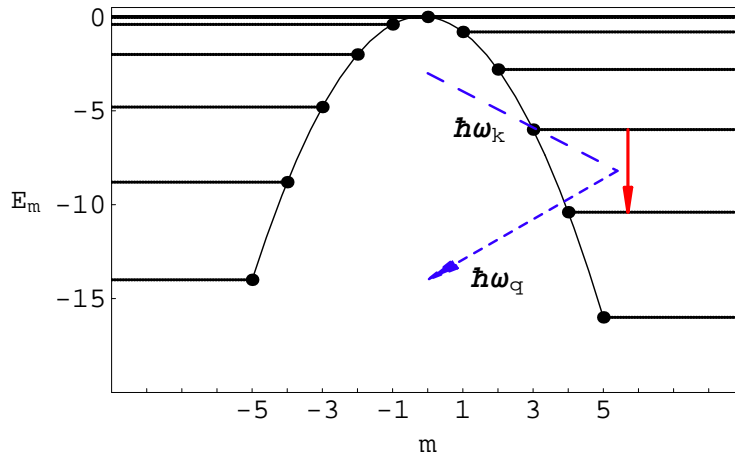


Figure 2.1: Transition between adjacent spin-energy levels of Hamiltonian (2.55) mediated by Raman processes.

and $l_{m,m\pm 1} = \sqrt{(S \mp m)(S \pm m + 1)}$.

Then $M_R = M_R^{(2)}$ and the transition rate is given by

$$\Gamma_R^{m \rightarrow m\pm 1} = \sum_{\substack{\mathbf{k}\lambda_{\mathbf{k}} \\ \mathbf{q}\lambda_{\mathbf{q}}}} \frac{2\pi}{\hbar} |M_R^{(2)}|^2 \delta(\hbar\omega_{\mathbf{q}} - \hbar\omega_{\mathbf{k}} - \Delta E_1), \quad (2.62)$$

where $\Delta E_1 = E_m - E_{m\pm 1}$ is the energy between the spin states. Note that in the sums over the polarizations $\lambda_{\mathbf{k}}$ and $\lambda_{\mathbf{q}}$, only the two transverse modes are considered.

To complete the calculation, we make use of

$$[\mathbf{k} \times \mathbf{e}_{\mathbf{k}t}] = \pm k \mathbf{e}_{\mathbf{k}t'} \quad (2.63)$$

$$\sum_{t=t_1, t_2} (\mathbf{e}_{\mathbf{k}t} \cdot \mathbf{a})(\mathbf{e}_{\mathbf{k}t} \cdot \mathbf{b}) = \mathbf{a} \cdot \mathbf{b} - \frac{(\mathbf{k} \cdot \mathbf{a})(\mathbf{k} \cdot \mathbf{b})}{k^2} \quad (2.64)$$

and the replacement of $\sum_{\mathbf{k}}$ by $V \int d^3k / (2\pi)^3$ to obtain

$$\Gamma_R^{m \rightarrow m\pm 1} = \frac{1}{\hbar} \frac{l_{m,m\pm 1}^2 I_{R1}}{\pi^3} \frac{[D(-2m \mp 1)]^2}{\mathcal{E}_t^8} (k_B T)^7, \quad (2.65)$$

where

$$\mathcal{E}_t \equiv (\hbar^3 \rho v_t^5)^{1/4} \quad (2.66)$$

is a characteristic energy in the problem. In these expressions ρ is the mass density and v_t is velocity of transverse sound. I_{R1} is given by

$$I_{R1} = \frac{1}{1152} \int_0^{\theta_D/T} dx x^3 (x + \epsilon_1)^3 \frac{e^{x+\epsilon_1}}{(e^x - 1)(e^{x+\epsilon_1} - 1)}, \quad (2.67)$$

where

$$\epsilon_1 = \frac{\Delta E_1}{k_B T} = \frac{D(\pm 2m + 1) \pm g\mu_B H}{k_B T}. \quad (2.68)$$

We remind the reader that in the above formulas the choice of upper and lower sign corresponds the choice of \pm in Eq. (2.59). We use $m + 1$ for positive m and we use $m - 1$ for negative m , so that $\Delta E_1 > 0$.

Note that the integral I_{R1} given by Eq. (2.67) that is contained in the expression of the Raman relaxation rate, Eq. (2.65), is in general temperature-dependent. This results in a different dependence on temperature of the relaxation rate for different temperature ranges.

For $k_B T \ll \Delta E_1 \ll \theta_D$, $I_{R1} = (\pi^4/17280) \epsilon_1^3$ so that the relaxation rate is

$$\Gamma_R^{m \rightarrow m \pm 1} = \frac{1}{\hbar} \frac{\pi l_{m,m \pm 1}^2}{17280} \frac{[D(-2m \mp 1)]^2 (\Delta E_1)^3}{\mathcal{E}_t^8} (k_B T)^4. \quad (2.69)$$

For $\Delta E_1 \ll k_B T \ll \theta_D$, $I_{R1} = \pi^6/1512$ and the relaxation rate is

$$\Gamma_R^{m \rightarrow m \pm 1} = \frac{1}{\hbar} \frac{\pi^3 l_{m,m \pm 1}^2}{1512} \frac{[D(-2m \mp 1)]^2}{\mathcal{E}_t^8} (k_B T)^7. \quad (2.70)$$

For $k_B T \gg \theta_D \gg \Delta E_1$, $I_{R1} = (\theta_D/T)^5 (1/5760)$ so that the Raman relaxation rate is given by

$$\Gamma_R^{m \rightarrow m \pm 1} = \frac{1}{\hbar} \frac{l_{m,m \pm 1}^2}{5760 \pi^3} \frac{[D(-2m \mp 1)]^2}{\mathcal{E}_t^8} (k_B \theta_D)^5 (k_B T)^2 \quad (2.71)$$

within the Debye model.

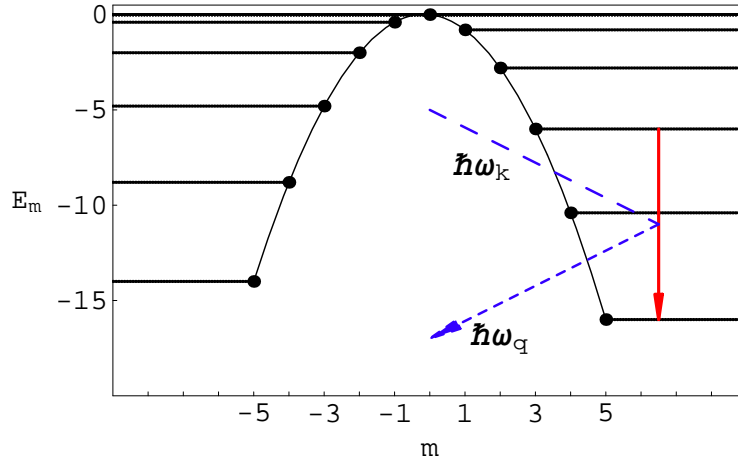


Figure 2.2: Transition between the spin-energy levels of Hamiltonian (2.55) $m \rightarrow m+2$ due to Raman scattering.

Non-adjacent spin levels, $m \rightarrow m \pm 2$

It is clear from equations (2.57) and (2.58) that the only allowed transitions between non-adjacent spin levels are those with

$$|m_+\rangle = |m\rangle, \quad |m_-\rangle = |m \pm 2\rangle. \quad (2.72)$$

In this case, represented in Fig. 2.2, equations (2.57) and (2.58) give

$$\begin{aligned} M_R^{(2)} &= D l_{m,m\pm 1} l_{m\pm 1,m\pm 2} M_{\text{ph-R}}^{\pm\pm} \\ M_R^{(1+1)} &= -\frac{D^2}{2} (\pm 2m + 3)(\pm 2m + 1) l_{m,m\pm 1} l_{m\pm 1,m\pm 2} \\ &\times \left(\frac{M_{\text{ph-R}}^{\pm\pm}}{E_{m\pm 1} - E_m + \hbar\omega_{\mathbf{k}}} + \frac{M_{\text{ph-R}}^{\pm\pm}}{E_{m\pm 1} - E_m - \hbar\omega_{\mathbf{q}}} \right), \end{aligned} \quad (2.73)$$

where

$$\begin{aligned} M_{\text{ph-R}}^{--} &= \frac{1}{2} [M_{\text{ph-R}}^{xx} + i(M_{\text{ph-R}}^{xy} + M_{\text{ph-R}}^{yx}) - M_{\text{ph-R}}^{yy}] \\ M_{\text{ph-R}}^{++} &= \frac{1}{2} [M_{\text{ph-R}}^{xx} - i(M_{\text{ph-R}}^{xy} + M_{\text{ph-R}}^{yx}) - M_{\text{ph-R}}^{yy}]. \end{aligned} \quad (2.74)$$

The transition rate can be obtained by computing

$$\Gamma_R^{m \rightarrow m \pm 2} = \sum_{\substack{\mathbf{k} \lambda_{\mathbf{k}} \\ \mathbf{q} \lambda_{\mathbf{q}}}} \frac{2\pi}{\hbar} |M_R|^2 \delta(\hbar\omega_{\mathbf{q}} - \hbar\omega_{\mathbf{k}} - \Delta E_2), \quad (2.75)$$

where $\Delta E_2 = E_m - E_{m \pm 2}$ and M_R is given by equations (2.45) and (2.73). Again, we use equations (2.63) and (2.64) and the replacement of $\sum_{\mathbf{k}}$ by $V d^3k / (2\pi)^3$ (with V being the volume of the crystal) to obtain the final result

$$\Gamma_R^{m \rightarrow m \pm 2} = \frac{1}{\hbar} \frac{l_{m,m \pm 1}^2 l_{m \pm 1, m \pm 2}^2 I_{R2} D^2}{\pi^3 \mathcal{E}_t^8} (k_B T)^7, \quad (2.76)$$

where

$$I_{R2} = \frac{1}{288} \int_0^{\theta_D/T} dx \frac{(x + \epsilon_2)^3 x^3 e^{(x + \epsilon_2)}}{[e^x - 1][e^{(x + \epsilon_2)} - 1]} \left\{ 1 - \frac{1}{2} (\pm 2m + 1)(\pm 2m + 3) \left[\frac{D/k_B T}{\epsilon_1 + x} + \frac{D/k_B T}{\epsilon_1 - \epsilon_2 - x} \right] \right\}^2 \quad (2.77)$$

with

$$\epsilon_2 = \frac{\Delta E_2}{k_B T} = \frac{4D(\pm m + 1) \pm 2g\mu_B H}{k_B T}. \quad (2.78)$$

Again, the integral I_{R2} given by Eq. (2.77) that is contained in the expression of the Raman relaxation rate, Eq. (2.76), is in general temperature-dependent. This causes a different temperature-dependence of the relaxation rate for different temperature ranges.

For $k_B T \ll \Delta E_2 \ll \theta_D$, $I_{R2} = A(\pi^4/4320) \epsilon_2^3$ so that the relaxation rate is

$$\Gamma_R^{m \rightarrow m \pm 2} = \frac{1}{\hbar} \frac{A\pi l_{m,m \pm 1}^2 l_{m \pm 1, m \pm 2}^2 D^2 (\Delta E_2)^3}{4320 \mathcal{E}_t^8} (k_B T)^4 \quad (2.79)$$

with A given by

$$A = \left(1 - \frac{(\pm 2m + 1)(\pm 2m + 3)}{2} \left[\frac{D}{\Delta E_1} - \frac{D}{\Delta E_2 - \Delta E_1} \right] \right)^2 \quad (2.80)$$

For $\Delta E_2 \ll k_B T \ll \theta_D$, $I_{R2} = \pi^6/378$ and the relaxation rate is

$$\Gamma_R^{m \rightarrow m \pm 2} = \frac{1}{\hbar} \frac{\pi^3 l_{m, m \pm 1}^2 l_{m \pm 1, m \pm 2}^2}{378} \frac{D^2}{\mathcal{E}_t^8} (k_B T)^7. \quad (2.81)$$

For $k_B T \gg \theta_D \gg \Delta E_2$, $I_{R2} = (\theta_D/T)^5 (1/1440)$ so that the Raman relaxation rate is given by

$$\Gamma_R^{m \rightarrow m \pm 2} = \frac{1}{\hbar} \frac{l_{m, m \pm 1}^2 l_{m \pm 1, m \pm 2}^2}{1440 \pi^3} \frac{D^2}{\mathcal{E}_t^8} (k_B \theta_D)^5 (k_B T)^2 \quad (2.82)$$

within the Debye model.

Transitions between tunnel-split states

Consider now a biaxial spin Hamiltonian with strong uniaxial anisotropy

$$\hat{\mathcal{H}}_S = \hat{\mathcal{H}}_A - g\mu_B \mathbf{H} \cdot \mathbf{S}, \quad \hat{\mathcal{H}}_A = -DS_z^2 + E[S_x^2 - S_y^2], \quad (2.83)$$

where $D \gg E > 0$ and $DS \gg g\mu_B H_\perp$, with H_\perp being the transverse magnetic field. Consequently, $\hat{\mathcal{H}}_A$ nearly commutes with S_z . The energy levels of this Hamiltonian are approximately given by Eq. (2.56). The two levels m and m' are in resonance for the values of the magnetic field $H_{z, mm'}^{(res)} = (m + m')D/(g\mu_B)$. The level bias is given by

$$W \equiv E_m - E'_m = g\mu_B \left(H_z - H_{z, mm'}^{(res)} \right) (m' - m). \quad (2.84)$$

The two state model

Due to the terms in $\hat{\mathcal{H}}_S$ that do not commute with S_z , the true eigenstates of $\hat{\mathcal{H}}_S$ far from a resonance are given by expansions over the complete $|m\rangle$ basis:

$$|\phi_m\rangle = \sum_{m''=-S}^S c_{mm''} |m''\rangle, \quad (2.85)$$

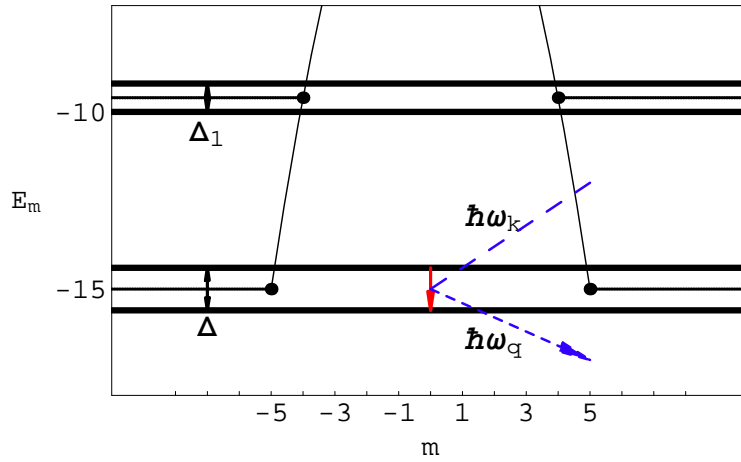


Figure 2.3: Transition between tunnel-split states due to Raman scattering.

where $|c_{mm}| \simeq 1$ and all the other coefficients are small. Hybridization of the states $|\phi_m\rangle$ and $|\phi_{m'}\rangle$ when they are close to resonance can be taken into account in the framework of the two-state model

$$\begin{aligned} \langle \phi_{m_i} | \hat{\mathcal{H}}_S | \phi_{m_i} \rangle &= E_{m_i}, \quad m_i = m, m' \\ \langle \phi_m | \hat{\mathcal{H}}_S | \phi_{m'} \rangle &= \frac{1}{2}\Delta, \end{aligned} \quad (2.86)$$

where Δ is the tunnel splitting of the levels m and m' that can be calculated from the exact spin Hamiltonian $\hat{\mathcal{H}}_S$ [42] or determined experimentally. Diagonalizing this 2×2 matrix yields the eigenvalues

$$E_{\pm} = \frac{1}{2} \left(E_m + E_{m'} \pm \sqrt{W^2 + \Delta^2} \right). \quad (2.87)$$

The corresponding eigenvectors can be represented in the form

$$|\psi_{\pm}\rangle = \frac{1}{\sqrt{2}} (C_{\pm}|\phi_m\rangle \pm C_{\mp}|\phi_{m'}\rangle), \quad (2.88)$$

where

$$C_{\pm} = \sqrt{1 \pm \frac{W}{\sqrt{W^2 + \Delta^2}}}. \quad (2.89)$$

Far from the resonance, $|W| \gg \Delta$, the eigenstates and energy eigenvalues reduce to those of $|\phi_m\rangle$ and $|\phi_{m'}\rangle$ states.

Matrix elements

Here we consider Raman processes involving spin transitions between tunnel-split states (see Fig. 2.3). That is, the spin eigenstates in Eq. (2.43) are given by Eq. (2.88). In order to compute the matrix element of the Raman process, we can rewrite $M_R^{(2)}$ by adding and subtracting $\hat{\mathcal{H}}_Z$ in the spin matrix element of Eq. (2.50)

$$\begin{aligned} \langle \psi_- | \left[\left[\hat{\mathcal{H}}_A, S_\alpha \right], S_\beta \right] | \psi_+ \rangle &= \langle \psi_- | \left[\left[\hat{\mathcal{H}}_S, S_\alpha \right], S_\beta \right] | \psi_+ \rangle \\ &\quad - \langle \psi_- | \left[\left[\hat{\mathcal{H}}_Z, S_\alpha \right], S_\beta \right] | \psi_+ \rangle. \end{aligned} \quad (2.90)$$

Taking into account that $|\psi_\pm\rangle$ are the eigenstates of $\hat{\mathcal{H}}_S$ and inserting the identity $1 = \sum_\xi |\psi_\xi\rangle\langle\psi_\xi|$ we can express the first term of the right hand side as

$$\langle \psi_- | \left[\left[\hat{H}_S, S_\alpha \right], S_\beta \right] | \psi_+ \rangle = \sum_\xi (E_- + E_+ - 2E_\xi) \langle \psi_- | S_\alpha | \psi_\xi \rangle \langle \psi_\xi | S_\beta | \psi_+ \rangle. \quad (2.91)$$

Then,

$$\begin{aligned} M_R^{(2)} &= - \left\{ \sum_\xi (E_- + E_+ - 2E_\xi) \langle \psi_- | S_\alpha | \psi_\xi \rangle \times \right. \\ &\quad \left. \langle \psi_\xi | S_\beta | \psi_+ \rangle - \langle \psi_- | \left[\left[\hat{\mathcal{H}}_Z, S_\alpha \right], S_\beta \right] | \psi_+ \rangle \right\} \tilde{M}_{\text{ph-R}}^{\alpha\beta}. \end{aligned} \quad (2.92)$$

Following the same procedure, we can rewrite $M_R^{(1+1)}$ from Eq. (2.54) as an expansion on powers of H :

$$M_R^{(1+1)} = M_R^{(1+1)}(H^0) + M_R^{(1+1)}(H^1) + O(H^2) \quad (2.93)$$

with

$$\begin{aligned}
M_R^{(1+1)}(H^0) &= - \sum_{\xi} (E_- - E_{\xi}) (E_{\xi} - E_+) \langle \psi_- | S_{\alpha} | \psi_{\xi} \rangle \langle \psi_{\xi} | S_{\beta} | \psi_+ \rangle \\
&\times \left[\frac{M_{\text{ph-R}}^{\alpha\beta}}{E_+ + \hbar\omega_{\mathbf{k}} - E_{\xi}} + \frac{M_{\text{ph-R}}^{\beta\alpha}}{E_+ - E_{\xi} - \hbar\omega_{\mathbf{q}}} \right]
\end{aligned} \tag{2.94}$$

and

$$\begin{aligned}
M_R^{(1+1)}(H^1) &= \\
&\sum_{\xi} \frac{\langle \psi_- | [\hat{H}_Z, S_{\alpha}] | \psi_{\xi} \rangle \langle \psi_{\xi} | [\hat{H}_S, S_{\beta}] | \psi_+ \rangle}{E_+ + \hbar\omega_{\mathbf{k}} - E_{\xi}} M_{\text{ph-R}}^{\alpha\beta} \\
&+ \sum_{\xi} \frac{\langle \psi_- | [\hat{H}_S, S_{\alpha}] | \psi_{\xi} \rangle \langle \psi_{\xi} | [\hat{H}_Z, S_{\beta}] | \psi_+ \rangle}{E_+ + \hbar\omega_{\mathbf{k}} - E_{\xi}} M_{\text{ph-R}}^{\alpha\beta} \\
&+ \sum_{\xi} \frac{\langle \psi_- | [\hat{H}_Z, S_{\alpha}] | \psi_{\xi} \rangle \langle \psi_{\xi} | [\hat{H}_S, S_{\beta}] | \psi_+ \rangle}{E_+ - E_{\xi} - \hbar\omega_{\mathbf{q}}} M_{\text{ph-R}}^{\beta\alpha} \\
&+ \sum_{\xi} \frac{\langle \psi_- | [\hat{H}_S, S_{\alpha}] | \psi_{\xi} \rangle \langle \psi_{\xi} | [\hat{H}_Z, S_{\beta}] | \psi_+ \rangle}{E_+ - E_{\xi} - \hbar\omega_{\mathbf{q}}} M_{\text{ph-R}}^{\beta\alpha}.
\end{aligned} \tag{2.95}$$

Transition rate for $H = 0$

At $H = 0$ one obtains

$$\begin{aligned}
M_R &= - \sum_{\xi} \langle \psi_- | S_{\alpha} | \psi_{\xi} \rangle \langle \psi_{\xi} | S_{\beta} | \psi_+ \rangle \left[M_{\text{ph-R}}^{(\alpha\beta)} \times \right. \\
&\left. \left(\frac{E_- + E_+}{2} - E_{\xi} + \frac{(E_- - E_{\xi})(E_{\xi} - E_+)}{E_+ + \hbar\omega_{\mathbf{k}} - E_{\xi}} \right) + \right. \\
&\left. M_{\text{ph-R}}^{(\beta\alpha)} \left(\frac{E_- + E_+}{2} - E_{\xi} + \frac{(E_- - E_{\xi})(E_{\xi} - E_+)}{E_+ - E_{\xi} - \hbar\omega_{\mathbf{q}}} \right) \right]
\end{aligned} \tag{2.96}$$

It is convenient to consider the terms with $\xi = \pm$ and $\xi \neq \pm$ separately. The contribution from $\xi = \pm$ is

$$M_R = -(E_+ - E_-) \left(\langle \psi_- | S_\alpha | \psi_- \rangle \langle \psi_- | S_\beta | \psi_+ \rangle - \langle \psi_- | S_\alpha | \psi_+ \rangle \langle \psi_+ | S_\beta | \psi_+ \rangle \right) \tilde{M}_{\text{ph-R}}^{\alpha\beta}. \quad (2.97)$$

Using the time-reversal symmetry, we obtain

$$\langle \psi_\pm | \mathbf{S} | \psi_\pm \rangle = -\langle \psi_\pm | \mathbf{S} | \psi_\pm \rangle^*. \quad (2.98)$$

For the biaxial model with $E > 0$ the states $|\psi_\pm\rangle$ are real. Then,

$$\langle \psi_\pm | S_z | \psi_\pm \rangle = \langle \psi_\pm | S_x | \psi_\pm \rangle = 0. \quad (2.99)$$

On the other hand, $\langle \psi_\pm | S_y | \psi_\pm \rangle = 0$ because of the factorization of the Hilbert space: $\mathcal{H} = \mathcal{H}_1^{(1)} \otimes \mathcal{H}_1^{(2)}$, $(-S, -S+2, \dots, S) \in \mathcal{H}_1^{(1)}$ and $(-S+1, -S+3, \dots, S-1) \in \mathcal{H}_1^{(2)}$. Thus Eq. (2.97) yields a zero result.

Let us consider now the terms with $\xi \neq \pm$. In this case, the difference between the energies of the doublet is much smaller than the energy distance to the other states, $|E_+ - E_-| \ll |E_\pm - E_\xi|$, so that one can replace E_\pm with E and $\hbar\omega_{\mathbf{q}}$ with $\hbar\omega_{\mathbf{k}}$ in the matrix elements. We consider the case of low temperature, when $\hbar\omega_{\mathbf{k}} \ll |E - E_\xi|$ for thermal phonons. Then M_R can be simplified to

$$M_R \simeq 2 (\hbar\omega_{\mathbf{k}})^2 \tilde{M}_{\text{ph-R}}^{\alpha\beta} A_{\alpha\beta}, \quad (2.100)$$

with

$$A_{\alpha\beta} \equiv \sum_{\xi} \prime \frac{\langle \psi_- | S_\alpha | \psi_\xi \rangle \langle \psi_\xi | S_\beta | \psi_+ \rangle}{E - E_\xi}, \quad (2.101)$$

where prime means that $\xi = \pm$ have been excluded. Note that the quadratic dependence on $\omega_{\mathbf{q}}$ in Eq. (2.100) results from cancellations between terms from $M_R^{(2)}$

and terms from $M_R^{(1+1)}$. Consequently, the relaxation rate will have a different temperature dependence from the result that one would obtain if one added the rates stemming from $M_R^{(2)}$ and $M_R^{(1+1)}$ independently. The rate is given by

$$\begin{aligned}\Gamma_{R0}^{+\rightarrow-} &= \sum_{\mathbf{k}, \lambda_{\mathbf{k}}} \sum_{\mathbf{q}, \lambda_{\mathbf{q}}} \frac{2\pi}{\hbar} |M_R|^2 \delta(\hbar\omega_{\mathbf{q}} - \hbar\omega_{\mathbf{k}}) \\ &= \frac{1}{18\hbar(2\pi)^3} \sum_{\alpha\beta} A_{\alpha\beta} (A_{\alpha\beta}^* + A_{\beta\alpha}^*) \frac{(k_B T)^{11}}{\mathcal{E}_t^8} I_{10}\end{aligned}\tag{2.102}$$

where equations (2.63) and (2.64) have been used and the continuum limit has been taken. The constant I_{10} is

$$I_{10} = \int_0^\infty dx \frac{x^{10} e^x}{(e^x - 1)^2} = \Gamma(11)\zeta(10).\tag{2.103}$$

For transitions between the lowest doublet $m = -S, m' = S$ specified in Eq. (2.88) one can evaluate $A_{\alpha\beta}$ by considering also the first excited doublet $m = -S + 1, m' = S - 1$

$$|\psi_{1\pm}\rangle = \frac{1}{\sqrt{2}} (C_{1\pm} |\phi_{m+1}\rangle \pm C_{1\mp} |\phi_{m'-1}\rangle)\tag{2.104}$$

with $C_{1\pm}$ given by Eq. (2.89) with $\Delta \rightarrow \Delta_1$ and $W \rightarrow W_1$. Hence the only non zero matrix elements are

$$A_{\pm\mp} = \frac{1}{E_m - E_{m+1}} \bar{A}_{\pm\mp},\tag{2.105}$$

where

$$\bar{A}_{\pm\mp} \equiv \sum_{\eta=\pm} \langle \psi_- | S_{\pm} | \psi_{1\eta} \rangle \langle \psi_{1\eta} | S_{\mp} | \psi_+ \rangle.\tag{2.106}$$

Evaluation of these matrix elements yields

$$\sum_{\alpha\beta} A_{\alpha\beta} (A_{\alpha\beta}^* + A_{\beta\alpha}^*) = \frac{S^2}{(E_{-S} - E_{-S+1})^2} \frac{\Delta^2}{W^2 + \Delta^2}.\tag{2.107}$$

For the case under consideration $W = 0$ and the transition rate is, then

$$\Gamma_{R0}^{+\rightarrow-} = \frac{80 \pi^7 S^2}{297 \hbar} \frac{(k_B T)^{11}}{(E_{-S} - E_{-S+1})^2 \mathcal{E}_t^8}. \quad (2.108)$$

Transition rate in the presence of a magnetic field

Here we are going to evaluate the contribution of the magnetic field \mathbf{H} to the rate of the transition between the tunnel-split ground-state levels. We consider magnetic fields with very small longitudinal component, $g\mu_B H_z \sim \Delta$. For longitudinal fields $g\mu_B H_z \gg \Delta$ the Raman processes die out. We are also restricted to not very large transverse magnetic fields, $g\mu_B H_\perp \ll DS$. In this case, it is sufficient to compute the lowest-order contribution of the magnetic field to the transition rate. This contribution can be essential because of the cancellation that occurs in the matrix element for the $H = 0$ case, Eq. (2.100). This cancellation leads to the $\Gamma_R^{+\rightarrow-} \propto T^{11}$ dependence. As we shall see, there is no such cancellation in the field-dependent term, so that the result shows a T^7 -dependence.

According to Eq. (2.92), the linear order contribution of H to $M_R^{(2)}$ is given by

$$\delta M_R^{(2)} = \langle \psi_- | \left[\left[\hat{H}_Z, S_\alpha \right], S_\beta \right] | \psi_+ \rangle \tilde{M}_{\text{ph-R}}^{\alpha\beta}. \quad (2.109)$$

The double commutator equals

$$\left[\left[\hat{H}_Z, S_\alpha \right], S_\beta \right] = g\mu_B (H_\beta S_\alpha - H_\gamma S_\gamma \delta_{\alpha\beta}) \quad (2.110)$$

so that

$$\begin{aligned} \delta M_R^{(2)} &= g\mu_B (H_\beta \delta_{\alpha z} - H_z \delta_{\alpha\beta}) \tilde{M}_{\text{ph-R}}^{\alpha\beta} \langle \psi_- | S_z | \psi_+ \rangle \\ &= g\mu_B K_{\alpha\beta}^{(2)} \tilde{M}_{\text{ph-R}}^{\alpha\beta}, \end{aligned} \quad (2.111)$$

where

$$K_{\alpha\beta}^{(2)} = - (H_\beta \delta_{\alpha z} - H_z \delta_{\alpha\beta}) \frac{\Delta}{\sqrt{W^2 + \Delta^2}} \frac{m' - m}{2}. \quad (2.112)$$

The phonon matrix element $\tilde{M}_{\text{ph-R}}^{\alpha\beta}$ is symmetric in $\alpha\beta$. Thus, it is possible and convenient to replace $K_{\alpha\beta}^{(2)}$ in Eq. (2.111) by the symmetrized tensor

$$\tilde{K}_{\alpha\beta}^{(2)} = \frac{1}{2} \left(K_{\alpha\beta}^{(2)} + K_{\beta\alpha}^{(2)} \right). \quad (2.113)$$

On the other hand, the linear order contribution of H to $M_R^{(1+1)}$ is given by Eq. (2.95).

By using Eq. (2.110) and assuming $\hbar\omega_{\mathbf{k}} \ll E_{m+1} - E_m$ we obtain

$$\begin{aligned} \delta M_R^{(1+1)} &\cong ig\mu_B 2H_\gamma (\epsilon_{\gamma\alpha\delta} \bar{A}_{\delta\beta} - \epsilon_{\gamma\beta\delta} \bar{A}_{\alpha\delta}) \tilde{M}_{\text{ph-R}}^{\alpha\beta} \\ &\equiv g\mu_B K_{\alpha\beta}^{(1+1)} \tilde{M}_{\text{ph-R}}^{\alpha\beta}, \end{aligned} \quad (2.114)$$

where

$$K_{\alpha\beta}^{(1+1)} = i2H_\gamma (\epsilon_{\gamma\alpha\delta} \bar{A}_{\delta\beta} - \epsilon_{\gamma\beta\delta} \bar{A}_{\alpha\delta}). \quad (2.115)$$

Again, it is convenient to replace $K_{\alpha\beta}^{(1+1)}$ in Eq. (2.114) by the symmetrized version

$$\tilde{K}_{\alpha\beta}^{(1+1)} = \frac{1}{2} \left(K_{\alpha\beta}^{(1+1)} + K_{\beta\alpha}^{(1+1)} \right). \quad (2.116)$$

The addition to the Raman matrix element due to $H \neq 0$ is, then

$$\delta M_R \equiv \delta M_R^{(2)} + \delta M_R^{(1+1)} = g\mu_B \tilde{K}_{\alpha\beta} \tilde{M}_{\text{ph-R}}^{\alpha\beta}, \quad (2.117)$$

with $\tilde{K}_{\alpha\beta} = \tilde{K}_{\alpha\beta}^{(2)} + \tilde{K}_{\alpha\beta}^{(1+1)}$. The transition rate is based upon $|M_R + \delta M_R|^2$. Here, $|M_R|^2$ was taken into account above. The interference term can be shown to be proportional to H_z and thus negligibly small. Therefore, the field effect is entirely contained in the term $|\delta M_R|^2$. Applying the same procedure as in the previous section, one obtains the following addition to the relaxation rate

$$\delta\Gamma_R^{+\leftrightarrow-} = \frac{1}{\hbar} \frac{\pi^3}{3024} (g\mu_B)^2 \sum_{\alpha\beta} |\tilde{K}_{\alpha\beta}|^2 \frac{(k_B T)^7}{\mathcal{E}_t^8}. \quad (2.118)$$

Evaluation of $\sum_{\alpha\beta} |\tilde{K}_{\alpha\beta}|^2$ for the lowest doublet $m = -S, m' = S$ yields

$$\sum_{\alpha\beta} |\tilde{K}_{\alpha\beta}|^2 = 2 \left(H_z^2 + \frac{1}{4} H_\perp^2 \right) \frac{\Delta^2}{W^2 + \Delta^2} S^2. \quad (2.119)$$

Therefore, the transition rate in the presence of a magnetic field is

$$\Gamma_R^{+\rightarrow-}(\mathbf{H}) \simeq \frac{\Delta^2}{W^2 + \Delta^2} (\Gamma_{R0}^{+\rightarrow-} + \delta\Gamma_{R0}^{+\rightarrow-}), \quad (2.120)$$

where $\Gamma_{R0}^{+\rightarrow-}$ is given by Eq. (2.108) and

$$\delta\Gamma_{R0}^{+\rightarrow-} = \frac{\pi^3 S^2}{6048\hbar} \frac{H_\perp^2 (g\mu_B)^2 (k_B T)^7}{\mathcal{E}_t^8}. \quad (2.121)$$

Note that we have used $H_z \ll H_\perp$ in the last expression. One can see from Eq. (2.120) that the relaxation rate due to Raman processes dies out when going out of resonance, $W \gg \Delta$.

2.2.3 Processes involving emission of two phonons

For processes involving emission of two phonons of, say, wave vectors \mathbf{k} and \mathbf{q} we use the following designations:

$$|\phi_+\rangle \equiv |n_{\mathbf{k}}, n_{\mathbf{q}}\rangle, \quad |\phi_-\rangle \equiv |n_{\mathbf{k}} + 1, n_{\mathbf{q}} + 1\rangle \quad (2.122)$$

In this case, conservation of energy reads:

$$E_+ - E_- = \hbar\omega_{\mathbf{k}} + \hbar\omega_{\mathbf{q}}. \quad (2.123)$$

The matrix element for this process is, again, the sum of the matrix element with $\hat{\mathcal{H}}_{\text{s-ph}}^{(2)}$ and that with $\hat{\mathcal{H}}_{\text{s-ph}}^{(1)}$ in the second order:

$$M_E = M_E^{(2)} + M_E^{(1+1)}, \quad (2.124)$$

where according to equations (2.40) and (2.46),

$$M_E^{(2)} = -\frac{1}{2} \left\langle \psi_- \left| \left[\left[\hat{\mathcal{H}}_A, S_\alpha \right], S_\beta \right] \right| \psi_+ \right\rangle \langle n_{\mathbf{k}} - 1, n_{\mathbf{q}} + 1 | \delta\phi_\alpha \delta\phi_\beta | n_{\mathbf{k}}, n_{\mathbf{q}} \rangle.$$

In this case it is convenient to express the phonon matrix element as:

$$\langle n_{\mathbf{k}} + 1, n_{\mathbf{q}} + 1 | \delta\phi_\alpha \delta\phi_\beta | n_{\mathbf{k}}, n_{\mathbf{q}} \rangle = M_{\text{ph-E}}^{\alpha\beta} + M_{\text{ph-E}}^{\beta\alpha} \equiv 2\tilde{M}_{\text{ph-E}}^{\alpha\beta}, \quad (2.125)$$

where

$$\begin{aligned} M_{\text{ph-E}}^{\alpha\beta} &= \langle n_{\mathbf{q}} + 1 | \delta\phi_\alpha | n_{\mathbf{q}} \rangle \langle n_{\mathbf{k}} + 1 | \delta\phi_\beta | n_{\mathbf{k}} \rangle \\ &= \frac{\hbar^2}{8\rho V} \frac{[\mathbf{k} \times \mathbf{e}_{\mathbf{k}\lambda_{\mathbf{k}}}]_\alpha [\mathbf{q} \times \mathbf{e}_{\mathbf{q}\lambda_{\mathbf{q}}}]_\beta}{\sqrt{\hbar\omega_{\mathbf{k}\lambda_{\mathbf{k}}}\hbar\omega_{\mathbf{q}\lambda_{\mathbf{q}}}}} \sqrt{(n_{\mathbf{q}} + 1)(n_{\mathbf{k}} + 1)}. \end{aligned} \quad (2.126)$$

Transitions between eigenstates of S_z

As stated above, the spin-phonon relaxation by emission of two phonons may be more important than the relaxation by Raman processes only if the energy difference between the spin-states satisfies $\Delta E \ll k_B T$. Provided that the energy difference between tunnel-split levels, Δ , is very small, only the relaxation by the emission of two phonons between eigenstates of S_z will be considered.

To this end, we will make use of the spin-Hamiltonian (2.55) and the transitions between its eigenstates, $|m\rangle$.

Adjacent spin levels, $m \rightarrow m \pm 1$

The matrix elements in this case are

$$\begin{aligned} M_E^{(2)} &= D(\mp 2m + 1) l_{m, m \pm 1} \tilde{M}_{\text{ph-E}}^{z\pm} \\ M_E^{(1+1)} &= 0, \end{aligned} \quad (2.127)$$

with

$$\tilde{M}_{\text{ph-E}}^{z\pm} = \frac{1}{2} \left[\tilde{M}_{\text{ph-E}}^{zx} \mp i \tilde{M}_{\text{ph-E}}^{zy} \right]. \quad (2.128)$$

The decay rate is then given by

$$\Gamma_E^{m \rightarrow m \pm 1} = \sum_{\substack{\mathbf{k}\lambda_{\mathbf{k}} \\ \mathbf{q}\lambda_{\mathbf{q}}}} \frac{2\pi}{\hbar} |M_E^{(2)}|^2 \delta(\hbar\omega_{\mathbf{k}} + \hbar\omega_{\mathbf{q}} - \Delta E_1). \quad (2.129)$$

Using the same techniques as in the previous calculations, one obtains

$$\Gamma_E^{m \rightarrow m \pm 1} = \frac{1}{\hbar} \frac{l_{m,m\pm 1}^2 I_{E1}}{\pi^3} \frac{[D(2m \pm 1)]^2}{\mathcal{E}_t^8} (k_B T)^7, \quad (2.130)$$

where

$$I_{E1} = \frac{1}{1152} \int_0^{\epsilon_1} dx \frac{x^3 (\epsilon_1 - x)^3 e^{\epsilon_1}}{(e^x - 1)(e^{(\epsilon_1 - x)} - 1)}. \quad (2.131)$$

The integral I_{E1} given by Eq. (2.131) that is contained in the expression of the relaxation rate, Eq. (2.130), is in general temperature-dependent. This results in a different dependence on temperature of the relaxation rate for different ranges of temperature.

For $k_B T \ll \Delta E_1$, $I_{E1} = \epsilon_1^7/161280$ so that the relaxation rate is temperature-independent and given by

$$\Gamma_E^{m \rightarrow m \pm 1} = \frac{1}{\hbar} \frac{l_{m,m\pm 1}^2}{161280\pi^3} \frac{[D(2m \pm 1)]^2 (\Delta E_1)^7}{\mathcal{E}_t^8}. \quad (2.132)$$

For $k_B T \gg \Delta E_1$, $I_{E1} = \epsilon_1^5/34560$ and the relaxation rate is

$$\Gamma_E^{m \rightarrow m \pm 1} = \frac{1}{\hbar} \frac{l_{m,m\pm 1}^2}{34560\pi^3} \frac{[D(2m \pm 1)]^2 (\Delta E_1)^5}{\mathcal{E}_t^8} (k_B T)^2. \quad (2.133)$$

Non-adjacent spin levels, $m \rightarrow m \pm 2$

In this case, the matrix elements are

$$\begin{aligned}
M_E^{(2)} &= D l_{m,m\pm 1} l_{m\pm 1,m\pm 2} M_{\text{ph-E}}^{\pm\pm} \\
M_E^{(1+1)} &= -\frac{D^2}{2} (\pm 2m + 3)(\pm 2m + 1) l_{m,m\pm 1} l_{m\pm 1,m\pm 2} \\
&\times \left(\frac{M_{\text{ph-E}}^{\pm\pm}}{E_{m\pm 1} - E_m + \hbar\omega_{\mathbf{k}}} + \frac{M_{\text{ph-E}}^{\pm\pm}}{E_{m\pm 1} - E_m - \hbar\omega_{\mathbf{q}}} \right),
\end{aligned} \tag{2.134}$$

where

$$M_{\text{ph-E}}^{\pm\pm} = \frac{1}{2} [M_{\text{ph-E}}^{xx} - M_{\text{ph-E}}^{yy} \mp i(M_{\text{ph-E}}^{xy} + M_{\text{ph-E}}^{yx})]. \tag{2.135}$$

The decay rate is

$$\Gamma_E^{m \rightarrow m \pm 2} = \frac{1}{\hbar} \frac{l_{m,m\pm 1}^2 l_{m\pm 1,m\pm 2}^2 I_{E2} D^2 (k_B T)^7}{\pi^3 \mathcal{E}_t^8}, \tag{2.136}$$

with

$$\begin{aligned}
I_{E2} &= \frac{1}{288} \int_0^{\epsilon_2} dx \frac{(\epsilon_2 - x)^3 x^3 e^{\epsilon_2}}{[e^x - 1][e^{(\epsilon_2 - x)} - 1]} \left\{ 1 - \right. \\
&\left. \frac{1}{2} (\pm 2m + 1)(\pm 2m + 3) \left[\frac{D/k_B T}{\epsilon_1 + x} + \frac{D/k_B T}{\epsilon_1 + \epsilon_2 - x} \right] \right\}^2.
\end{aligned} \tag{2.137}$$

The integral I_{E2} given by Eq. (2.137) that is contained in the expression of the decay rate, Eq. (2.136), is temperature-dependent. For different ranges of the temperature, the integral gives a different T-dependence.

For $k_B T \ll \Delta E_2$, $I_{E2} = I_{E2}^{(3)} (k_B T)^{-7}$ so that the relaxation rate is

$$\Gamma_E^{m \rightarrow m \pm 2} = \frac{1}{\hbar} \frac{l_{m,m\pm 1}^2 l_{m\pm 1,m\pm 2}^2 I_{E2}^{(3)} D^2}{\pi^3 \mathcal{E}_t^8}, \tag{2.138}$$

with

$$\begin{aligned}
I_{E_2}^{(n)} &= \frac{1}{288} \int_0^{\Delta E_2} dy (\Delta E_2 - y)^n y^n \left\{ 1 - \frac{1}{2} (\pm 2m + 1) \right. \\
&\times (\pm 2m + 3) \left[\frac{D}{\Delta E_1 + y} + \frac{D}{\Delta E_1 + \Delta E_2 - y} \right] \left. \right\}^2,
\end{aligned} \tag{2.139}$$

which is temperature-independent.

For $k_B T \gg \Delta E_2$, $I_{E_2} = I_{E_2}^{(2)} (k_B T)^{-5}$ and the relaxation rate becomes

$$\Gamma_E^{m \rightarrow m \pm 2} = \frac{1}{\hbar} \frac{l_{m, m \pm 1}^2 l_{m \pm 1, m \pm 2}^2}{\pi^3} \frac{I_{E_2}^{(2)} D^2}{\mathcal{E}_t^8} (k_B T)^2. \tag{2.140}$$

2.2.4 Discussion

Let us now compare transition rates obtained for direct, or one-phonon, processes obtained in Section 2.1 and the rates of the same transitions due to Raman processes.

Let us first compute the ratio of the Raman rate and the direct rate for spin transitions between adjacent eigenstates of the spin Hamiltonian (2.55). In the limit of $k_B T \ll \Delta E_1 < \theta_D$ the ratio is given by

$$\frac{\Gamma_R^{m \rightarrow m+1}}{\Gamma_D^{m \rightarrow m+1}} = \frac{\pi^2}{720} \left(\frac{k_B T}{\mathcal{E}_t} \right)^4. \tag{2.141}$$

and transitions are clearly dominated by direct processes. When $\Delta E_1 \ll k_B T < \theta_D$ one has

$$\frac{\Gamma_R^{m \rightarrow m+1}}{\Gamma_D^{m \rightarrow m+1}} \sim \left(\frac{\mathcal{E}_t}{\Delta E_1} \right)^2 \left(\frac{k_B T}{\mathcal{E}_t} \right)^6. \tag{2.142}$$

In this case transitions can be easily dominated by the Raman processes. For example, for $S = 10$, $m = 5$, $D = 0.1K$, $g\mu_B H = 1K$ the energy difference is $\Delta E_1 = 2.1K$, so that at $T = 35K$ the rate of the direct process is $\Gamma_D^{m \rightarrow m+1} \simeq 10^5 s^{-1}$, while the

rate of the Raman process is $\Gamma_R^{m \rightarrow m+1} \simeq 10^6 s^{-1}$. Besides, note that the Raman decay rates between adjacent levels, Eq. (2.70), and between levels separated by $\Delta m = \pm 2$, Eq. (2.81), are of the same order, so that the effect of Raman scattering is even larger. In these estimates we used the value of $\mathcal{E}_t \sim 100\text{K}$. In such molecular magnets as Mn-12 and Fe-8, however, it will be difficult to have the corresponding Raman processes dominant because of large distances between adjacent spin levels and small Debye temperature. Processes involving the emission of two phonons cannot be dominant in any temperature range. In some range they can dominate over Raman processes but not over direct processes.

For spin transitions between tunnel-split states of the spin Hamiltonian (2.83) at $H = 0$, the ratio of the Raman rate over the direct rate at $\Delta \ll k_B T$ is given by

$$\frac{\Gamma_{R0}^{+\rightarrow-}}{\Gamma_D^{+\rightarrow-}} = \frac{960\pi^8}{297(2S-1)^2} \left(\frac{k_B T}{D}\right)^2 \left(\frac{k_B T}{\mathcal{E}_t}\right)^4 \left(\frac{k_B T}{\Delta}\right)^4. \quad (2.143)$$

Consequently, in zero field and temperatures significantly exceeding Δ , the Raman processes will have much higher probability than direct processes. At, e.g., $D = 0.5\text{K}$, $S = 10$, $\Delta = 10^{-2}\text{K}$ and $T = 5\text{K}$, the rate of the direct process gives $\Gamma_D^{+\rightarrow-} \simeq 10^{-4} s^{-1}$, while the rate of the Raman process will be $\Gamma_R^{+\rightarrow-} \simeq 5 \cdot 10^4 s^{-1}$. Note that at temperatures where Raman processes dominate over direct processes, contribution of the magnetic field to the rate, Eq. (2.121), is small compared to the zero-field rate, Eq. (2.108).

In application to molecular magnets an approximation that operates with a single spin \mathbf{S} of fixed length S is valid below certain temperature due to strong exchange interaction between individual atomic spins of the cluster. At higher temperature this approximation fails [44]. As temperature rises, spin manifolds corresponding to different S begin to contribute to the dynamics of the cluster and, eventually, the

description in terms of a single spin \mathbf{S} becomes meaningless. In this connection we would like to note that for our approach to be valid, only the mechanical rigidity of the cluster is required; the spin itself does not have to be rigid and can change its length, S , alongside with direction. Extension of our model to the situation when a single-spin approximation fails requires separate investigation.

Finally, we would like to comment that while our formulas are qualitatively similar to the ones that exist in literature, their attractiveness for application to rigid spin clusters (like certain molecular magnets) is due to the absence of any unknown spin-lattice interaction constants. In the past such interaction constants were determined from fitting theoretical formulas to experimental data. In the case of rigid spin clusters, however, theory can be compared with experiment without any fitting parameters, which is rather extraordinary in solid state physics.

Chapter 3

Relaxation of the electron spin in a quantum dot

In a semiconductor quantum dot the relaxation time for the electron spin is determined by its interaction with phonons, nuclear spins, impurities, etc. As in the case of molecular magnets, while impurities and nuclear spins can, in principle, be eliminated, the interaction with phonons cannot. Thus, spin-phonon interactions provide the most fundamental upper bound on the lifetime of electron spin states. The existing methods of computing electron spin-phonon rates in semiconductors rely upon phenomenological models of spin-orbit interaction, see, e.g., Refs. [45, 46, 47, 48, 49, 50, 51, 52, 53, 54]. These models contain unknown constants that must be obtained from experiment. Meantime, as has been noticed more than 50 years ago by Elliot [55] (see also Ref. [56]), the spin-orbit coupling in semiconductors determines the difference of the electron g-factor from the free electron value of $g_0 = 2.0023$. The question then arises whether the effect of the spin-orbit coupling on spin-phonon relaxation can be expressed via the difference between the electron gyromagnetic tensor $g_{\alpha\beta}$ ($\alpha, \beta = x, y, z$) and the vacuum tensor $g_0\delta_{\alpha\beta}$. Since $g_{\alpha\beta}$ can

be measured independently, this would enable one to compare the computed relaxation rates with experiment without any fitting parameters. In this section we show that this, indeed, can be done under certain reasonable simplifying assumptions.

Zeeman interaction of the electron with an external magnetic field, \mathbf{B} , is given by the Hamiltonian

$$\hat{\mathcal{H}}_Z = -\mu_B g_{\alpha\beta} s_{\alpha} B_{\beta}, \quad (3.1)$$

where μ_B is the Bohr magneton and $\mathbf{s} = \sigma/2$ is the dimensionless electron spin with σ_{α} being Pauli matrices. One can choose the axes of the coordinate system along the principal axes of the tensor $g_{\alpha\beta}$. Then $g_{\alpha\beta}$ is diagonal,

$$g_{\alpha\beta} = g_{\alpha} \delta_{\alpha\beta}, \quad (3.2)$$

represented by three numbers, g_x , g_y , and g_z that can be directly measured. Perturbation of Eq. (3.1) by phonons has been studied in the past [47, 48, 50] by writing all terms of the expansion of $g_{\alpha\beta}$ on the strain tensor, $u_{\alpha\beta}$, permitted by symmetry. This gives spin-phonon interaction of the form $A_{\alpha\beta\gamma\delta} u_{\alpha\beta} \sigma_{\gamma} B_{\delta}$ with unknown coefficients $A_{\alpha\beta\gamma\delta}$. To avoid this uncertainty we limit our consideration to local rotations generated by transverse phonons. The argument for doing this is three-fold. Firstly, the rate of the transition accompanied by the emission or absorption of a phonon is inversely proportional to the fifth power of the sound velocity [16]. Since the velocity of the transverse sound is always smaller than the velocity of the longitudinal sound [37], the transverse phonons must dominate the transitions. Secondly, for a dot that is sufficiently rigid to permit only tiny local rotations as a whole under an arbitrary elastic deformation, the emission or absorption of a quantum of the elastic twist will be the only spin-phonon relaxation mode. Finally, we notice that interaction of the electron spin with a local elastic twist generated by a transverse phonon does not

contain any unknown constants. Consequently, it gives parameter-free lower bound on the electron spin relaxation rate.

3.1 Direct processes [57]

The most studied (and often most significant) spin-phonon relaxation mechanisms are the direct processes, in which the spin transition is accompanied by the emission or absorption of a single phonon. To describe such processes only terms up to first order in phonon amplitudes are necessary in the Hamiltonian.

The angle of the local rotation of the crystal lattice in the presence of the deformation, $\mathbf{u}(\mathbf{r})$, is given by [37]

$$\delta\phi = \frac{1}{2}\nabla \times \mathbf{u}, \quad (3.3)$$

and the local angular velocity is $\delta\dot{\phi}$. The analysis of the effect of the rotation on the electron spin can be done in the coordinate frame that is rigidly coupled to the crystal lattice. In that coordinate frame the effect of the rotation is two-fold. Firstly, it results in the opposite rotation of the external magnetic field felt by the spin. The corresponding perturbation of the magnetic field is given by $\delta\mathbf{B} = \mathbf{B} \times \delta\phi$. Secondly, the Hamiltonian in the rotating frame acquires a kinematic term $-\hbar\mathbf{s} \cdot \delta\dot{\phi}$. The spin-phonon interaction in the lattice frame (marked by prime) to first order in phonon amplitudes is then given by

$$\hat{\mathcal{H}}'_{\text{s-ph}} = -\hbar\boldsymbol{\Omega}' \cdot \mathbf{s}, \quad \Omega'_\alpha = \delta\dot{\phi}_\alpha + (\mu_B/\hbar)g_{\alpha\beta} [\mathbf{B} \times \delta\phi]_\beta. \quad (3.4)$$

In these formulas $\delta\phi$ should be understood as an operator (see, in Section 1.2.3, Eq. (1.36)). Summation over repeated indices is implied. The total Hamiltonian in the

lattice frame is, then,

$$\hat{\mathcal{H}}' = \hat{\mathcal{H}}_0 + \hat{\mathcal{H}}'_{\text{s-ph}}, \quad \hat{\mathcal{H}}_0 = \hat{\mathcal{H}}_Z + \hat{\mathcal{H}}_{\text{ph}}, \quad (3.5)$$

where \hat{H}_Z is Zeeman Hamiltonian of Eq. (3.1) unperturbed by phonons and $\hat{\mathcal{H}}_{\text{ph}}$ is Hamiltonian of free phonons.

Spin-phonon transitions occur between the eigenstates of $\hat{\mathcal{H}}_0$. These eigenstates are direct products of the spin and phonon states

$$|\Psi_{\pm}\rangle = |\psi_{\pm}\rangle \otimes |\phi_{\pm}\rangle. \quad (3.6)$$

Here $|\psi_{\pm}\rangle$ are the eigenstates of $\hat{\mathcal{H}}_Z$ with energies E_{\pm} and $|\phi_{\pm}\rangle$ are the eigenstates of $\hat{\mathcal{H}}_{\text{ph}}$ with energies $E_{\text{ph}\pm}$, satisfying

$$E_+ + E_{\text{ph},+} = E_- + E_{\text{ph},-}. \quad (3.7)$$

For $\hat{\mathcal{H}}'_{\text{s-ph}}$ of Eq. (3.4), which is linear in phonon amplitudes, the states $|\phi_{\pm}\rangle$ differ by one emitted or absorbed phonon with a wave vector \mathbf{k} . We will use the following designations

$$|\phi_+\rangle \equiv |n_{\mathbf{k}}\rangle, \quad |\phi_-\rangle \equiv |n_{\mathbf{k}} + 1\rangle. \quad (3.8)$$

We need to compute the matrix element corresponding to the decay of the spin $|\Psi_+\rangle \rightarrow |\Psi_-\rangle$. With the help of Eq. (3.4) we get:

$$\langle \Psi_- | \hat{\mathcal{H}}'_{\text{s-ph}} | \Psi_+ \rangle = \mathbf{K} \cdot \langle \phi_- | \delta\boldsymbol{\phi} | \phi_+ \rangle, \quad (3.9)$$

where components of vector \mathbf{K} are given by

$$K_{\gamma} \equiv -\mu_B (g_{\alpha} - g_{\beta}) B_{\beta} \epsilon_{\alpha\beta\gamma} \langle \psi_- | s_{\alpha} | \psi_+ \rangle, \quad (3.10)$$

and the principal components of the gyromagnetic tensor, g_α , are defined by Eq. (3.2). To obtain Eq. (3.10), we have used the relation

$$\delta\dot{\phi} = \frac{i}{\hbar}[\hat{\mathcal{H}}_{\text{ph}}, \delta\phi], \quad (3.11)$$

to eliminate $\delta\dot{\phi}$ from Eq. (3.4), and the energy conservation, Eq. (3.7). Note that for the isotropic g -factor $K_\gamma = 0$ and thus phonons do not couple to the spin.

As an independent test, one can consider the problem in the laboratory frame. In the presence of the local rotation given by Eq. (3.3), the gyromagnetic tensor in the laboratory frame becomes

$$g_{\alpha\beta}^{(\text{ph})} = \mathbb{R}_{\alpha\alpha'}\mathbb{R}_{\beta\beta'}g_{\alpha'\beta'}, \quad (3.12)$$

where $\mathbb{R}_{\alpha\beta}$ is a 3×3 rotation matrix corresponding to $\delta\phi$. Substituting Eq. (3.12) into Eq. (3.1) and using the orthogonality of the rotation matrix, $\mathbb{R}_{\alpha\beta} = \mathbb{R}_{\beta\alpha}^{-1}$, we get for the Zeeman Hamiltonian in the presence of phonons

$$\hat{\mathcal{H}}_Z^{(\text{ph})} = -\mu_B g_{\alpha'\beta'} (\mathbb{R}_{\alpha'\alpha}^{-1} s_\alpha) (\mathbb{R}_{\beta'\beta}^{-1} B_\beta). \quad (3.13)$$

In the linear order in $\delta\phi$ one has

$$\mathbb{R}_{\alpha\beta} = \delta_{\alpha\beta} - \epsilon_{\alpha\beta\gamma}\delta\phi_\gamma, \quad (3.14)$$

so that the full Hamiltonian in the laboratory frame becomes

$$\hat{H} = \hat{\mathcal{H}}_0 + \hat{\mathcal{H}}_{\text{s-ph}}, \quad \hat{\mathcal{H}}_0 = \hat{\mathcal{H}}_Z + \hat{\mathcal{H}}_{\text{ph}}, \quad (3.15)$$

where

$$\hat{\mathcal{H}}_{\text{s-ph}} = -\hbar\boldsymbol{\Omega} \cdot \mathbf{s}, \quad (3.16)$$

and

$$\boldsymbol{\Omega}_\alpha = (\mu_B/\hbar)(g_\alpha - g_\beta) B_\beta \epsilon_{\alpha\beta\gamma} \delta\phi_\gamma. \quad (3.17)$$

One can see that the spin-phonon matrix element in the laboratory frame, $\langle \Psi_- | \hat{H}_{\text{s-ph}} | \Psi_+ \rangle$, is the same as that in the lattice frame, Eqs. (3.9) and (3.10).

To obtain the relaxation rate one can use the Fermi golden rule. Taking into account the quantization of phonons, Eq.(1.36), the transition matrix element of Eq. (3.9) can be expressed as

$$\langle \Psi_- | \hat{\mathcal{H}}_{\text{s-ph}} | \Psi_+ \rangle = \frac{\hbar}{\sqrt{N}} \sum_{\mathbf{k}\lambda} V_{\mathbf{k}\lambda} \langle n_{\mathbf{k}'} + 1 | a_{\mathbf{k}\lambda} + a_{-\mathbf{k}\lambda}^\dagger | n_{\mathbf{k}'} \rangle, \quad (3.18)$$

where

$$V_{\mathbf{k}\lambda} \equiv \frac{e^{i\mathbf{k}\mathbf{r}}}{\sqrt{8M\hbar\omega_{\mathbf{k}\lambda}}} \mathbf{K} \cdot [\mathbf{k} \times \mathbf{e}_{\mathbf{k}\lambda}]. \quad (3.19)$$

Note that only the transverse phonons contribute to the relaxation process. The decay rate W_{-+} of the upper spin state into the lower state, accompanied by the emission of a phonon, and the rate W_{+-} of the inverse process are given by

$$\begin{pmatrix} W_{-+} \\ W_{+-} \end{pmatrix} = W_0 \begin{pmatrix} n_{\omega_0} + 1 \\ n_{\omega_0} \end{pmatrix}, \quad (3.20)$$

where $n_{\omega_0} = (e^{\hbar\omega_0/(k_B T)} - 1)^{-1}$ is the phonon occupation number at equilibrium,

$$\hbar\omega_0 \equiv E_+ - E_- = \mu_B \left(\sum_{\gamma} g_{\gamma}^2 B_{\gamma}^2 \right)^{1/2} \quad (3.21)$$

is the distance between the two spin levels, and

$$W_0 = \frac{1}{N} \sum_{\mathbf{k}\lambda} |V_{\mathbf{k}\lambda}|^2 2\pi\delta(\omega_{\mathbf{k}\lambda} - \omega_0). \quad (3.22)$$

The balance equation for normalized populations of the upper spin state n_+ and the lower spin state n_- (satisfying $n_+ + n_- = 1$) is

$$\dot{n}_+ = -W_{-+}n_+ + W_{+-}n_- = -\Gamma n_+ + W_{+-} \quad (3.23)$$

where the relaxation rate is given by

$$\Gamma = W_{+-} + W_{-+} = W_0 \coth\left(\frac{\hbar\omega_0}{2k_B T}\right). \quad (3.24)$$

Using Eq. (3.19) and replacing $(1/N)\sum_{\mathbf{k}}\dots$ by $v_0\int d^3k/(2\pi)^3\dots$ in Eq. (3.22), v_0 being unit-cell volume, one obtains

$$W_0 = \frac{1}{12\pi\hbar} \frac{|\mathbf{K}|^2 \omega_0^3}{M v_t^2 \omega_D^3} = \frac{1}{12\pi\hbar} \frac{|\mathbf{K}|^2 \omega_0^3}{\rho v_t^5}. \quad (3.25)$$

Here v_t is the velocity of the transverse sound, ρ is the mass density, $\omega_D \equiv v_t v_0^{1/3}$ is the Debye frequency for the transverse phonons, and $|\mathbf{K}|^2 \equiv \sum K_\gamma^* K_\gamma$. With the help of Eq. (3.10) we get

$$|\mathbf{K}|^2 = \mu_B^2 \sum_{\alpha\beta} (g_\alpha - g_\beta)^2 (B_\beta^2 T_{\alpha\alpha} + B_\beta B_\alpha T_{\alpha\beta}), \quad (3.26)$$

where

$$T_{\alpha\beta} \equiv \frac{1}{2} (\langle \psi_- | s_\alpha | \psi_+ \rangle^* \langle \psi_- | s_\beta | \psi_+ \rangle + \text{c. c.}). \quad (3.27)$$

The eigenstates of \hat{H}_Z are

$$\begin{aligned} |\psi_+\rangle &= -\sin(\theta/2)e^{-i\varphi/2}|+\rangle + \cos(\theta/2)e^{i\varphi/2}|-\rangle \\ |\psi_-\rangle &= \cos(\theta/2)e^{-i\varphi/2}|+\rangle + \sin(\theta/2)e^{i\varphi/2}|-\rangle, \end{aligned} \quad (3.28)$$

where $|+\rangle, |-\rangle$ are the eigenstates of the operator s_z ,

$$s_z |\pm\rangle = \pm \frac{1}{2} |\pm\rangle, \quad (3.29)$$

and the spherical angles θ and φ are defined through

$$\begin{aligned} \mathbf{b} &= g_x B_x \mathbf{e}_x + g_y B_y \mathbf{e}_y + g_z B_z \mathbf{e}_z \\ &= |\mathbf{b}| (\sin\theta \cos\varphi \mathbf{e}_x + \sin\theta \sin\varphi \mathbf{e}_y + \cos\theta \mathbf{e}_z). \end{aligned} \quad (3.30)$$

This gives

$$\begin{aligned}
\langle \psi_- | s_x | \psi_+ \rangle &= \frac{1}{2} (i \sin \varphi + \cos \theta \cos \varphi) \\
\langle \psi_- | s_y | \psi_+ \rangle &= \frac{1}{2} (-i \cos \varphi + \cos \theta \sin \varphi) \\
\langle \psi_- | s_z | \psi_+ \rangle &= -\frac{1}{2} \sin \theta.
\end{aligned} \tag{3.31}$$

Direct calculation then yields

$$T_{\alpha\beta} = \frac{1}{4} \left(\delta_{\alpha\beta} - \frac{g_\alpha B_\alpha g_\beta B_\beta}{\sum_\gamma (g_\gamma B_\gamma)^2} \right). \tag{3.32}$$

Thus one obtains

$$\begin{aligned}
|\mathbf{K}|^2 &= \frac{\mu_B^2}{8} \sum_{\alpha\beta=x,y,z} (g_\alpha - g_\beta)^2 \\
&\quad \times \left[B_\alpha^2 + B_\beta^2 - \frac{(g_\alpha + g_\beta)^2 B_\alpha^2 B_\beta^2}{\sum_\gamma (g_\gamma B_\gamma)^2} \right].
\end{aligned} \tag{3.33}$$

With the help of Eq. (3.21), Eq. (3.24) now can be written in the final form

$$\Gamma = \frac{1}{3\pi\hbar} \frac{(\mu_B B)^5}{M v_t^2 (\hbar\omega_D)^3} F_T(\mathbf{n}) = \frac{\hbar}{3\pi\rho} \left(\frac{\mu_B B}{\hbar v_t} \right)^5 F_T(\mathbf{n}), \tag{3.34}$$

where $\mathbf{n} \equiv \mathbf{B}/B$ and

$$\begin{aligned}
F_T(\mathbf{n}) &= \frac{1}{32} \left(\sum_\gamma g_\gamma^2 n_\gamma^2 \right)^{3/2} \coth \left[\frac{\mu_B B}{2k_B T} \left(\sum_\gamma g_\gamma^2 n_\gamma^2 \right)^{1/2} \right] \\
&\quad \times \sum_{\alpha\beta} (g_\alpha - g_\beta)^2 \left[n_\alpha^2 + n_\beta^2 - \frac{(g_\alpha + g_\beta)^2 n_\alpha^2 n_\beta^2}{\sum_\gamma (g_\gamma n_\gamma)^2} \right].
\end{aligned} \tag{3.35}$$

Here α, β, γ run over x, y, z . It is apparent from Eq. (3.35) that the relaxation mechanism studied in this Letter requires anisotropy of the gyromagnetic tensor.

When the field is directed along the z -axis, Eq. (3.35) simplifies to

$$F_T(\mathbf{e}_z) = \frac{g_z^3}{16} [(g_z - g_x)^2 + (g_z - g_y)^2] \coth \left(\frac{g_z \mu_B B}{2k_B T} \right). \quad (3.36)$$

For the theory to be valid, ω_0 of Eq. (3.21) should not exceed ω_D , otherwise there will be no acoustic phonons responsible for the discussed spin-phonon relaxation mechanism. If g_α are of order unity, this is equivalent to the condition that the factor $(\mu_B B / \hbar v_t)$ in Eq. (3.34), that has dimensionality of the wave vector, is less than the Debye wave vector, $k_D = \omega_D / v_t$, for transverse phonons. This condition is almost always satisfied in the experimentally accessible field range. At $\hbar\omega_0 \gg k_B T$ the coth factor in equations (3.35) and (3.36) tends to one. In this case $\Gamma \propto B^5$ while F_T depends only on the direction of the field with respect to the principal axes of $g_{\alpha\beta}$. In the opposite limit of $k_B T \gg \hbar\omega_0$, the relaxation rate is proportional to $B^4 T$ while its dependence on the direction of the field is given by the factor

$$\sum_{\alpha\beta} (g_\alpha - g_\beta)^2 \left[n_\alpha^2 + n_\beta^2 - \frac{(g_\alpha + g_\beta)^2 n_\alpha^2 n_\beta^2}{\sum_\gamma (g_\gamma n_\gamma)^2} \right]. \quad (3.37)$$

A nice property of the spin relaxation mechanism studied above is its universal dependence on the strength and the direction of the magnetic field. Due to B^5 in Eq. (3.34) this mechanism can dominate electron spin relaxation at high fields. For, e.g., $\rho \sim 5 \text{ g/cm}^3$ and $v_t \sim 2 \times 10^5 \text{ cm/s}$, it gives $\Gamma \sim 3 \times 10^4 \text{ s}^{-1} F_T(\mathbf{n})$. The dependence of the rate on the direction of the field, $F_T(\mathbf{n})$, is entirely determined by the difference between principal values of the tensor $g_{\alpha\beta}$. Highly anisotropic $g_{\alpha\beta}$ has been theoretically predicted in two-dimensional systems [58] and experimentally detected in GaAs quantum wells [59]. In the mK temperature range, the spin relaxation times of order $100 \mu\text{s}$ have been observed [60] in GaAs electron quantum dots in the field of order 10T. Note that equations (3.34)-(3.37) allow a detailed comparison between theory

and experiment for the proposed mechanism of relaxation, which, thus, can be easily confirmed or ruled out for a particular quantum dot.

In conclusion, we have studied electron spin relaxation in quantum dots due to local rotations generated by transverse phonons. This is unavoidable relaxation channel that occurs when the electron gyromagnetic tensor, $g_{\alpha\beta}$, is anisotropic. It can dominate spin relaxation at high magnetic fields. The advantage of our theory is that it expresses the effect of unknown spin-orbit interactions on electron spin relaxation in terms of the tensor $g_{\alpha\beta}$ alone. The corresponding relaxation rate has universal dependence on the strength and direction of the field with respect to the principal axes of $g_{\alpha\beta}$. The important feature of the proposed mechanism is that it does not involve any unknown constants of the quantum dot and is entirely determined by the three principal values of $g_{\alpha\beta}$, which can be independently measured. This allows simple experimental test of the proposed theory.

3.2 Raman Processes [61]

Spin-lattice relaxation by Raman scattering is a two phonon mechanism consisting of a spin transition accompanied by the absorption of a phonon and the emission of another phonon of different frequency. In spite of being a second order process, its contribution can be important, since the phase space of the phonons triggering the transition is not limited to the distance between the levels as in the direct case. To describe such processes, we need to consider terms up to second order in phonon amplitudes in the Hamiltonian.

The gyromagnetic tensor $g_{\alpha\beta}$ is determined by the local environment of the quantum dot. In the presence of long wave deformations of the lattice, the whole environment is rotated so that the Zeeman Hamiltonian in the laboratory frame becomes (see Section 3.1),

$$\hat{\mathcal{H}}_Z^{(ph)} = -\mu_B g_{\alpha'\beta'} (\mathbb{R}_{\alpha'\alpha}^{-1} S_\alpha) (\mathbb{R}_{\beta'\beta}^{-1} H_\beta) . \quad (3.38)$$

In order to describe Raman processes we expand the 3×3 rotation matrix to second order in $\delta\phi$

$$\mathbb{R}_{\alpha\beta} = \delta_{\alpha\beta} - \epsilon_{\alpha\beta\gamma} \delta\phi_\gamma + \frac{1}{2} [\delta\phi_\alpha \delta\phi_\beta - \delta_{\alpha\beta} (\delta\phi)^2] . \quad (3.39)$$

The total Hamiltonian is then given by

$$\hat{\mathcal{H}} = \hat{\mathcal{H}}_0 + \hat{\mathcal{H}}_{s-ph} , \quad \hat{\mathcal{H}}_{s-ph} = \hat{\mathcal{H}}_{s-ph}^{(1)} + \hat{\mathcal{H}}_{s-ph}^{(2)} , \quad (3.40)$$

where $\hat{\mathcal{H}}_0$ is the Hamiltonian of non-interacting spins and phonons, Eq. (3.5), $\hat{\mathcal{H}}_{s-ph}^{(1)}$ is given by Eq. (3.16) and

$$\hat{\mathcal{H}}_{s-ph}^{(2)} = -\frac{1}{2} \mu_B (g_\alpha + g_\beta) S_\alpha H_\beta \delta\phi_\alpha \delta\phi_\beta - \mu_B g_\alpha (\mathbf{S} \times \delta\phi)_\alpha (\mathbf{H} \times \delta\phi)_\alpha . \quad (3.41)$$

Again, we will study the spin-phonon transitions between the eigenstates of $\hat{\mathcal{H}}_0$, $|\Psi_\pm\rangle = |\psi_\pm\rangle \otimes |\phi_\pm\rangle$. Here, again, $|\psi_\pm\rangle$ are the eigenstates of $\hat{\mathcal{H}}_Z$ with energies E_\pm and $|\phi_\pm\rangle$ the eigenstates of $\hat{\mathcal{H}}_{ph}$ with energies $E_{ph\pm}$. We consider Raman processes, in which a phonon with wave vector \mathbf{k} is absorbed and a phonon with a wave vector \mathbf{q} is emitted. We will use the following designations for the phonon states

$$|\phi_+\rangle \equiv |n_{\mathbf{k}}, n_{\mathbf{q}}\rangle, \quad |\phi_-\rangle \equiv |n_{\mathbf{k}} - 1, n_{\mathbf{q}} + 1\rangle . \quad (3.42)$$

To obtain the relaxation rate of the transition $|\Psi_+\rangle \rightarrow |\Psi_-\rangle$ one needs to evaluate the matrix element of the process, which is the sum of the matrix element with $\hat{\mathcal{H}}_{s-ph}^{(2)}$

and that with $\hat{\mathcal{H}}_{s-ph}^{(1)}$ in the second order: $M_R = M_R^{(2)} + M_R^{(1+1)}$, where

$$M_R^{(2)} = \langle \Psi_- | \hat{\mathcal{H}}_{s-ph}^{(2)} | \Psi_+ \rangle \quad (3.43)$$

and

$$\begin{aligned} M_R^{(1+1)} &= \sum_{\xi=\pm} \frac{\langle \Psi_- | \hat{\mathcal{H}}_{s-ph}^{(1)} | \Psi_\xi \rangle \langle \Psi_\xi | \hat{\mathcal{H}}_{s-ph}^{(1)} | \Psi_+ \rangle}{E_+ + \hbar\omega_{\mathbf{k}} - E_\xi} \\ &+ \sum_{\xi=\pm} \frac{\langle \Psi_- | \hat{\mathcal{H}}_{s-ph}^{(1)} | \Psi_\xi \rangle \langle \Psi_\xi | \hat{\mathcal{H}}_{s-ph}^{(1)} | \Psi_+ \rangle}{E_+ - E_\xi - \hbar\omega_{\mathbf{q}}}. \end{aligned} \quad (3.44)$$

The intermediate phonon states are $|n_{\mathbf{k}} - 1, n_{\mathbf{q}}\rangle$ in the first term and $|n_{\mathbf{k}}, n_{\mathbf{q}} + 1\rangle$ in the second term.

Raman processes may dominate over direct processes for a small energy difference between the spin states, $\hbar\omega_0 \ll k_B T$. Thus we will consider terms to the lowest order in H . For simplicity we will study the case where the field is directed along the z -axis. Then the matrix element becomes,

$$M_R = M_R^{(2)} = \frac{\mu_B H}{4} [(2g_y - g_x - g_z) \tilde{M}_{ph-R}^{xz} - i(2g_x - g_y - g_z) \tilde{M}_{ph-R}^{yz}], \quad (3.45)$$

where $\tilde{M}_{ph-R}^{\alpha\beta} = M_{ph-R}^{\alpha\beta} + M_{ph-R}^{\beta\alpha}$ with

$$\begin{aligned} M_{ph-R}^{\alpha\beta} &= \langle n_{\mathbf{q}} + 1 | \delta\phi_\alpha | n_{\mathbf{q}} \rangle \langle n_{\mathbf{k}} - 1 | \delta\phi_\beta | n_{\mathbf{k}} \rangle \\ &= \frac{\hbar^2}{8\rho V} \frac{[\mathbf{k} \times \mathbf{e}_{\mathbf{k}\lambda_{\mathbf{k}}}]_\alpha [\mathbf{q} \times \mathbf{e}_{\mathbf{q}\lambda_{\mathbf{q}}}]_\beta}{\sqrt{\hbar\omega_{\mathbf{k}\lambda_{\mathbf{k}}} \hbar\omega_{\mathbf{q}\lambda_{\mathbf{q}}}}} \sqrt{(n_{\mathbf{q}} + 1) n_{\mathbf{k}}} \end{aligned} \quad (3.46)$$

The Raman rate of the transition $|\Psi_+\rangle \rightarrow |\Psi_-\rangle$ can be obtained by using the Fermi golden rule,

$$\Gamma_R = [(2g_y - g_x - g_z)^2 + (2g_x - g_y - g_z)^2] \frac{\pi^3}{3024} \frac{k_B T}{\hbar} \left(\frac{\mu_B H}{E_t} \right)^2 \left(\frac{k_B T}{E_t} \right)^6. \quad (3.47)$$

The ratio of Raman and direct rates is of order $\Gamma_R/\Gamma_D \sim 10^{-2}(k_B T/\mu_B H)^2(k_B T/E_t)^4$. Consequently, Raman processes dominate over direct processes at high temperature and low field.

Chapter 4

Interaction of spins with ultrasound

4.1 Rabi oscillations from ultrasound in spin systems [62]

Let us consider an ensemble of spin clusters (e.g., a molecular magnets) non-interacting with each other whose magnetic cores are more rigid than their elastic environment. Then, as it has been shown in Section 1.2.3, the main effect of the distortions of the lattice on the spin is produced by the rigid rotation of the cluster. In the frame rigidly coupled to the magnetic cluster, the effect of such rotations is equivalent to the application of a magnetic field $\mathbf{B} = \boldsymbol{\Omega}/\gamma$, being γ the gyromagnetic ratio, $\mathcal{H}_{s-ph}^{(lat)} = -\hbar\mathbf{S}\cdot\boldsymbol{\Omega}$. This term can produce non-trivial dynamical effects. Consider, e.g., a spin cluster with the Hamiltonian $\hat{\mathcal{H}} = -D\hat{S}_z^2$ that preserves the direction of the spin along the anisotropy axis Z due to commutation of $\hat{\mathcal{H}}$ with \hat{S}_z . In the presence of the rotation about, e.g., the X-axis of the crystal the Hamiltonian in the rotating frame becomes $\hat{\mathcal{H}}' = -D\hat{S}_z^2 - \hbar\hat{S}_x\Omega$. This Hamiltonian, unlike $\hat{\mathcal{H}}$, does not commute with \hat{S}_z and, therefore, allows transitions between the two orientations of \mathbf{S} along the anisotropy axis. Thus, rotation alone can induce quantum transitions between spin states that

are prohibited by the Hamiltonian of a stationary system $\hat{\mathcal{H}}$. We should emphasize that switching from the laboratory-frame Hamiltonian, $\hat{\mathcal{H}}$, to the rotating-frame Hamiltonian, $\hat{\mathcal{H}}' = \hat{\mathcal{H}} - \hbar\hat{\mathbf{S}} \cdot \boldsymbol{\Omega}$, does not introduce any new spin-lattice interactions in addition to the crystal field. It is just another method to obtain solution of the problem, which, in the laboratory frame, requires introduction of the time dependence of the crystal field: e.g., $\hat{\mathcal{H}} = -D\hat{S}_z^2$, in the presence of rotation, becomes $\hat{\mathcal{H}} = -D[\mathbf{n}(t) \cdot \hat{\mathbf{S}}]^2$ with $\mathbf{n}(t)$ being the instantaneous direction of the anisotropy axis.

So far, quantum spin-rotation effects received little attention because only a very tiny magnetic field due to rotation can be produced in the rotating frame of a macroscopic body. Consequently, the corresponding quantum effects have very low probability. However, *local* rotations of the crystal lattice produced by high-frequency ultrasound can easily provide 10 G - 100 G fields in the rotating frame of a rigid spin cluster in a solid. Indeed, in the presence of the phonon displacement field, $\mathbf{u}(\mathbf{r}, t)$, the angular velocity of the local rotation that it produces, $\boldsymbol{\Omega}(\mathbf{r}, t)$, is given by

$$\boldsymbol{\Omega}(\mathbf{r}, t) = \frac{1}{2}\nabla \times \dot{\mathbf{u}}(\mathbf{r}, t). \quad (4.1)$$

For a transverse sound wave of frequency $f \sim 3$ GHz and amplitude $u_0 \sim 1$ nm, this gives $B = \Omega/\gamma \sim 10$ G in the rotating frame coupled to the local crystallographic axes. Even greater local fields can be achieved with surface acoustic waves that have been recently used in experiments on molecular magnets [63, 64].

The equivalence of the effect of high-frequency transverse acoustic waves to the effect of high-amplitude ac magnetic field on paramagnetic spins immediately suggests that one can try to generate Rabi spin oscillations with the help of high-frequency ultrasound. Rabi effect [65] corresponds to the oscillation of the occupation numbers of two quantum levels in the presence of an ac field which frequency is close to

the distance between the levels. At resonance, the frequency of Rabi oscillations is proportional to the amplitude of the ac field. The effort to observe Rabi oscillations between quantum states of molecular magnets in experiments employing ac magnetic fields [66, 67, 68, 69] has been going for some time. For such experiments to succeed, the Rabi frequency must be greater than the spin decoherence rate. This typically requires the amplitude of the ac field to be greater than 1 G, which is not easy to achieve with electromagnetic waves but, as we have seen, is possible with surface acoustic waves. Note that the condition of the validity of the elastic theory, $u_0 \ll \lambda$ (where λ is the phonon wavelength) automatically provides the condition $\Omega \ll \omega = 2\pi f$, which allows one to treat local rotations classically while treating the two-level system with level separation $\hbar\omega$ quantum-mechanically.

4.1.1 Hamiltonian

For certainty we consider a crystal of molecular magnets with the anisotropy Hamiltonian

$$\hat{\mathcal{H}}_A = -D\hat{S}_z^2 + \hat{V}, \quad (4.2)$$

where \hat{V} is a small term responsible for the tunnel splitting, Δ , of spin-up and spin-down states. The spin cluster is assumed to be more rigid than its elastic environment, so that the long-wave crystal deformations can only rotate it as a whole but cannot change its inner structure responsible for the parameters of the Hamiltonian $\hat{\mathcal{H}}_A$. This approximation should apply to many molecular magnets as they typically have a compact magnetic core inside a large unit cell of the crystal. We choose geometry in which surface acoustic waves are running along the X -axis with the solid extending towards $y > 0$, see Fig. 4.1. Using standard formulas [37] for the displacement field

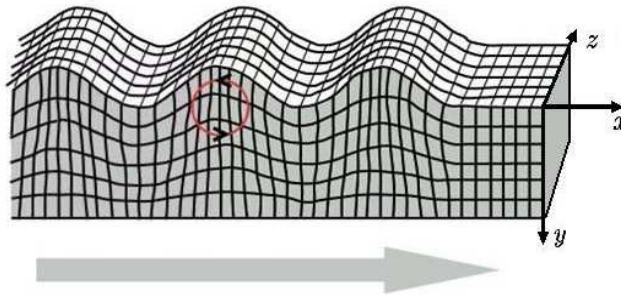


Figure 4.1: Geometry of the problem.

in a surface acoustic wave, \mathbf{u}_{SAW} , one obtains for the angle of rigid rotations

$$\delta\phi(\mathbf{r}) = \frac{1}{2}\nabla \times \mathbf{u}_{SAW} = \frac{1}{2}\frac{\omega}{c_t}u_0 e^{-k_t y} \cos(kx - \omega t) \mathbf{e}_z \equiv \delta\phi(x, t) \mathbf{e}_z, \quad (4.3)$$

where $\omega = c_t k \xi$, $k_t \equiv k\sqrt{1 - \xi^2}$, ξ is a real number between 0 and 1 satisfying

$$\xi^6 - 8\xi^4 + 8\xi^3 \left(3 - 2\frac{c_t^2}{c_l^2}\right) - 16 \left(1 - \frac{c_t^2}{c_l^2}\right) = 0, \quad (4.4)$$

and $c_{t,l}$ are velocities of transverse and longitudinal sound.

In the presence of deformations of the crystal lattice, $\mathbf{u}(\mathbf{r}, t)$, the spin Hamiltonian in the laboratory frame becomes (see Section 1.2.3)

$$\hat{\mathcal{H}} = e^{-i\hat{\mathbf{S}}\cdot\delta\phi} \hat{\mathcal{H}}_A e^{i\hat{\mathbf{S}}\cdot\delta\phi}. \quad (4.5)$$

In order to find the laboratory-frame wave function $|\Psi\rangle$, it is useful to introduce the *lattice-frame* wave function $|\Psi^{(lat)}\rangle$, defined through the unitary transformation

$$|\Psi^{(lat)}\rangle = e^{i\delta\phi\cdot\hat{\mathbf{S}}} |\Psi\rangle. \quad (4.6)$$

Differentiating it on time it is easy to see that this function satisfies Schrödinger equation with the lattice-frame Hamiltonian

$$\hat{\mathcal{H}}^{(lat)} = \hat{\mathcal{H}}_A - \hbar\hat{\mathbf{S}} \cdot \boldsymbol{\Omega} \quad (4.7)$$

where

$$\boldsymbol{\Omega} = \frac{\partial \delta \phi}{\partial t} = \frac{1}{2} \frac{\omega^2}{c_t} u_0 e^{-k_t y} \sin(kx - \omega t) \mathbf{e}_z. \quad (4.8)$$

To this point we have not made any assumptions about the magnitude of $\delta \phi$, so that the equations (4.5) and (4.7) are exact. An interesting observation for the comparison of the effects of ultrasound and ac magnetic field is that the Hamiltonian (4.7) resembles the Hamiltonian of a particle of spin $\hat{\mathbf{S}}$ in the ac magnetic field which amplitude scales as the square of the frequency.

4.1.2 Rabi oscillations

We are interested in the Rabi oscillations between the two lowest states of $\hat{\mathcal{H}}_A$:

$$|\phi_{\pm}\rangle = \frac{1}{\sqrt{2}}(|S\rangle \pm |-S\rangle), \quad (4.9)$$

where $|\pm S\rangle$ satisfy $\hat{S}_z |\pm S\rangle = \pm S |\pm S\rangle$. It makes sense, therefore, to project our Hamiltonian on the $|\pm S\rangle$ states, making the problem essentially a two-state problem.

This gives

$$\hat{h}_{eff}^{(lat)} = -\frac{\Delta}{2} \hat{\sigma}_1 - \hbar \omega_R \sin(kx - \omega t) \hat{\sigma}_3, \quad (4.10)$$

where Δ is the energy distance between the ground state $|\phi_+\rangle$ and the first excited state $|\phi_-\rangle$, $\hat{\sigma}_1 \equiv |S\rangle\langle -S| + |-S\rangle\langle S|$, $\hat{\sigma}_3 \equiv |S\rangle\langle S| - |-S\rangle\langle -S|$, and

$$\omega_R = \frac{1}{2c_t} \omega^2 u_0 S e^{-k_t y}. \quad (4.11)$$

The two-state approach will be valid if Δ and $\hbar \omega$ are small in comparison with the distances to other spin levels. Note that the tunnel splitting Δ originates from the term \hat{V} in $\hat{\mathcal{H}}_A$ that does not commute with \hat{S}_z .

It is easy to check that at $\omega \sim \Delta/\hbar$, which is our case of interest for consideration of Rabi oscillations, the second term in Eq. (4.10) can be treated as a perturbation

as long as the wavelength of the acoustic wave satisfies $\lambda \gg Su_0$. For a not very large S this condition is always fulfilled by surface acoustic waves. The unperturbed eigenstates of the problem are then the eigenstates of σ_1 given by Eq. (4.9). Their energies are $\pm\Delta/2$. The time-dependent perturbation produces transitions between these states, resulting in the Rabi oscillations when $\hbar\omega \simeq \Delta$. The standard way to obtain the evolution of the wave function is to apply the *rotating wave approximation* [65]. Note that the coordinates x and y in Eq. (4.10) can be viewed as parameters. Expressing the wave function as

$$|\Psi(t)^{(lat)}\rangle = C_+(t)|\phi_+\rangle + C_-(t)|\phi_-\rangle, \quad (4.12)$$

and starting with $C_-(0) = 0$, $C_+(0) = 1$ at $t = 0, x = 0$, one obtains

$$\begin{aligned} C_-(t) &= \frac{\omega_R}{\Omega_R} e^{-\frac{i}{2}\omega t} \sin\left(\frac{\Omega_R t}{2}\right) \\ C_+(t) &= \left[\cos\left(\frac{\Omega_R t}{2}\right) + i \frac{\Delta/\hbar - \omega}{\Omega_R} \sin\left(\frac{\Omega_R t}{2}\right) \right] e^{\frac{i}{2}\omega t}, \end{aligned} \quad (4.13)$$

where

$$\Omega_R = \sqrt{(\Delta/\hbar - \omega)^2 + \omega_R^2}. \quad (4.14)$$

Assuming that every spin was in the ground state $|\phi_+\rangle$ before the sound wave arrived, the spatial dependence of the wave function can be obtained by making a replacement $t \rightarrow t - kx/\omega$ in Eq. (4.13). In the absence of spatial derivatives in the Hamiltonian (4.10), $|\Psi(t)^{(lat)}\rangle$ is defined up to the phase factor $\exp[i\theta(x, y)]$ with θ being an arbitrary real function of coordinates. From Eq. (4.6) the wave function of the system in the laboratory frame is $|\Psi\rangle = e^{-i\delta\phi\cdot\mathbf{S}}|\Psi^{(lat)}\rangle$. Because of the smallness of $\delta\phi$, the dynamics of $|\Psi\rangle$ essentially coincides with the dynamics of $|\Psi^{(lat)}\rangle$ and is given by Rabi oscillations between the states $|\phi_\pm\rangle$ at the frequency Ω_R . This is confirmed by

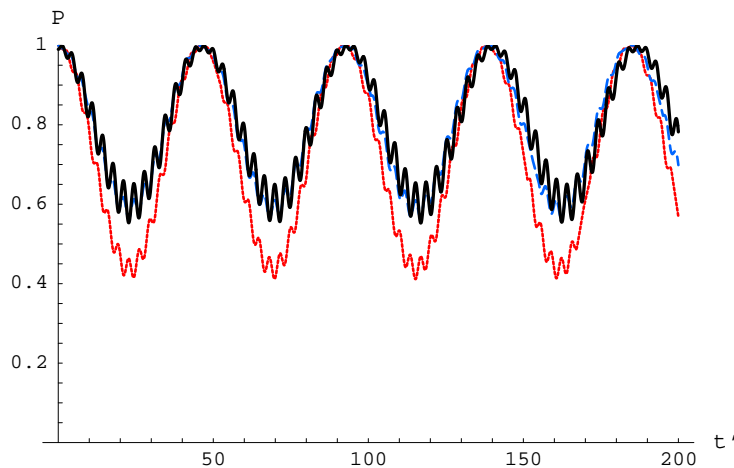


Figure 4.2: Time dependence ($t' \equiv t\Delta/\hbar$) of the probability to find the spin in the state $|\phi_+\rangle$ at $x = 0$, $S = 10$, $\omega_R = 0.1\omega$, and $\omega = 0.9(\Delta/\hbar)$. Dotted line (red): Numerical result for the laboratory-frame Hamiltonian (4.18). Dash line (blue): Numerical result for the lattice-frame Hamiltonian (4.10). Solid line (black): Analytical result given by Eq. (4.13).

numerical calculations with the lattice-frame and laboratory-frame Hamiltonians, see Fig. 4.2.

The expectation value of the projection of the spin onto the anisotropy axis (the Z-axis) is given by

$$\begin{aligned} \langle \Psi(t) | \hat{S}_z | \Psi(t) \rangle &= 2S \frac{\omega_R}{\Omega_R^2} \times \\ &\left\{ \left(\omega - \frac{\Delta}{\hbar} \right) \sin(\omega t - kx) \sin^2 \left[\frac{1}{2} (\Omega_R t - K_R x) \right] \right. \\ &\left. + \frac{1}{2} \Omega_R \cos(\omega t - kx) \sin(\Omega_R t - K_R x) \right\}, \end{aligned} \quad (4.15)$$

where $K_R = (\Omega_R/\omega)k \ll k$ can be called the ‘‘Rabi’’ wave vector. Thus, the space-time Rabi oscillations of the occupation numbers of spin states generate space-time oscillations of the magnetization of the crystal. On resonance, when $\omega = \Delta/\hbar$, Eq. (4.15) simplifies to

$$\langle \Psi(t) | \hat{S}_z | \Psi(t) \rangle = S \cos(kx - \omega t) \sin(\omega_R t - k_R x), \quad (4.16)$$

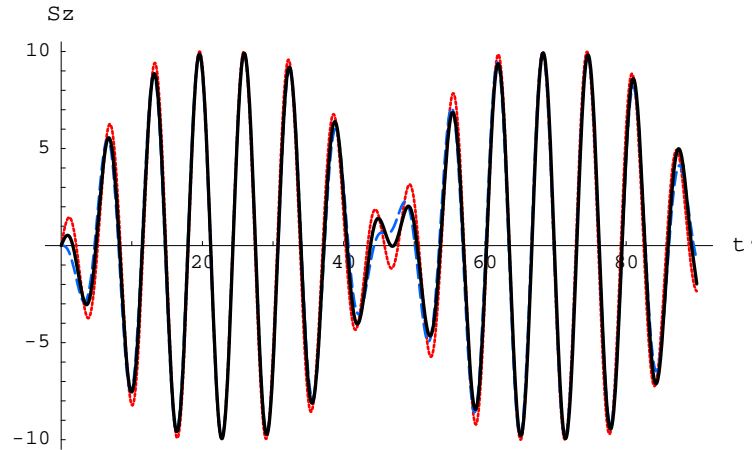


Figure 4.3: Time dependence ($t' \equiv t\Delta/\hbar$) of the expectation value of the projection of the spin on the anisotropy axis at $x = 0$, $S = 10$, $\omega_R = 0.1\omega$ and $\omega = 0.9(\Delta/\hbar)$. Dotted line (red): Numerical result for the laboratory-frame Hamiltonian (4.18). Dash line (blue): Numerical result for the lattice-frame Hamiltonian (4.10). Solid line (black): Analytical result given by Eq. (4.15).

with $k_R = (\omega_R/\omega)k \ll k$. The condition $\omega_R \ll \omega$ ($Su_0 \ll \lambda$) implies that the time dependence of $\langle \hat{S}_z \rangle$ at any point in space consists of the oscillations at frequency ω with beats of frequency ω_R . Similarly, $\langle \hat{S}_z \rangle$ at any moment of time oscillates in space with the wave vector k and exhibits beats with the wave vector $k_R \ll k$.

Our conclusions can be checked by obtaining the full solution of the problem in the laboratory frame in a particular case of a biaxial symmetry, when \hat{V} in Eq. (4.2) equals $E(\hat{S}_x^2 - \hat{S}_y^2)$. In this case Eq. (4.5) reduces to

$$\hat{\mathcal{H}} = -D\hat{S}_z^2 + \frac{E}{2} \left\{ \hat{S}_+^2 e^{-2i\delta\phi(x,t)} + \hat{S}_-^2 e^{2i\delta\phi(x,t)} \right\}, \quad (4.17)$$

where $\hat{S}_\pm = \hat{S}_x \pm i\hat{S}_y$. The second term can be treated as a perturbation provided that $E \ll D$. At $\omega \ll (2S + 1)D/\hbar$ the dynamics of the wave function involves only a superposition of the $|\pm S\rangle$ states. As in the lattice-frame consideration, it is then convenient to project the Hamiltonian (4.17) onto these two states. In order to obtain such an effective two-state Hamiltonian that accounts for the tunnel splitting of the

lowest energy states, one must apply perturbation theory for the degenerate states $|\pm S\rangle$ to the S -th order [43]. This results in

$$\hat{h}_{eff} = -\frac{\Delta}{2} \{e^{2iS\delta\phi(x,t)}|S\rangle\langle -S| + e^{-2iS\delta\phi(x,t)}|-S\rangle\langle S|\}. \quad (4.18)$$

Here $\Delta = 8D(2S)![(S-1)!]^{-2}(E/8D)^S$ is the tunnel-splitting for the biaxial model in the absence of lattice distortions [42]. Numerical solution for $\langle\hat{S}_z\rangle$ that follows from Eq. (4.18), and its comparison with the analytical solution given by Eq. (4.15), are illustrated in Fig. 4.3. The beats discussed above are clearly seen in the figure.

4.1.3 Discussion

We shall now discuss conditions under which the above effects can be observed. The first condition is that the rate of decoherence of the spin states is lower than the frequencies involved. The lowest of these frequencies is $\omega_R = 2\pi^2 f^2 u_0 S / c_t$, where f , u_0 , and c_t are the frequency, the amplitude, and the velocity of the sound. For, e.g., $f = 3$ GHz, $u_0 = 1$ nm, $S = 10$, and $c_t = 10^3$ m/s, one obtains $\omega_R \sim 2$ GHz $\ll \omega = 2\pi f \sim 20$ GHz. If such a high value of ω_R were to be produced by an electromagnetic wave, it would require the ac magnetic field of amplitude 10 G, which is not easy to achieve in experiment. Note, however, that the Rabi oscillations of $\langle\hat{S}_z\rangle$ generated in a crystal of molecular magnets by ultrasound, contrary to the Rabi oscillations generated in a small crystal by an electromagnetic wave, will have a pronounced wave dependence on coordinates so that $\langle\hat{S}_z\rangle$ averaged over the wavelength of the sound, λ , will be zero. Consequently, measurements of the oscillations of $\langle\hat{S}_z\rangle$ should be done on the scale that is small compared to λ .

Another restriction comes from the inevitable presence of the dc magnetic fields that generate the Zeeman energy bias for the $|\pm S\rangle$ states. Such fields can be of dipolar

origin or they can be any stray fields in the system. They are not likely to affect our results qualitatively if the Zeeman energy bias is small compared to $\hbar\omega \sim \Delta$. Note that the tunnel splitting, Δ , can be controlled by a transverse magnetic field. Thus, the above condition translates into $B_l \leq 2\pi f/(\gamma S)$ for the longitudinal field B_l . For $f \sim 3$ GHz one then needs $B_l \leq 100$ G. In the case of a greater bias field (and/or higher decoherence), higher frequencies of the acoustic waves will be required. In principle, surface acoustic waves of frequency as high as 100 GHz have been generated in experiment [70]. However, since $\omega_R \propto \omega^2$, raising ω significantly may eventually violate the condition $\omega_R \ll \omega$ under which our results were derived.

In Conclusion, we have shown that transversal acoustic waves in the GHz range provide spin-rotation coupling that can be used to generate space-time Rabi oscillations in molecular magnets. When frequency of ultrasound, ω , equals the distance between tunnel-split spin states, the magnetization on the surface of the crystal oscillates as $\langle \hat{S}_z \rangle = S \cos(kx - \omega t) \sin[\omega_R t - k_R x]$, where $\omega_R = \omega^2 u_0 S / (2c_t)$ and $k_R = (\omega_R / \omega) k$, with u_0 and c_t being the amplitude and the speed of the sound respectively.

4.2 Magneto-elastic waves in crystals of magnetic molecules [72]

Hybridization of electron paramagnetic resonance (EPR) with longitudinal ultrasonic waves has been studied by Jacobsen and Stevens [73] within a phenomenological model of magneto-elastic interaction proportional to the magnetic field. General theory of magneto-elastic effects on the phonon dispersion and the sound velocity in conventional paramagnets has been developed by Dohm and Fulde [23]. The advantage of molecular magnets is that they, unlike conventional paramagnets, can be prepared in

a variety of magnetic states even in the absence of the magnetic field. Spontaneous transitions between spin levels in molecular magnets are normally due to the emission and absorption of phonons. Interactions of molecular spins with phonons have been studied in the context of magnetic relaxation [74, 75, 76, 77], conservation of angular momentum [33, 34, 36], phonon Raman processes [41], and phonon superradiance [35]. Parametric excitation of acoustic modes in molecular magnets has been studied [78, 79]. It has been suggested that surface acoustic waves can produce Rabi oscillations of magnetization in crystals of molecular magnets (see Section 4.1). In this Section we study coupled dynamics of paramagnetic spins and elastic deformations at a macroscopic level.

When considering magneto-elastic waves in paramagnets the natural question is why the adjacent spins should rotate in unison rather than behave independently. In ferromagnets the local alignment of spins is due to the strong exchange interaction. Due to this interaction the length of the local magnetization is a constant throughout the ferromagnet. We shall argue now that a somewhat similar quantum effect exists in a system of weakly interacting two-level entities described by a fictitious spin 1/2. Indeed, since any product of Pauli matrices reduces to a single Pauli matrix σ_α , interaction of N independent two-state systems with an arbitrary field $\mathbf{A}(\mathbf{r})$ should be linear on σ_α ,

$$\mathcal{H} = \sum_{n=1}^N g_{\alpha\beta} \sigma_\alpha^{(n)} A_\beta(\mathbf{r}_n) , \quad (4.19)$$

where $\sigma^{(n)}$ describes a two-state system located at a point $\mathbf{r} = \mathbf{r}_n$. If \mathbf{A} was independent of coordinates, then the Hamiltonian (4.19) would reduce to

$$\mathcal{H} = g_{\alpha\beta} \Sigma_\alpha A_\beta , \quad (4.20)$$

where

$$\Sigma = \sum_{n=1}^N \sigma^{(n)} \quad (4.21)$$

is the total fictitious spin of the system. In this case the interaction Hamiltonian would commute with Σ^2 , thus preserving the length of the total fictitious “magnetization”. This observation is crucial for understanding Dicke superradiance [39]: A system of independent two-state entities behaves collectively in a field whose wavelength significantly exceeds the size of the system. When the wavelength of the field is small compared to the size of the system but large compared to the distance between the two-state entities, the same argument can be made about the rigidity of $\Sigma = \sum \sigma^{(n)}$ summed up over the distances that are small compared to the wavelength. Consequently, the system that has been initially prepared in a state with all spins up, and then is allowed to evolve through interaction with a long-wave Bose field, should conserve the length of the local “magnetization” in the same way as ferromagnets do.

The relevance of the above argument to the dynamics of magnetic molecules interacting with elastic deformations becomes obvious when only two spin levels are important. This is the case when the low-energy dynamics of the molecular magnet is dominated by, e.g., tunnel split spin-levels or when the magneto-acoustic wave is generated by a pulse of sound of resonant frequency. Recently, experiments with surface acoustic waves in the GHz range have been performed in crystals of molecular magnets [63]. The existing techniques, in principle, allow generation of acoustic frequencies up to 100 GHz [70]. This opens the possibility of resonant interaction of generated ultrasound with spin excitations. Here we study coupled magneto-elastic waves in the ground state of a crystal of molecular magnets. We derive equations

describing macroscopic dynamics of sound and magnetization and show that high-frequency ultrasound interacts strongly with molecular spins when the frequency of the sound equals the distance between spin levels. We obtain the dispersion relation for magneto-elastic waves and show that non-linear equations of motion also possess solutions describing solitary waves of magnetization coupled to the elastic twists.

The model of spin-phonon coupling is discussed in Section 4.2.1 where coupled magneto-elastic equation are derived. Linear magneto-elastic waves are studied in Section 4.2.2 where we obtain dispersion laws for bulk and surface acoustic waves. Non-linear solitary waves are studied in Section 4.2.3. Suggestions for experiments are made in Section 4.2.4.

4.2.1 Model of magneto-elastic coupling

We consider a molecular magnet interacting with a local crystal field described by a phenomenological anisotropy Hamiltonian $\hat{\mathcal{H}}_A$. The spin cluster is assumed to be more rigid than its elastic environment, so that the long-wave crystal deformations can only rotate it as a whole but cannot change its inner structure responsible for the parameters of the Hamiltonian $\hat{\mathcal{H}}_A$. This approximation should apply to many molecular magnets as they typically have a compact magnetic core inside a large unit cell of the crystal. For these systems, the Hamiltonian in the presence of deformations $\mathbf{u}(\mathbf{r})$ of the crystal lattice is (see Section 1.2.3)

$$\hat{\mathcal{H}} \simeq \hat{\mathcal{H}}_0 + \hat{\mathcal{H}}_{s-ph}, \quad (4.22)$$

where $\hat{\mathcal{H}}_0$ is the Hamiltonian of non-interacting spins and phonons

$$\hat{\mathcal{H}}_0 = \hat{\mathcal{H}}_S + \hat{\mathcal{H}}_{ph}, \quad \hat{\mathcal{H}}_S = \hat{\mathcal{H}}_A + \hat{\mathcal{H}}_Z, \quad (4.23)$$

and $\hat{\mathcal{H}}_{s-ph}$ is the spin-phonon interaction term, given by

$$\hat{\mathcal{H}}_{s-ph} = i \left[\hat{\mathcal{H}}_A, \hat{\mathbf{S}} \right] \cdot \delta\boldsymbol{\phi}. \quad (4.24)$$

Coupling of spins to the elastic twists

For certainty, we consider a crystal of molecular magnets with the anisotropy Hamiltonian

$$\hat{\mathcal{H}}_A = -D\hat{S}_z^2 + \hat{V}, \quad (4.25)$$

where \hat{V} is a small term that does not commute with the \hat{S}_z operator. This term is responsible for the tunnel splitting, Δ , of the levels on resonance.

At low temperature and small magnetic field, $k_B T, g\mu_B B \lesssim \Delta$, when the frequency of the displacement field $\mathbf{u}(\mathbf{r})$ satisfies $\omega \ll 2DS/\hbar$, only the two lowest states of $\hat{\mathcal{H}}_A$ are involved in the evolution of the system. Thus, one can reduce the spin-Hamiltonian of the molecular magnet to an effective two-state Hamiltonian in terms of pseudospin-1/2 operators $\hat{\sigma}_i$,

$$\hat{\mathcal{H}}_S^{(eff)} = -\frac{1}{2} (W\mathbf{e}_z + \Delta\mathbf{e}_x) \cdot \hat{\boldsymbol{\sigma}}, \quad (4.26)$$

where $\hat{\sigma}_i$ are the Pauli matrices in the basis of the \hat{S}_z -states close to the resonance between $|S\rangle$ and $| -S\rangle$, and $W = E_S - E_{-S}$ is the energy difference for the resonant states at $\Delta = 0$. The non-degenerate eigenfunctions of $\hat{\mathcal{H}}_S^{(eff)}$ are

$$|\psi_{\mp}\rangle = \frac{1}{\sqrt{2}} (C_{\pm}|S\rangle \mp C_{\mp}| -S\rangle) \quad (4.27)$$

with

$$C_{\pm} = \sqrt{1 \pm \frac{W}{\sqrt{\Delta^2 + W^2}}}. \quad (4.28)$$

In terms of $|\psi_{\mp}\rangle$ the Hamiltonian (4.26) can be written as

$$\hat{\mathcal{H}}_S^{(eff)} = -\frac{1}{2}\sqrt{W^2 + \Delta^2}\hat{\sigma}_z, \quad (4.29)$$

where $\hat{\sigma}_i$ are now the Pauli matrices in the new basis $|\psi_{\pm}\rangle$, i.e., $\hat{\sigma}_z = |\psi_+\rangle\langle\psi_+| - |\psi_-\rangle\langle\psi_-|$. The projection of the spin-phonon interaction Hamiltonian (4.24) onto this new two-state basis results in

$$\hat{\mathcal{H}}_{s-ph}^{(eff)} = \sum_{i,j=\pm} \langle\psi_i|\hat{\mathcal{H}}_{s-ph}|\psi_j\rangle|\psi_i\rangle\langle\psi_j| = \delta\phi_z S \Delta \hat{\sigma}_y, \quad (4.30)$$

with $\hat{\sigma}_y = -i|\psi_+\rangle\langle\psi_-| + i|\psi_-\rangle\langle\psi_+|$. The total Hamiltonian (4.22) of a single molecular magnet becomes

$$\begin{aligned} \hat{\mathcal{H}}^{(eff)} &= -\frac{1}{2}\mathbf{b}^{(eff)} \cdot \hat{\boldsymbol{\sigma}} + \hat{\mathcal{H}}_{ph}, \\ \mathbf{b}^{(eff)} &= \sqrt{W^2 + \Delta^2}\mathbf{e}_z - 2\delta\phi_z S \Delta \mathbf{e}_y. \end{aligned} \quad (4.31)$$

Here we have assumed that the perturbation introduced by the spin-phonon interaction is much smaller than the perturbation \hat{V} producing the splitting Δ , which will usually be the case. Note also that Δ and W can in general be made \mathbf{r} -dependent to account for possible inhomogeneities of the crystal.

When considering magneto-elastic excitations we will need to know whether they are accompanied by a non-zero local magnetization of the crystal. For that reason it is important to have the magnetic moment of the molecule,

$$m_z = g\mu_B\langle S_z \rangle, \quad (4.32)$$

(with g being the gyromagnetic ratio and μ_B being the Bohr magneton), in terms of its wave function

$$|\Psi\rangle = K_+|\psi_+\rangle + K_-|\psi_-\rangle, \quad (4.33)$$

where K_{\pm} are arbitrary complex numbers satisfying $|K_-|^2 + |K_+|^2 = 1$. With the help of Eq. (4.27) one obtains

$$\begin{aligned} \frac{\langle S_z \rangle}{S} &= \frac{W}{\sqrt{W^2 + \Delta^2}} (|K_-|^2 - |K_+|^2) + \frac{\Delta}{\sqrt{W^2 + \Delta^2}} (K_+^* K_- + K_+ K_-^*) \\ &= \frac{\Delta \langle \hat{\sigma} \rangle_x - W \langle \hat{\sigma} \rangle_z}{\sqrt{W^2 + \Delta^2}}. \end{aligned} \quad (4.34)$$

Magneto-elastic equations

We want to describe our system of N spins in terms of the spin field

$$\hat{\mathbf{n}}(\mathbf{r}) = \sum_i^N \hat{\boldsymbol{\sigma}}_i \delta(\mathbf{r} - \mathbf{r}_i), \quad (4.35)$$

satisfying commutation relations

$$[\hat{n}_\alpha(\mathbf{r}), \hat{n}_\beta(\mathbf{r}')] = 2i\epsilon_{\alpha\beta\gamma} \hat{n}_\gamma(\mathbf{r}) \delta(\mathbf{r} - \mathbf{r}'). \quad (4.36)$$

In terms of this field the total Hamiltonian becomes

$$\hat{\mathcal{H}} = -\frac{1}{2} \int d^3r \hat{\mathbf{n}}(\mathbf{r}) \cdot \mathbf{b}^{(eff)}(\mathbf{r}) + \hat{\mathcal{H}}_{ph}. \quad (4.37)$$

The classical pseudo-spin field $\mathbf{n}(\mathbf{r}, t)$ can be defined as

$$\mathbf{n}(\mathbf{r}, t) = \langle \hat{\mathbf{n}}(\mathbf{r}) \rangle, \quad (4.38)$$

where $\langle \dots \rangle$ contains the average over quantum spin states and the statistical average over spins inside a small volume around the point \mathbf{r} . If the size of that volume is small compared to the wavelength of the phonon displacement field, then, as has been discussed in the Introduction, $\mathbf{n}^2(\mathbf{r})$ should be approximately constant in time. According to equations (4.32), (4.34) and (4.35), the magnetization is given by

$$M_z(\mathbf{r}) = g\mu_B S \frac{\Delta n_x(\mathbf{r}) - W n_z(\mathbf{r})}{\sqrt{W^2 + \Delta^2}}. \quad (4.39)$$

The dynamical equation for the classical pseudo-spin field $\mathbf{n}(\mathbf{r}, t)$ is

$$i\hbar \frac{\partial \mathbf{n}(\mathbf{r}, t)}{\partial t} = \langle [\hat{\mathcal{H}}, \hat{\mathbf{n}}] \rangle, \quad (4.40)$$

which, with the help of Eq. (4.36), can be written as

$$\hbar \frac{\partial \mathbf{n}(\mathbf{r}, t)}{\partial t} = \mathbf{n}(\mathbf{r}, t) \times \mathbf{b}^{(eff)}(\mathbf{r}, t). \quad (4.41)$$

In this treatment we are making a common assumption that averaging over spin and phonon states can be done independently. This approximation is expected to be good in the long-wave limit.

The dynamical equation for the displacement field is

$$\rho \frac{\partial^2 u_\alpha}{\partial t^2} = \sum_\beta \frac{\partial \sigma_{\alpha\beta}}{\partial x_\beta}, \quad (4.42)$$

where $\sigma_{\alpha\beta} = \partial h / \partial e_{\alpha\beta}$ is the stress tensor, $e_{\alpha\beta} = \partial u_\alpha / \partial x_\beta$ is the strain tensor, h is the Hamiltonian density of the system in $\hat{\mathcal{H}} = \int d^3r h(\mathbf{r})$, and ρ is the mass density. Note that the stress tensor has an antisymmetric part originating from the magneto-elastic interaction in the Hamiltonian,

$$\begin{aligned} \sigma_{\alpha\beta} &= \sigma_{\alpha\beta}^{(s)} + \sigma_{\alpha\beta}^{(a)}, \\ \sigma_{\alpha\beta}^{(a)} &= \frac{1}{2} S \Delta n_y(\mathbf{r}) \epsilon_{z\alpha\beta}. \end{aligned} \quad (4.43)$$

This implies that at each point \mathbf{r} there is a torque per unit volume,

$$\tau_\alpha(\mathbf{r}) = -\delta_{\alpha z} S \Delta n_y(\mathbf{r}), \quad (4.44)$$

created by the interaction with the magnetic system. This effect can be viewed as the local Einstein – de Haas effect: Spin rotation produces a torque in the crystal lattice

due to the necessity to conserve angular momentum. With the help of equations (4.31), (4.37), and (4.42), using standard results of the theory of elasticity, one obtains

$$\frac{\partial^2 u_\alpha}{\partial t^2} - c_t^2 \nabla^2 u_\alpha - (c_l^2 - c_t^2) \nabla_\alpha (\nabla \cdot \mathbf{u}) = \frac{S\Delta}{2\rho} \epsilon_{z\alpha\beta} \nabla_\beta n_y, \quad (4.45)$$

where c_l and c_t are velocities of longitudinal and transverse sound. The source of deformation in the right hand side of this equation is due to the above-mentioned torque generated by the spin rotation.

Equations (4.41) and (4.45) describe coupled motion of the pseudospin field $\mathbf{n}(\mathbf{r}, t)$ and the displacement field $\mathbf{u}(\mathbf{r}, t)$. It is easy to see from these equations that in accordance with the argument presented in the Introduction $n_x^2 + n_y^2 + n_z^2$ is independent of time. It may, nevertheless, depend on coordinates, reflecting the structure of the initial state. We will study cases in which the crystal of molecular magnets was initially prepared in the ground state $\mathbf{n} = n_0 \mathbf{e}_z$ with n_0 being the concentration of magnetic molecules. In this case the dynamics of $\mathbf{n}(\mathbf{r})$ described by equations (4.41) and (4.45) reduces to its rotation, with the length of $\mathbf{n}(\mathbf{r})$ being a constant n_0 . Remarkably, this situation is similar to a ferromagnet, despite the absence of the exchange interaction.

4.2.2 Linear magneto-elastic waves

Bulk waves

For magnetic molecules whose magnetic cores are more rigid than their environments, only the transverse part of the displacement field (with $\nabla \cdot \mathbf{u}(\mathbf{r}) = 0$) interacts with the magnetic degrees of freedom. This is a consequence of the fact that the elastic deformation produced by the rotation of local magnetization is a local twist of the crystal lattice, required by the conservation of angular momentum. Let us consider then a transverse plane wave propagating along the X-axis. From Eqs.(4.41) and

(4.45) one obtains

$$\begin{aligned}
\frac{\partial^2 u_y}{\partial t^2} - c_t^2 \frac{\partial^2 u_y}{\partial x^2} &= -\frac{S\Delta}{2\rho} \frac{\partial n_y}{\partial x} \\
\hbar \frac{\partial n_x}{\partial t} &= n_y \sqrt{W^2 + \Delta^2} - n_z S\Delta \frac{\partial u_y}{\partial x} \\
\hbar \frac{\partial n_y}{\partial t} &= -n_x \sqrt{W^2 + \Delta^2} \\
\hbar \frac{\partial n_z}{\partial t} &= S\Delta n_x \frac{\partial u_y}{\partial x} .
\end{aligned} \tag{4.46}$$

We shall study linear waves around the ground state $|\psi_+\rangle$ corresponding to $n_z = n_0, n_{x,y} = 0, u_y = 0$. The perturbation around this state results in nonzero $n_{x,y}$ and u_y . Linearized equations of motion are

$$\begin{aligned}
\frac{\partial^2 u_y}{\partial t^2} - c_t^2 \frac{\partial^2 u_y}{\partial x^2} &= -\frac{S\Delta}{2\rho} \frac{\partial n_y}{\partial x} \\
\hbar \frac{\partial n_x}{\partial t} &= n_y \sqrt{W^2 + \Delta^2} - S\Delta n_0 \frac{\partial u_y}{\partial x} \\
\hbar \frac{\partial n_y}{\partial t} &= -n_x \sqrt{W^2 + \Delta^2} .
\end{aligned} \tag{4.47}$$

For $u_y, n_{x,y} \propto \exp(iqx - i\omega t)$, the above equations become

$$\begin{aligned}
(\omega^2 - c_t^2 q^2) u_y - iq \frac{S\Delta}{2\rho} n_y &= 0 \\
iq \frac{n_0 S\Delta \sqrt{W^2 + \Delta^2}}{\hbar^2} u_y + \left(\omega^2 - \frac{W^2 + \Delta^2}{\hbar^2} \right) n_y &= 0 .
\end{aligned} \tag{4.48}$$

The spectrum of coupled excitations is given by

$$(\omega^2 - c_t^2 q^2) \left(\omega^2 - \frac{W^2 + \Delta^2}{\hbar^2} \right) = \frac{n_0 S^2 \Delta^2 \sqrt{W^2 + \Delta^2}}{2\rho \hbar^2} q^2 . \tag{4.49}$$

In the vicinity of the resonance,

$$c_t q_0 = \frac{\sqrt{W^2 + \Delta^2}}{\hbar} \equiv \omega_0 , \tag{4.50}$$

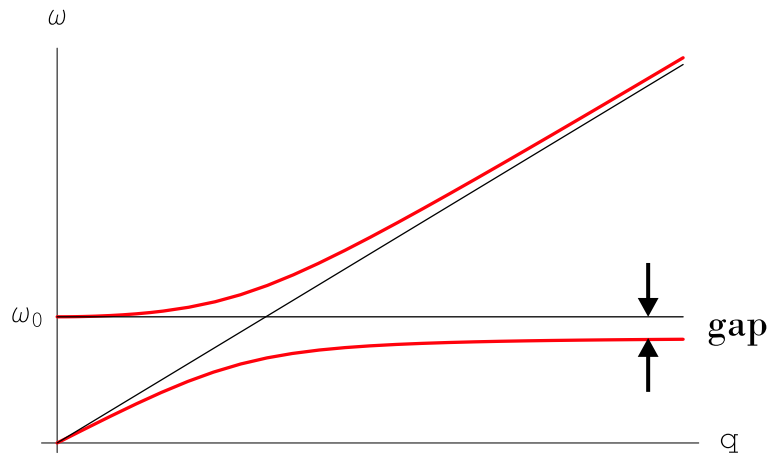


Figure 4.4: Interacting sound and spin modes. Notice the gap below spin resonance ω_0 .

one can write

$$\omega = \omega_0(1 + \delta) \quad (4.51)$$

with δ to be determined by the dispersion relation. Substituting equations (4.50) and (4.51) into Eq. (4.49), one obtains

$$\delta = \pm \sqrt{\frac{n_0 S^2 \Delta^2}{8\rho c_t^2 \hbar \omega_0}}, \quad (4.52)$$

that describes the splitting of two coupled modes at the resonance. The repulsion of elastic and spin modes is illustrated in Fig. 4.4. The relative splitting of the modes reaches maximum at $W = 0$ ($\hbar\omega_0 = \Delta$):

$$2|\delta_{max}| = \sqrt{\frac{n_0 S^2 \Delta}{2\rho c_t^2}} = S \sqrt{\frac{\Delta}{2Mc_t^2}}, \quad (4.53)$$

where $M = \rho/n_0$ is the mass of the volume containing one molecule of spin S . Notice also another consequence of Eq. (4.49): The presence of the energy gap below $\omega_0 = \sqrt{W^2 + \Delta^2}/\hbar$ (see Fig. 4.4). The value of the gap follows from Eq. (4.49) at large q . It equals $2\delta^2\omega_0$. This effect is qualitatively similar to the one obtained in Ref. [73] from an *ad hoc* model of spin-phonon interaction. In contrast with that model our

results for the splitting of the modes and for the gap do not contain any unknown interaction constants as they are uniquely determined by the conservation of the total angular momentum (spin + crystal lattice).

According to equations (4.48) and (4.49) the Fourier transforms of n_y and u_y are related through

$$\frac{n_y}{n_0} = iS \frac{\omega_0^2}{\omega_0^2 - \omega^2} \frac{\Delta}{\hbar\omega_0} qu_y. \quad (4.54)$$

Due to the condition of the elastic theory $qu_y \ll 1$, the absolute value of the ratio n_y/n_0 is generally small, unless ω is close to ω_0 . This means that away from the resonance the sound cannot significantly change the population of excited spin states. At the magneto-elastic resonance, substituting equations (4.51) and (4.52) into the above equation, one obtains:

$$\frac{|n_y|_{res}}{n_0} = \left(\frac{2M\omega_0}{\hbar} \right)^{1/2} |u_y|. \quad (4.55)$$

Although this relation is valid only at $|n_y| \ll n_0$, it allows one to estimate the amplitude of ultrasound that will significantly affect populations of spin states. We shall postpone the discussion of this effect until Section 4.2.4. Meantime let us compute the magnetization generated by the linear elastic wave, $u_y = u_0 \cos[q_0(x - c_t t)]$, in resonance with our two-state spin system. The last of Eqs. (4.47) yields $n_x = i(\omega/\omega_0)n_y$. Then, with the help of Eq. (4.39) and Eq. (4.55) one obtains

$$M_z = g\mu_B S \frac{\Delta}{\hbar\omega_0} \left(\frac{2Mc_t^2}{\hbar\omega_0} \right)^{1/2} q_0 u_0 \cos[q_0(x - c_t t)]. \quad (4.56)$$

So far we have investigated coupled magneto-elastic waves in the vicinity of the ground state, $n_z = n_0$. Eqs. (4.46) also allow one to obtain the increment, Γ , of the decay of the unstable macroscopic state of the crystal, $n_z = -n_0$, in which all molecules are initially in the excited state $|\psi_-\rangle$. In fact, the result can be immediately

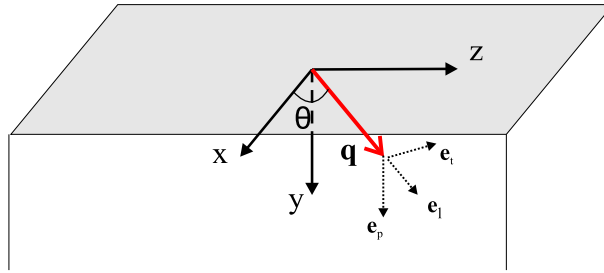


Figure 4.5: Geometry of the problem with surface acoustic waves.

obtained from equations (4.47) – (4.49) by replacing n_0 with $-n_0$. It is then easy to see from Eq. (4.49) that in the vicinity of the resonance the frequency acquires an imaginary part that attains maximum at the resonance where

$$\omega = \omega_0(1 \pm i|\delta|). \quad (4.57)$$

The mode growing at the rate $\Gamma = \omega_0|\delta|$ represents the decay of $|\psi_-\rangle$ spin states into $|\psi_+\rangle$ spin states, separated by energy $\hbar\omega_0$. This decay is accompanied by the exponential growth of the amplitude of ultrasound of frequency ω_0 .

Surface waves

Magneto-elastic coupling in crystals of molecular magnets can be studied with the help of surface acoustic waves (see Discussion). To describe the surface waves we chose a geometry in which the surface of interest is the XZ -plane and the solid extends to $y > 0$ with waves running along the direction that makes an angle θ with the X -axis, see Fig. 4.5. As usual [37] we assume that the displacement field $\mathbf{u}(\mathbf{r}, t)$ and the components $n_x(\mathbf{r}, t), n_y(\mathbf{r}, t)$ have the form

$$A = A_0 e^{-\alpha y} e^{i(q_x x + q_z z)} e^{-i\omega t}. \quad (4.58)$$

It is convenient to express the components of the displacement field in the coordinate system defined by $(\mathbf{e}_l, \mathbf{e}_t, \mathbf{e}_p)$, see Fig. 4.5,

$$\begin{aligned} u_x &= u_l \cos \theta - u_t \sin \theta \\ u_y &= u_p \\ u_z &= u_l \sin \theta + u_t \cos \theta . \end{aligned} \tag{4.59}$$

Equations of motion for u_l , u_t , and u_p follow from Eq. (4.45):

$$\begin{aligned} [\omega^2 + c_t^2(\alpha^2 - q^2)] u_t + \frac{S}{2\rho} \alpha \Delta \sin \theta n_y &= 0 \\ [\omega^2 + c_t^2 \alpha^2 - c_l^2 q^2] u_l - i \alpha q (c_l^2 - c_t^2) u_p \\ &- \frac{S}{2\rho} \alpha \Delta \cos \theta n_y = 0 \\ [\omega^2 + c_l^2 \alpha^2 - c_t^2 q^2] u_p - i \alpha q (c_l^2 - c_t^2) u_l \\ &- \frac{iS}{2\rho} \Delta q \cos \theta n_y = 0 . \end{aligned} \tag{4.60}$$

It is easy to see that for $\theta \neq k\pi$, $k = 0, 1, 2, \dots$ and $n_y \neq 0$, the transverse component u_t cannot be zero, contrary to the case of Rayleigh waves. This is the signature of magneto-elastic coupling.

As in the analysis of bulk waves, we shall study the linear waves around the ground state corresponding to the pseudospin field polarized in the Z -direction, $n_z = n_0, n_{x,y} = 0$. The excitations above this state are described by Eqs. (4.41), which become

$$\begin{aligned} -i\hbar\omega n_x &= S\Delta [-\alpha(u_l \cos \theta - u_t \sin \theta) - iq_{\parallel} \cos \theta u_p] \\ &+ \sqrt{W^2 + \Delta^2} n_y \\ -i\hbar\omega n_y &= -\sqrt{W^2 + \Delta^2} n_x . \end{aligned} \tag{4.61}$$

Substitution of these two equations into Eqs. (4.60) leads to a homogeneous system of algebraic equations for u_l , u_t , and u_p , that have a non-zero solution only if its determinant equals zero. From this condition we obtain three values of the coefficient α that describe the decay of the wave away from the surface:

$$\begin{aligned}\alpha_1 &= \sqrt{q^2 - \frac{\omega^2}{c_l^2}}, & \alpha_2 &= \sqrt{q^2 - \frac{\omega^2}{c_t^2}}, \\ \alpha_3 &= \sqrt{\frac{c_t^2 q^2 - \omega^2 + \eta q^2 \cos^2 \theta}{\eta + c_t^2}},\end{aligned}\quad (4.62)$$

where

$$\eta \equiv \frac{S^2 \Delta^2 \sqrt{W^2 + \Delta^2}}{2M [\hbar^2 \omega^2 - (W^2 + \Delta^2)]}. \quad (4.63)$$

Note that if there are no spins ($S = 0$), then $\alpha_3 = \alpha_2$ and one obtains decay coefficients for ordinary Rayleigh waves.

The general plane wave solution for the components of the displacement field can be written as

$$u_i = \sum_{k=1}^3 u_{i0}^{(k)} e^{-\alpha_k y} e^{i(q_x x + q_z z)} e^{-i\omega t}, \quad (4.64)$$

where $u_{i0}^{(k)}$ is the amplitude corresponding to each α_k and $i = l, t, p$. For each k , the amplitudes $u_{l0}^{(k)}, u_{t0}^{(k)}, u_{p0}^{(k)}$ are related through Eqs. (4.60) (there are two independent equations, so we can express, e.g., $u_{t0}^{(k)}, u_{p0}^{(k)}$ in terms of $u_{l0}^{(k)}$). Therefore, there still are three unknowns, say $u_{l0}^{(1)}, u_{l0}^{(2)}, u_{l0}^{(3)}$. The boundary conditions for the stress tensor at the surface, $\sigma_{iy}|_{y=0} = 0$, provide a system of homogeneous equations for $u_{l0}^{(1)}, u_{l0}^{(2)}$ and $u_{l0}^{(3)}$, whose determinant must be zero to allow for non-trivial solution. From this

last condition we obtain the dispersion relation for surface magneto-elastic waves:

$$\begin{aligned}
& -4q^2 \sqrt{q^2 - \frac{\omega^2}{c_l^2}} \left[\left(q^2 - \frac{\omega^2}{c_t^2} \right)^{3/2} \sin^2 \theta - \frac{\omega^2}{c_t^2} \cos^2 \theta \times \right. \\
& \left. \sqrt{\frac{q^2 S^2 \Delta^2 \omega_0 \cos^2 \theta + 2M c_t^2 \hbar (\omega^2 - \omega_0^2) (q^2 - \omega^2 / c_t^2)}{S^2 \Delta^2 \omega_0 + 2M c_t^2 \hbar (\omega^2 - \omega_0^2)}} \right] \\
& + \left(2q^2 - \frac{\omega^2}{c_t^2} \right)^2 \left(q^2 \sin^2 \theta - \frac{\omega^2}{c_t^2} \right) = 0. \tag{4.65}
\end{aligned}$$

This equation should be solved numerically to obtain the dispersion law for magneto-elastic modes. Qualitatively, the repulsion of the modes is similar to the one shown in Fig. 4.4.

4.2.3 Non-linear magneto-elastic waves

An interesting feature of Eqs. (4.46) is the existence of transverse non-linear plane wave solutions of the form $u_i = u_i(x - vt)$, $n_i = n_i(x - vt)$. For such a choice, Eq. (4.46) gives

$$\frac{du_y}{d\bar{x}} = \frac{S\Delta}{2\rho(c_t^2 - v^2)} n_y, \tag{4.66}$$

where $\bar{x} \equiv x - vt$ and the constant of integration was put zero assuming that there is no $du_y/d\bar{x}$ independent from n_y . Substituting this into the equations of motion for \mathbf{n} , Eqs. (4.46), one obtains

$$\begin{aligned}
-\frac{dn_x}{d\xi} &= n_y - \gamma n_y n_z \\
-\frac{dn_y}{d\xi} &= -n_x \\
-\frac{dn_z}{d\xi} &= \gamma n_x n_y, \tag{4.67}
\end{aligned}$$

where

$$\xi \equiv \frac{\bar{x} \sqrt{W^2 + \Delta^2}}{\hbar v} \quad \gamma \equiv \frac{S^2 \Delta^2}{2\rho(c_t^2 - v^2) \sqrt{W^2 + \Delta^2}} \tag{4.68}$$

The system of Eqs. (4.67) can be reduced to

$$n_z = C - \frac{1}{2}\gamma n_y^2 \quad (4.69)$$

$$\frac{d^2 n_y}{d\xi^2} = -n_y \left(1 - \gamma C + \frac{1}{2}\gamma^2 n_y^2 \right), \quad (4.70)$$

where C is a constant of integration. The first integral of the last differential equation is

$$\frac{1}{2} \left(\frac{dn_y}{d\xi} \right)^2 = -\frac{1}{2}(1 - \gamma C)n_y^2 - \frac{\gamma^2}{8}n_y^4 + A \geq 0, \quad (4.71)$$

where A is another integration constant.

We are interested in real bounded solutions of Eq. (4.70) with n_y vanishing at $x - vt \rightarrow \pm\infty$, so that the integration constant A must be zero. In this case, for the right hand side of Eq. (4.71) to be positive we must have $1 - \gamma C < 0$. Then, the solution of Eq. (4.70) is

$$n_y(\xi) = \frac{\sqrt{\gamma C - 1} e^{\pm\sqrt{\gamma C - 1}(\xi - \xi_0)}}{\gamma + \gamma e^{\pm 2\sqrt{\gamma C - 1}(\xi - \xi_0)}}. \quad (4.72)$$

From the equations

$$n_x = \frac{dn_y}{d\xi}, \quad n_z = C - \frac{1}{2}\gamma n_y^2 \quad (4.73)$$

one determines with the help of the condition $n_x^2 + n_y^2 + n_z^2 = n_0^2$ that $C = \pm n_0$. Therefore, γ must satisfy $|\gamma| > 1/n_0$ for the equation (4.70) to have a solution satisfying the conditions specified above. Setting the reference point $\xi_0 = 0$ one obtains

$$n_y(\xi) = \pm \frac{2}{|\gamma|} \sqrt{|\gamma|n_0 - 1} \operatorname{sech} \left[\sqrt{|\gamma|n_0 - 1} \xi \right], \quad (4.74)$$

so that

$$n_z(\xi) = \pm 1 \mp 2 \frac{|\gamma|n_0 - 1}{|\gamma|} \operatorname{sech}^2 \left[\sqrt{|\gamma|n_0 - 1} \xi \right]. \quad (4.75)$$

In these formulas, the upper sign corresponds to $\gamma > 0$ and the lower sign to $\gamma < 0$.

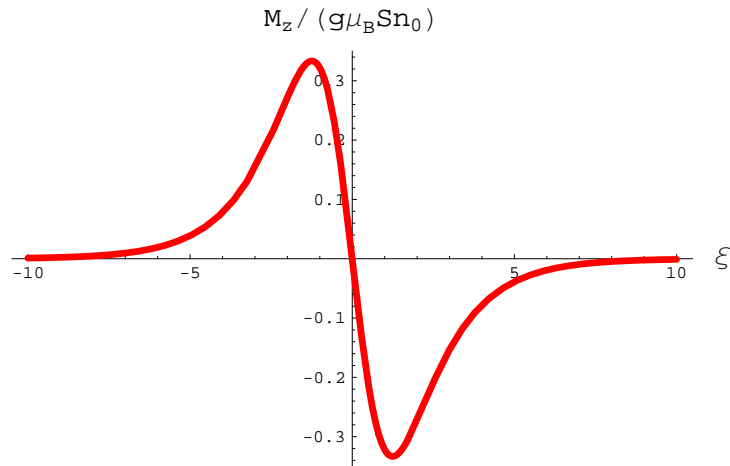


Figure 4.6: Magnetization inside the soliton as a function of ξ for $W = 0$.

Eq. (4.75) describes a solitary wave of a characteristic width

$$l_0 \sim \frac{1}{\sqrt{|\gamma|n_0 - 1}} \frac{\hbar v}{\sqrt{W^2 + \Delta^2}}, \quad (4.76)$$

travelling at a speed v . The parameter γ given by Eq. (4.68) is determined by v , which is the only free parameter of the soliton. The magnetization inside the soliton is given by Eq. (4.39) with n_x and n_z defined by equations (4.73) – (4.75). At, e.g., $W = 0$

$$\begin{aligned} M_z = & \mp g\mu_B \frac{2S(|\gamma|n_0 - 1)}{|\gamma|} \times \\ & \times \operatorname{sech} \left[\sqrt{|\gamma|n_0 - 1} \xi \right] \tanh \left[\sqrt{|\gamma|n_0 - 1} \xi \right]. \end{aligned} \quad (4.77)$$

The condition

$$n_0|\gamma| = \frac{1}{|1 - v^2/c_t^2|} \frac{S^2\Delta}{2Mc_t^2} \frac{\Delta}{\sqrt{W^2 + \Delta^2}} > 1 \quad (4.78)$$

requires v to be very close to the speed of sound c_t . This is a consequence of Δ being very small compared to Mc_t^2 . Note that the maximal value of the magnetization inside the soliton,

$$|M_z| = g\mu_B S \left(n_0 - \frac{1}{|\gamma|} \right), \quad (4.79)$$

is, in general, of the order of saturation magnetization $M_0 = g\mu_B S n_0$. We should also note that although the above non-linear solution of the equations of motion formally allows v to be both slightly lower or slightly higher than c_t , the supersonic soliton should be unstable with respect to Cherenkov radiation of sound waves.

4.2.4 Discussion

Eq. (4.53) provides the splitting of the bulk sound frequency in a magnetized crystal of magnetic molecules in the vicinity of the resonance between sound and spin levels. At a zero field bias ($W = 0$) the resonant condition, $\Delta = \hbar c_t q$, should be easily accessible at low Δ . However, the splitting given by Eq. (4.53) will be very small unless Δ is in the GHz range or higher. Such a large Δ will be also beneficial for decreasing inhomogeneous broadening of Δ and for insuring low decoherence of quantum spin states. Surface acoustic waves can, in principle, be generated up to 100GHz [70]. They may also be easier to use for the observation of the discussed splitting. By order of magnitude it will still be given by Eq. (4.53). Substituting into this equation $S = 10$, $\Delta \sim 0.1$ K (frequency f in the GHz range), $Mc_t^2 \sim 10^5$ K, one obtains $\delta_{max} \sim 10^{-2}$. This will be observable if the quality factor of ultrasound in the GHz range exceeds 100. The magneto-elastic nature of the splitting can be confirmed through its dependence on the angle between the wave vector and the easy magnetization axis of the crystal, see Sec. III-B. Observation of the gap, $2\delta^2\omega_0$, in the excitation spectrum (see Fig. 4.4) will be more challenging. For practical values of δ the gap is likely to be small compared to the width of the spin resonance and the width of the ultrasonic mode in the GHz range.

Eq. (4.55) shows that at $M \sim 10^{-21}$ g and $\omega_0 \sim 10^{10}$ s $^{-1}$ ultrasound of amplitude

$u_0 \sim 0.1$ nm will significantly affect population of spin levels. Moreover, it will result in the oscillating magnetization of large amplitude, Eq. (4.56). We have also demonstrated that one can prepare the crystal in the excited spin state and generate ultrasound due to the decay of the population of that state. This result is another confirmation of the phonon laser effect suggested in Ref. [35]. Equations (4.57) and (4.53) show that at $\omega_0 \sim 10^{10}\text{s}^{-1}$ the amplitude of the sound wave may grow at the rate as high as $\Gamma \sim 10^8\text{s}^{-1}$. Magneto-elastic effects studied here should be sensitive to the decoherence of spin states. However, when the oscillation of spin population is driven by the external acoustic wave, the latter should force the phase coherence upon the spin system. To provide the resonance condition, the broadening of the level splitting due to disorder and dipolar fields should be small compared to Δ . If it is not, the tunnel splitting, Δ , should be increased by applying a sufficiently large transverse magnetic field.

One fascinating prediction of our theory is the existence in molecular magnets of solitary waves of the magnetization reversal coupled to elastic twists. Such waves have quantum origin as they are related to the quantum splitting of spin-up and spin-down states. They can be ignited in experiment that starts with all molecules in the ground state. Such a state of the crystal has zero magnetization as the molecules are in a superposition of spin-up and spin-down states. The soliton discussed above is characterized by a narrow region of a large non-zero magnetization that propagates through the solid with the velocity close to the speed of transverse sound. It can be generated by, e.g., a localized pulse of the magnetic field or by a localized mechanical twist, and detected through local measurements of the magnetization. In general the

width of the soliton, given by Eq. (4.76), is of order of the wavelength of sound of frequency $\sqrt{W^2 + \Delta^2}/\hbar$, though wider solitons are allowed if $|\gamma|n_0 \rightarrow 1$. In experiment this width should depend on the width of the field pulse or the size of the twisted region that generates the soliton.

Part II

Dynamical Landau-Zener effects in spin systems

Chapter 5

Quantum dynamics of a nanomagnet in a rotating field [80]

5.1 Landau-Zener theory in molecular magnets

As mentioned in the introduction, in a time dependent magnetic field, molecular magnets exhibit stepwise magnetic hysteresis due to resonant quantum tunneling between spin levels [2]. This phenomenon has been intensively studied theoretically within models employing Landau-Zener-Stueckelberg (LZS) effect [110]. The formulation of the problem, independently studied by Landau, Zener, and Stueckelberg at the inception of quantum theory is this. Consider a system characterized by quantum states $|1\rangle$ and $|2\rangle$ with energies E_1 and E_2 respectively. Let the system be initially prepared in the lower-energy state, $|1\rangle$, and the field be changing such (due to, e.g., Zeeman interaction of the magnetic field with a spin) that E_1 is shifting up while E_2 is shifting down. After the levels cross and the distance between them continues to increase, the system, with LZS probability, $P = \exp(-\pi\Delta^2/2\hbar v)$, remains in the state $|1\rangle$. Here Δ is the tunnel splitting of $|1\rangle$ and $|2\rangle$ at the crossing, and v is the rate at which the energy bias between $|1\rangle$ and $|2\rangle$ is changing with time. This picture, of course, does not take into account any disturbance of the quantum states, $|1\rangle$ and $|2\rangle$,

by the dissipative environment. Application of the conventional LZS effect to molecular magnets was initially suggested in Refs. [81, 82]. Its dissipative counterpart was developed in Refs. [83, 84, 85, 86, 87, 111, 90, 88, 89]. The amazing property of the LZS formula is that it is very robust against any effect of the environment [91, 86, 111]. This has allowed experimentalists to use the LZS expression to extract Δ in molecular magnets from bulk magnetization measurements [4, 92, 112, 93].

Our purpose is to study in detail quantum spin transitions and the effect of the environment in experiments with a rotating magnetic field. Quantum tunneling rates for a spin system in a rotating field have been studied before [94]. Here we are taking a different angle at this problem, by computing the occupation numbers for quantum spin states. This approach can be useful for the description of experiments that measure the time dependence of the magnetization. A weak high-frequency rotating field, $H_0 \sim 1$ Oe, can be easily achieved electronically, by applying $H_x = H_0 \cos(\omega t)$ and $H_z = H_0 \sin(\omega t)$. The rotating field of large amplitude can be achieved by rotating the sample in a constant magnetic field. In a typical molecular magnet, a rotating field not exceeding a few kOe will result in the crossing of two spin levels only, preserving the two-state approximation. We will compute the time evolution of the probability to occupy one of the two spin levels after a number of revolutions. We will demonstrate that this evolution depends crucially on whether the system is subject to the dissipative noise and that it depends strongly on the frequency of the noise. The model and the approach are formulated in Sec. 5.2. The rotating-field counterpart of the LZS effect is studied in Sec. 5.3. The effects of low- and high-frequency stationary noise are considered in Sec. 5.4. Consequences for experiment

are discussed at the end of the Chapter.

5.2 Hamiltonian

We shall start with the Hamiltonian

$$\mathcal{H} = -DS_z^2 - g\mu_B\mathbf{H} \cdot \mathbf{S}, \quad (5.1)$$

where D is the uniaxial anisotropy constant, g is the gyromagnetic factor, μ_B is the Bohr magneton, and \mathbf{H} is the magnetic field, and S is an integer spin. We shall assume that the magnetic field rotates in the XZ -plane,

$$\mathbf{H} = H \sin(\omega t)\mathbf{e}_z + H \cos(\omega t)\mathbf{e}_x. \quad (5.2)$$

At $\mathbf{H} = 0$, the ground state of the model is double degenerate. The lowest energy states correspond to the parallel ($m = S$) and antiparallel ($m = -S$) orientation of \mathbf{S} with respect to the anisotropy axis, with m being the magnetic quantum number for \mathbf{S} . The effect of the external magnetic field is twofold. The Z -component of the field removes the degeneracy. The X -component produces a term in the Hamiltonian that does not commute with S_z . Consequently, at $H_x \neq 0$ the $|m\rangle$ states are no longer the eigenstates of the system. However, at

$$g\mu_B H \ll (2S - 1)D \quad (5.3)$$

we can treat the non-commuting term in the Hamiltonian as a perturbation. Throughout this article it will be assumed that the system is prepared initially in one of the saturated magnetic states, say $| -S \rangle$ for certainty. This can be easily achieved at low temperature in molecular magnets with high easy-axis anisotropy.

For the perturbation $V(t) = g\mu_B \mathbf{H} \cdot \mathbf{S}$ the time-dependent perturbation theory gives the following expression for the transition amplitude from the initial state, $|-S\rangle$, to any $|m'\rangle$ state with $m' \neq -S$:

$$\begin{aligned}
c_{m'}(t) = & e^{-i\frac{E_{m'}t}{\hbar}} \left[-\frac{i}{\hbar} \langle m' | g\mu_B H S_x | -S \rangle \times \right. \\
& \int_0^t dt_1 e^{i\frac{(E_{m'} - E_{-S})t_1}{\hbar}} \cos(\omega t_1) + \left(\frac{-i}{\hbar} \right)^2 \times \\
& \sum_{m''} \langle m' | g\mu_B H S_x | m'' \rangle \langle m'' | g\mu_B H S_x | -S \rangle \times \\
& \int_0^t dt_1 e^{i\frac{(E_{m'} - E_{m''})t_1}{\hbar}} \cos(\omega t_1) \times \\
& \left. \int_0^{t_1} dt_2 e^{i\frac{(E_{m''} - E_{-S})t_2}{\hbar}} \cos(\omega t_2) + \dots \right], \tag{5.4}
\end{aligned}$$

where $E_m = -Dm^2$ are the eigenstates of $\mathcal{H}_0 = -DS_z^2$. When $\omega \ll (E_{m'} - E_{-S})/\hbar$ for all m' , then the perturbation can be treated adiabatically. This requires the condition

$$\hbar\omega \ll (2S - 1)D, \tag{5.5}$$

that will be used throughout the analysis. In molecular magnets, D is of the order of 1 K. Consequently, any ω at or below GHz range satisfies Eq. (5.5).

At $T = 0$, equations (5.3) and (5.5), and the initial condition, allow one to limit the consideration by the two lowest states, $|S\rangle$ and $|-S\rangle$, of the unperturbed Hamiltonian. Time-independent perturbation theory based upon the condition (5.5) permits the usual reduction of the spin Hamiltonian to the effective two-state Hamiltonian for the tunnel split states originating from $m = S$ and $m = -S$,

$$\mathcal{H}_{eff} = -\frac{1}{2}h_0 \sin(\tau)\sigma_z + \frac{1}{2}\Delta(\tau)\sigma_x. \tag{5.6}$$

Here $\sigma_{z,x}$ are the Pauli matrices, $h_0 = 2Sg\mu_B H$ is the amplitude of the energy bias, $\tau = \omega t$ is dimensionless time, and $\Delta(\tau)$ is the tunnel splitting of $|S\rangle$ and $|-S\rangle$ due to

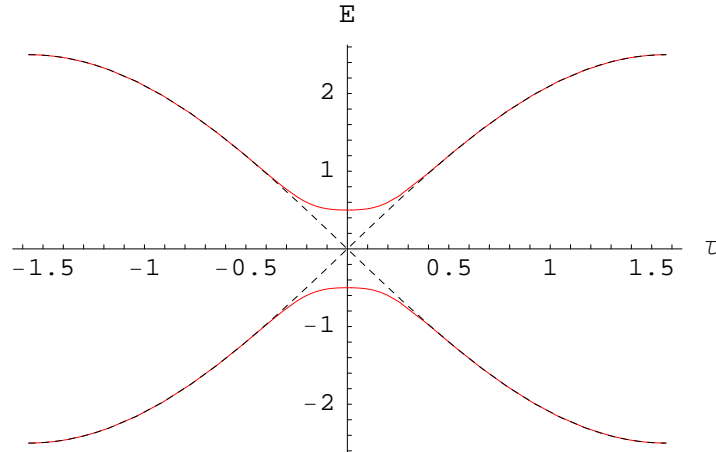


Figure 5.1: Time dependence of the energy levels (normalized by D) of the Hamiltonian (5.6) (solid line) at $S = 4$ and $g\mu_B H/D = 3.1$. Dash line shows the distance between the energy levels if they were unperturbed by the second term in Eq. (5.6).

the transverse field $H_x(\tau)$ [42],

$$\Delta(\tau) = \Delta_0 \cos^{2S}(\tau), \quad (5.7)$$

where

$$\Delta_0 = \frac{8S^2 D}{(2S)!} \left(\frac{h_0}{4DS} \right)^{2S}. \quad (5.8)$$

An important observation that follows from Eq. (5.7) is that at $\tau_n = (2n + 1)\pi/2$ (with $n = 0, \pm 1, \pm 2, \dots$) the splitting is exactly zero. According to Eq. (5.7), at large S , it decreases very fast as one moves away from the level crossing, that occurs at $\tau_n = n\pi/2$. This guarantees that the transitions between the two states are localized in time at the level crossing. This is clearly seen in Figure 1 that shows the effect of the perturbation on the energy levels.

For real systems, the Hamiltonian may contain additional terms that do not commute with S_z . Such terms provide an additional tunnel splitting Δ_E . Quantum dynamics of the system is dominated by the rotating magnetic field if $\Delta_E \ll \Delta_0$. In the case of, e.g., the transverse anisotropy, ES_x^2 , contribution to the Hamiltonian, Δ_E

is given by [42],

$$\Delta_E = 8D \frac{(2S)!}{[(S-1)!]^2} \left(\frac{E}{16D} \right)^S. \quad (5.9)$$

The condition $\Delta_E \ll \Delta_0$ is satisfied when

$$\frac{E}{D} < \left(\frac{g\mu_B H}{SD} \right)^2. \quad (5.10)$$

5.3 Dynamics without noise

5.3.1 A single revolution

In order to describe the evolution of the magnetization in a magnetic field rotating in the XZ -plane, we shall compute first the probability of staying at the initial state after a rotation by 180 degrees, when a single level crossing takes place.

The Schrödinger equation for the coefficients of the wave function,

$$|\Psi\rangle = c_{-S} | -S\rangle + c_S | S\rangle, \quad (5.11)$$

can be expressed as:

$$\begin{aligned} i\hbar \frac{d}{dt} \tilde{c}_{-S}(t) &= \frac{\Delta(t)}{2} \tilde{c}_S(t) \\ i\hbar \frac{d}{dt} \tilde{c}_S(t) &= -h_0 \sin(\omega t) \tilde{c}_S(t) + \frac{\Delta(t)}{2} \tilde{c}_{-S}(t) \end{aligned} \quad (5.12)$$

where $\tilde{c}_i(t) = c_i(t) \exp[\frac{i}{2\hbar} \int_{t_0}^t dt' h_0 \sin(\omega t')]$. In terms of the dimensionless variable,

$$u = \frac{h_0 \tau}{\Delta_0}, \quad (5.13)$$

Eq. (5.12) turns into:

$$\begin{aligned} i \frac{d}{du} \tilde{c}_{-S}(u) &= \frac{\tilde{\epsilon}}{2} \cos^{2S}(\gamma u) \tilde{c}_S(u) \\ i \frac{d}{du} \tilde{c}_S(u) &= -\frac{\tilde{\epsilon}}{\gamma} \sin(\gamma u) \tilde{c}_S(u) + \frac{\tilde{\epsilon}}{2} \cos^{2S}(\gamma u) \tilde{c}_{-S}(u) \end{aligned} \quad (5.14)$$

The problem is now defined by two dimensionless parameters:

$$\tilde{\epsilon} = \frac{\Delta_0^2}{\hbar\omega h_0}, \quad (5.15)$$

which is similar to the parameter used in the LZS theory [95, 81], and

$$\gamma = \frac{\Delta_0}{h_0}, \quad (5.16)$$

which is a measure of the magnitude of the magnetic field. Notice that this parameter equals $\tau_c = \omega t_c$, where $t_c = \Delta_0/(\omega h_0)$ is the characteristic time of crossing the resonance. Thus, the condition $\gamma \ll 1$ is needed for the crossing to be well localized in time on the time scale of one revolution. This condition is required for the self-consistency of the method.

From Eqs. (5.14) one can compute numerically the time evolution of the coefficients c_{-S} and c_S , and, thus, the time evolution of the occupation numbers for any $\tilde{\epsilon}, \gamma$. In the fast ($\tilde{\epsilon} \ll 1$) and slow ($\tilde{\epsilon} \gg 1$) rotation regimes, analytical formulas for the occupation probabilities can be obtained. These formulas are useful for further analysis. Inspection of Eqs.(5.14) reveals that the deviation from the LZS result for slow rotation is small, since within the relevant time of the transition $\delta u \sim 1$ and $\Delta(\tau)$ is nearly constant. On the contrary, for the fast rotation regime, ($\tilde{\epsilon} \ll 1$), the relevant time interval is wider, $\delta u \sim \tilde{\epsilon}^{-1/2}$. This allows a significant change of Δ during the transition and makes possible a considerable deviation from the LZS result.

Fast rotation ($\tilde{\epsilon} \ll 1$)

Following the procedure devised by Garanin and Schilling [95], we can obtain the probability of staying at the initial state after a 180-degree rotation of the external magnetic field. We choose the direction of the magnetic field to be initially antiparallel

to the Z -axis. In the zero-th order of the perturbation theory $\tilde{c}_1(u) = 1$. In the first order, such probability is then given by

$$P = 1 - \frac{1}{4} \left| \frac{\tilde{\epsilon}}{\gamma} \int_{-\frac{\pi}{2}}^{\frac{\pi}{2}} \cos^{2S}(z) \exp \left[i \frac{\tilde{\epsilon}}{\gamma^2} \cos(z) \right] dz \right|^2 \quad (5.17)$$

It is clear from this expression that for $\gamma \ll 1$, only $|z| \ll 1$ contribute to the integral. This is in accordance with the fact that the transition takes place during the time interval $\Delta_0/h_0\omega$, which is of order γ compared with the time of the integration. Consequently, one can approximate $\cos(z)$ by

$$\cos(z) \approx 1 - \frac{z^2}{2}, \quad \cos^b(z) \approx e^{-\frac{b}{2}z^2}, \quad (5.18)$$

where the exponential form is chosen to insure fast convergence of the integral, and set infinite integration limits in Eq. (5.17):

$$\begin{aligned} P &= 1 - \frac{1}{4} \left| \frac{\tilde{\epsilon}}{\gamma} \int_{-\infty}^{\infty} \exp \left[- \left(\frac{i\tilde{\epsilon}}{\gamma^2} + S \right) z^2 \right] dz \right|^2 \\ &= 1 - \frac{\pi}{2} \frac{\tilde{\epsilon}}{\sqrt{1 + (2S\gamma^2/\tilde{\epsilon})^2}}. \end{aligned} \quad (5.19)$$

The probability, P , of staying at the initial state $|-S\rangle$ after a 180-degree rotation is shown in Fig. 5.2 for different values of $\tilde{\epsilon}$. In the figure, the numerical results are compared with the result given by Eq. (5.19), and with the LZS result,

$$P_{LZS} = \exp[-\pi\tilde{\epsilon}/2]. \quad (5.20)$$

Note that Eq. (5.20) would be our result for the probability if we applied the LZS theory to the version of the Hamiltonian (5.6) that is linearized on τ . As can be seen from Fig. 5.2, at $\gamma, \tilde{\epsilon} \ll 1$, Eq. (5.19) provides a good approximation. The difference between the numerical result and the LZS result is considerable. Fig. 5.3 shows P for different γ at $\tilde{\epsilon} = 0.1$. Here again Eq. (5.19), but not the LZS formula, provides a good approximation for the γ -dependence of the staying probability.

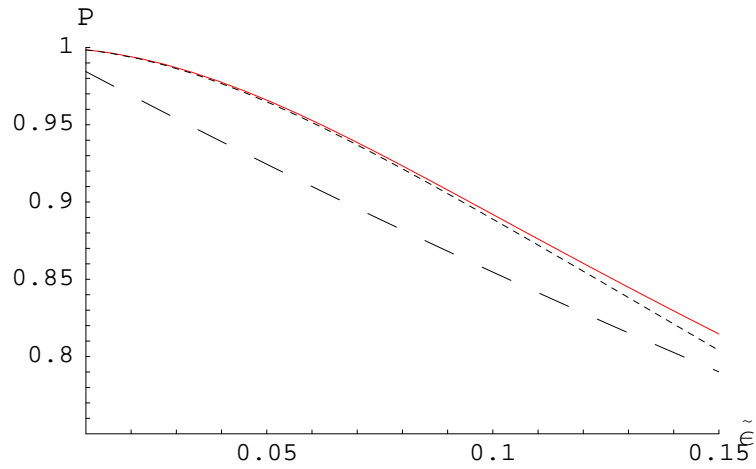


Figure 5.2: Probability of staying at $|-S\rangle$, P , as a function of parameter $\tilde{\epsilon}$ at $\gamma = 0.1$ and $S = 5$. The solid line represents the numerical data, the short-dash line is the analytical result, Eq. (5.19), and the long-dash line is the LZS result (see explanation in the text).

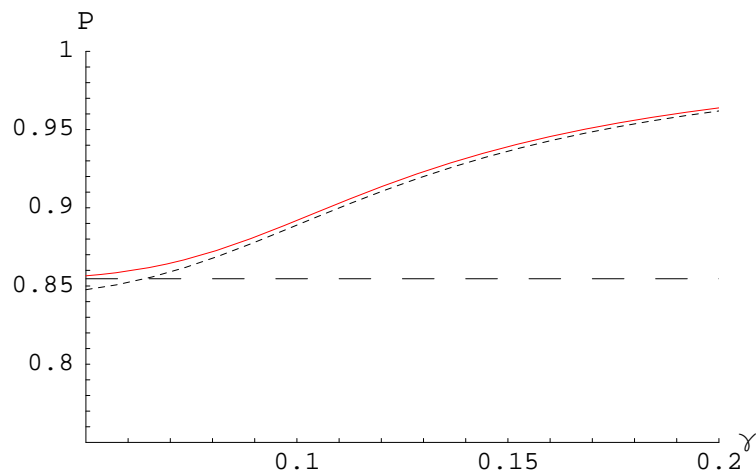


Figure 5.3: Probability of staying at the initial state, P , as a function of γ at $\tilde{\epsilon} = 0.1$ and $S = 5$. The solid line represents numerical data, the short-dash line is the analytical result Eq. (5.19), and the long-dash line is the LZS result.

Slow rotation ($\tilde{\epsilon} \gg 1$)

In the case of a slow rotation it is convenient to seek the solution of the Schrödinger's equation in the adiabatic basis of the two-state Hamiltonian. Then, one can follow a procedure similar to that used for the fast rotation regime. The adiabatic basis is given by:

$$|\Psi_{\pm}\rangle = \frac{1}{\sqrt{2}}(\pm k_{\pm} |-S\rangle + k_{\mp} |S\rangle) \quad (5.21)$$

where

$$k_{\pm}(\tau) = \sqrt{1 \pm \frac{W(\tau)}{\sqrt{W^2(\tau) + \Delta^2(\tau)}}}. \quad (5.22)$$

with $W(\tau) = h_0 \sin(\tau)$ and $\Delta(\tau) = \Delta_0 \cos^{2S}(\tau)$. The corresponding adiabatic energy levels are

$$E_{\pm}(\tau) = \pm \frac{1}{2} \sqrt{W^2(\tau) + \Delta^2(\tau)}. \quad (5.23)$$

Expressing the wave function as

$$|\Psi\rangle = c_+ |\Psi_+\rangle + c_- |\Psi_-\rangle \quad (5.24)$$

we can now write the Schrödinger equation for

$$\tilde{c}_{\pm}(t) = \exp \left[\frac{i}{\hbar} \int dt E_{\pm}(t) \right] c_{\pm}(t) \quad (5.25)$$

in terms of the dimensionless variable u defined above:

$$\begin{aligned} \frac{d}{du} \tilde{c}_+ &= -i\tilde{\epsilon}\Omega(\gamma u)\tilde{c}_+ - \frac{1}{2} \frac{dw/du}{(1+w^2)} \tilde{c}_- \\ \frac{d}{du} \tilde{c}_- &= \frac{1}{2} \frac{dw/du}{(1+w^2)} \tilde{c}_+, \end{aligned} \quad (5.26)$$

where

$$\Omega(z) = \sqrt{\frac{1}{\gamma^2} \sin^2(z) + \cos^{4S}(z)} \quad (5.27)$$

and $w(z) = W(z)/\Delta(z)$.

The asymptotic behavior of $\tilde{c}_-(u)$ is $\tilde{c}_-(u) \rightarrow 1$ for $\tilde{\epsilon} \rightarrow \infty$. At $\tilde{\epsilon} \gg 1$ the coefficient $\tilde{c}_-(u)$ remains close to 1. Also, far from the crossing point, $\tilde{c}_+(u) \approx c_{-S}$, as can be seen from Eqs. (5.21) and (5.22). These two facts allow one to obtain the probability of staying at the initial state in the first order of perturbation theory:

$$P = \frac{1}{4} \left| \int_{-\frac{\pi}{2}}^{\frac{\pi}{2}} dz \frac{dw/dz}{(1+w^2)} \exp \left[i \frac{\tilde{\epsilon}}{\gamma} \int_0^z dz' \Omega(z') \right] \right|^2 \quad (5.28)$$

At $\gamma \ll 1$ the integral is dominated by z close to zero. The correct prefactor can be obtained by applying the procedure outlined in Ref. [95]. With the accuracy to γ^2 this gives:

$$P = \exp \left\{ -\frac{\pi\tilde{\epsilon}}{2} \left[1 + \left(S - \frac{1}{8} \right) \gamma^2 \right] \right\} \quad (5.29)$$

This probability is shown in Fig. 5.4 for different values of $\tilde{\epsilon}$. The numerical results are compared in the figure with the result given by Eq. (5.29), and with the LZS result. As can be seen from Fig. 5.4, at $\gamma \ll 1$, Eq. (5.29) provides a good approximation for $\tilde{\epsilon} > 5$.

5.3.2 Continuous rotation

Our treatment of the continuous rotation is based upon the smallness of the transition time in comparison with the period of the rotation. Periodically driven two-state systems of that kind have been studied before [88].

The individual crossing is described by the transfer matrix:

$$M = \begin{pmatrix} \sqrt{P} & e^{-i\theta} \sqrt{1-P} \\ -e^{i\theta} \sqrt{1-P} & \sqrt{P} \end{pmatrix} \quad (5.30)$$

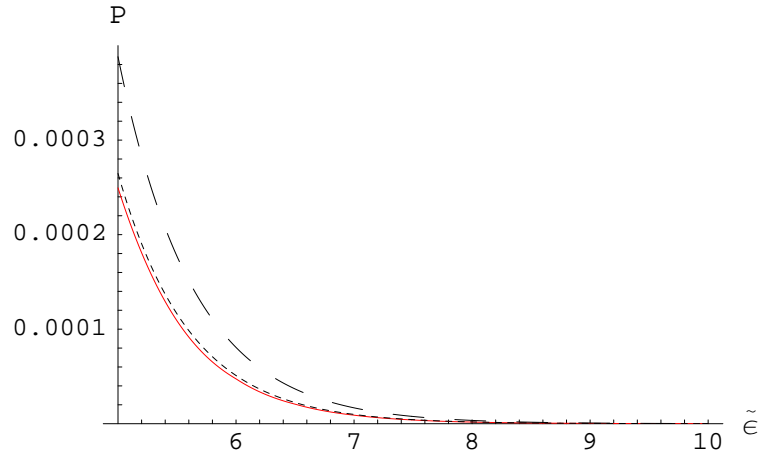


Figure 5.4: Probability of staying at the initial state, P , as a function of the parameter $\tilde{\epsilon}$ at $\gamma = 0.1$ and $S = 5$. The solid line represents the numerical data, the short-dash line is the analytical result, Eq. (5.29), and the long-dash line is the LZS result

where θ is the Stokes phase given by:

$$\theta = \frac{\pi}{4} + \arg \left[\Gamma \left(1 - i \frac{\tilde{\epsilon}}{4} \right) \right] + \frac{\tilde{\epsilon}}{4} \left[\ln \frac{\tilde{\epsilon}}{4} - 1 \right]. \quad (5.31)$$

This matrix transforms a given initial state into the after-crossing final state in terms of the unperturbed basis. The above expression corresponds to the crossing in which the $| -S \rangle$ level moves up towards the $| S \rangle$ level that is moving down. In the opposite case, M should be replaced by the transpose matrix, M^T .

To describe the evolution of the system between crossings it must be noted that, as we have shown before, far from the crossings the unperturbed basis $| -S \rangle, | S \rangle$ almost coincides with the adiabatic basis $| + \rangle, | - \rangle$, see equations (5.21) and (5.22). In this region, the evolutions of $| -S \rangle$ and $| S \rangle$ are then considered independent, so that they can be described by the propagator

$$G_n = \begin{pmatrix} \exp[(-1)^{n+1}i\alpha] & 0 \\ 0 & \exp[(-1)^n i\alpha] \end{pmatrix} \quad (5.32)$$

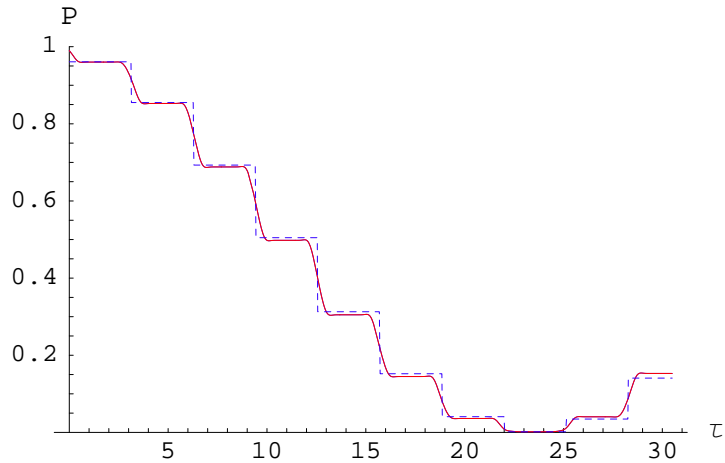


Figure 5.5: Time dependence of the probability of finding a continuously rotating system in the initial state $| -S \rangle$ for $\tilde{\epsilon} = 0.04$, $\gamma = 0.06$ and $S = 5$. The solid line represents numerical data. The dash line shows analytical result obtained by successive application of M , M^T and G_n .

where

$$\alpha = \frac{1}{2} \left(\frac{D}{\hbar\omega} \right) \int_0^{\frac{\pi}{2}} d\tau \sqrt{W(\tau)^2 + \Delta(\tau)^2}. \quad (5.33)$$

With the help of Eq. (5.30) and Eq. (5.32) one can compute the time evolution of the coefficients c_{-S}, c_S in Eq. (5.11). Starting with the initial state, the state of the system after the n -th crossing can be obtained by the successive action of M , M^T and G_n . The time-dependence of the probability of finding a continuously rotating system in the initial state $| -S \rangle$ is shown in Fig. 5.5. The figure shows good agreement of the above analytical method with numerical calculation. It is important to notice that in the absence of dissipation the system does not arrive to any asymptotic state at $\tau \rightarrow \infty$. The behavior of the probability shows a long-term memory of the initial state, which is somewhat surprising. This prediction of the theory can be tested in real experiment.

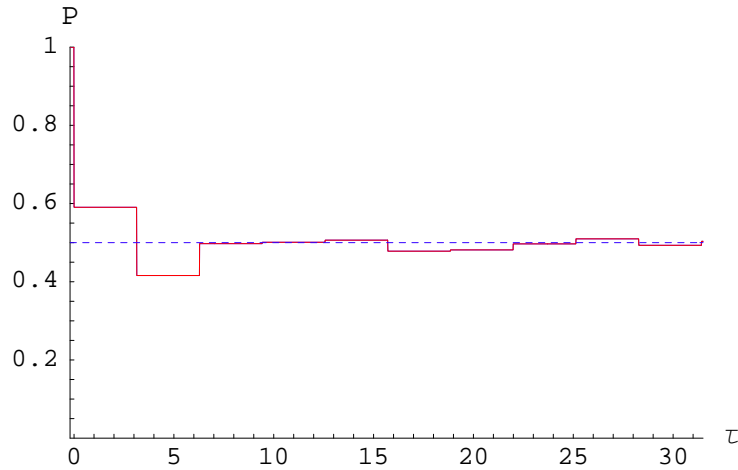


Figure 5.6: Time dependence of the probability of finding a particle in the state $|-S\rangle$ in the presence of a low-frequency noise for $\tilde{\epsilon} = 1/3$, $S = 10$, and $\gamma = 0.01$. The plotted probability is the average over an ensemble of 20 two-state dissipative systems.

5.4 Dynamics with noise.

When considering the effect of the noise, it is important to distinguish between the following three regimes:

$$\gamma \ll 1 \ll \omega/\Gamma \quad (5.34)$$

$$\gamma \ll \omega/\Gamma \ll 1 \quad (5.35)$$

$$\omega/\Gamma \ll \gamma \ll 1 \quad (5.36)$$

where Γ is the characteristic frequency of the noise. The first of these conditions corresponds to the situation when a few revolutions may occur before any contribution of the noise becomes apparent. Consequently, during the time interval satisfying $t < 1/\Gamma$ one can use the results for the probability obtained in the previous section. Under the condition (5.35), one can use the previously obtained results for a singular crossing but needs to take into account the destruction of the relative phase of the two states by the noise before the next crossing takes place. Under the condition

(5.36) the results of the previous section do not apply because the coherence of the quantum state is destroyed by the noise on a timescale that is less than the crossing time.

We shall only consider a stationary noise which is independent of the time evolution of the system. Note that it might not be the case when a nanomagnet is coupled to nuclear spins [91].

5.4.1 Low-frequency noise, $\gamma \ll \omega/\Gamma \ll 1$

The situation corresponding to the condition (5.35) can be easily described by the Hamiltonian

$$\mathcal{H}_{eff} = -\frac{1}{2}h_0 \sin(\tau)\sigma_z + \frac{1}{2}\Delta(\tau)\sigma_x - \eta\sigma_z, \quad (5.37)$$

where $\eta(\tau) \ll h_0$ is a random magnetic field in the Z -direction, with the correlator

$$\langle \eta(\tau)\eta(\tau') \rangle = \eta_0^2 \Theta [(\omega/\Gamma) - |\tau - \tau'|], \quad (5.38)$$

Θ being the theta-function.

The time dependence of the probability of finding the system in the state $|-S\rangle$ is shown in Fig. (5.6) for $\tilde{\epsilon} = 1/3$, $S = 10$, and $\gamma = 0.01$. In accordance with the expectation, the probability for the system to occupy the state with $m = -S$ (or $m = S$), after going through a few oscillations, tends to the asymptotic value of 0.5. For molecular magnets, only the average of the probability over an ensemble of two-state dissipative systems is of practical importance. The probability shown in Fig. (5.6) is such an average.

5.4.2 High-frequency noise, $\omega/\Gamma \ll \gamma \ll 1$

In this limit the coherence is completely suppressed, by, e.g., interaction with phonons, and the evolution of the population of energy levels must be described by the density matrix. In this case the population, N_{-S} , of the initially occupied state $|-S\rangle$ is given by [75, 111]

$$\frac{dN_{-S}}{dt} = -\frac{\Delta(t)^2}{2} \frac{\hbar\Gamma}{W(t)^2 + (\hbar\Gamma)^2} (N_{-S} - N_S). \quad (5.39)$$

The solution is

$$N_{-S} = \frac{1}{2} \left\{ 1 + \exp \left[-\frac{\tilde{\epsilon}}{2} g \left(\tau; 2S; \frac{\hbar\Gamma}{h_0} \right) \right] \right\}, \quad (5.40)$$

where $g(z; b; \alpha)$ is given by

$$g(z; b; \alpha) = \quad (5.41)$$

$$\begin{aligned} & (2n+2)f_1\left(\frac{\pi}{2}\right) - f_1\left(\frac{\pi}{2} - \xi\right), \quad \text{if } z = (2n+1)\frac{\pi}{2} + \xi \\ & g(z; b; \alpha) = 2nf_1\left(\frac{\pi}{2}\right) + f_1(\xi), \quad \text{if } z = n\pi + \xi, \end{aligned} \quad (5.42)$$

where $n = 0, 1, 2, \dots$, $0 < \xi < \pi/2$,

$$f_1(z) = F_1 \left(\frac{1}{2}; \frac{1}{2} - b, 1; \frac{3}{2}; \sin^2(z), -\frac{\sin^2(z)}{\alpha^2} \right) \frac{\sin(z)}{\alpha}, \quad (5.43)$$

and $F_1(a, b_1, b_2; c; x, y)$ is the Appell hypergeometric function of two variables.

The time-dependence of the occupation of the state $|-S\rangle$ is shown in Fig. 5.7 for $\tilde{\epsilon} = 1/3$, $S = 10$, $\hbar\Gamma/h_0 = 0.01$. As in the case of a low-frequency noise, the probability to occupy either of the two levels tends to 0.5 after a few revolutions. The difference between the two regimes is that in the case of the high-frequency noise the probability monotonically approaches the asymptotic value without exhibiting any oscillation.

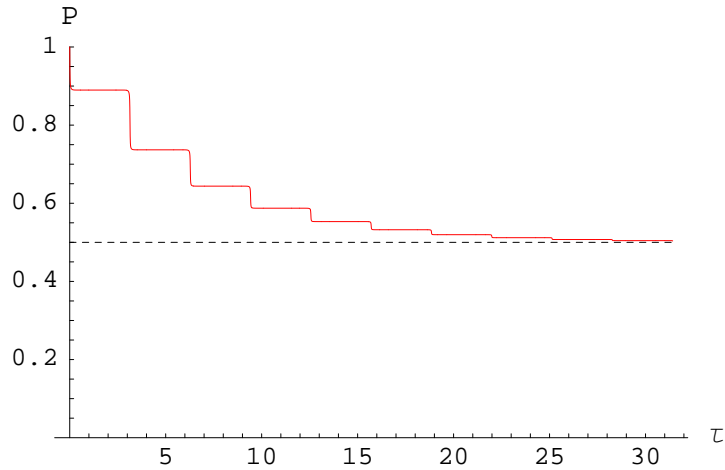


Figure 5.7: Time dependence of the probability of finding a particle in the state $|-S\rangle$ in the presence of a high-frequency noise for $S = 10$, $\tilde{\epsilon} = 1/3$ and $(\Gamma/h_0) = 0.01$.

5.5 Conclusions

We have studied the equivalent of the LZS effect for a spin system in a rotating magnetic field. Typical time dependence of the probability of staying at the initial state has been computed for three different situations. The first is the situation when the noise is irrelevant on the time scale of the measurement, Fig. 5.5. In this case the system exhibits coherent behavior and long-term memory effects. The second situation corresponds to the noise that decohere quantum states within the time of each revolution but is slow enough to provide pure quantum dynamics during the level crossing, Fig. 5.6. The third situation corresponds to a very fast noise that does not allow the use of wave functions for the description of the crossing and requires the density-matrix formalism, Fig. 5.7. When the noise becomes important, the occupation probability of each level approaches $1/2$ after several revolutions. However, the asymptotic behavior depends on the frequency of the noise. The three regimes discussed above are given by equations (5.34),(5.35),(5.36). One must be able to switch between different regimes by changing the angular velocity of the rotating

field and/or temperature. Experiments of that kind can shed light on the effect of dissipative environment on the resonant spin tunneling in molecular magnets. To be on a cautious side, one should notice that the evolution of the magnetization in a crystal of magnetic molecules also depends on the dipolar interactions between the molecules [96, 97, 98] and on their interaction with nuclear spins [96, 99, 91]. The theory based upon Eq. (5.1) is likely to be relevant to molecular magnets when the amplitude of the rotating field significantly exceeds dipolar fields, hyperfine fields, and the effective field due to transverse anisotropy, see Eq. (5.10). A good candidate could be, e.g., Ni-4 molecular nanomagnet [100, 68] that has $S = 4$, uniaxial anisotropy of $D = 0.75$ K, no nuclear spins, and no (or very weak) transverse anisotropy.

Chapter 6

Collective electromagnetic relaxation in crystals of molecular magnets [8]

Paramagnetic crystals of high-spin molecular magnets, like Mn_{12} , Fe_8 and others, exhibit unusual magnetic properties related to the macroscopic time of the transition between spin-up and spin-down states of individual magnetic molecules [1]. The latter is due to the high magnetic anisotropy and a large value of spin, $S \gg 1$. For, e.g., a biaxial molecule (Fe_8 of $S = 10$), in the magnetic field, \mathbf{H} , parallel to the anisotropy axis Z , the spin Hamiltonian is

$$\mathcal{H} = -DS_z^2 + AS_x^2 - g\mu_B H_z S_z, \quad (6.1)$$

where g is the gyromagnetic factor, μ_B is the Bohr magneton, and $D > A > 0$. For small A , the approximate energy states of \mathcal{H} are the eigenstates of S_z : $S_z|m\rangle = m|m\rangle$. At $H_z = kD/g\mu_B$, with $k = 0, \pm 1, \pm 2, \dots$, the levels $m < 0$ and m' satisfying $m + m' = -k$ come to resonance. For the even S , the tunnel splitting of the resonant levels, Δ_m , appears (for even k) in the $[(m' - m)/2]$ -th order of the perturbation theory on A : $\Delta_{(m=-S)} \propto (A/D)^{(m'-m)/2}$. At, e.g., $k = 0$ (see Fig. 6.1), $\Delta_{(m=-S)} \propto (A/D)^S$

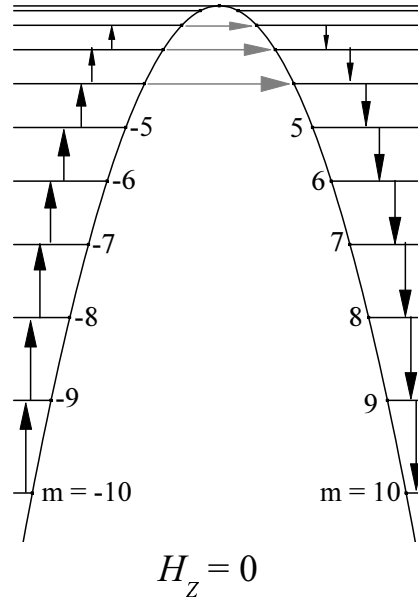


Figure 6.1: Approximate energy levels of a spin-10 molecule in a zero magnetic field. The tunnel splitting of the degenerate levels is not shown. Arrows show the relaxation path from $m = -10$ to $m = 10$ through thermally assisted quantum tunneling.

and, thus, at $S = 10$, the probability of the transition between spin-up and spin-down states is low. Consequently, at low temperature, the crystal can be prepared in a state with inverse population of the spin energy levels, e.g., magnetized against the direction of the magnetic field. This allows one to observe, in a macroscopic experiment, such quantum effects as resonant spin tunneling [2, 3], spin Berry phase [4], crossover between quantum tunneling and thermal activation [101, 102, 103], and quantum selection rules in the absorption of electromagnetic radiation [104].

Recently, it has been suggested [7, 105, 106] that a crystal of molecular nanomagnets can be a source of coherent electromagnetic radiation in the millimeter wavelength range, highly desirable for applications [107]. Some experimental evidence of this effect has been obtained [105, 108, 109]. The effect is related to Dicke superradiance [39]. Normally, atoms or molecules of a gas, initially prepared in the excited energy state, decay independently by spontaneous emission of light. The power of

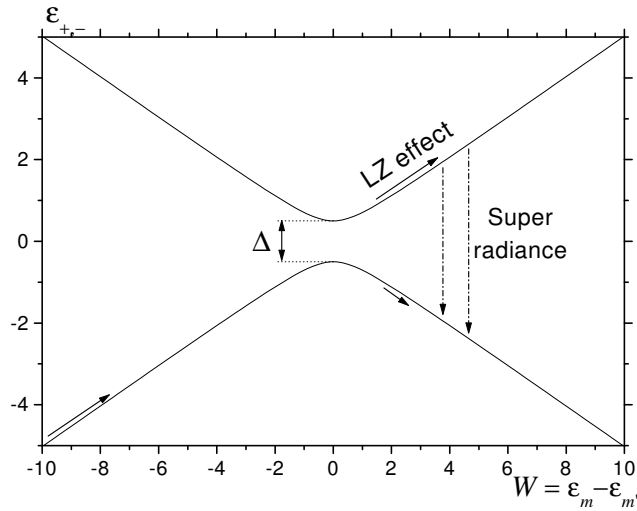


Figure 6.2: A pair of tunnel-split levels vs. energy bias W . The Landau-Zener (LZ) transition is followed by the emission of the coherent light via superradiance.

the radiation obeys the law $P \propto N \exp(-t/\tau)$ where N is the total number of atoms and τ is the lifetime of the excited state. Dicke argued that N atoms confined within a volume of size d , which is small compared to the wavelength of the radiation λ , cannot radiate independently from each other. At $d < \lambda$ a spontaneous phase locking of the atomic dipoles takes place, that results in the coherent radiation burst of power $P_{SR} \propto N^2$, emitted within a time of order $\tau_{SR} \sim \tau/N$. This phenomenon, called superfluorescence, has been widely observed in gases. It can occur in any system of identical quantum objects if the system is not very large compared to the wavelength of the radiation [35]. For crystals of molecular magnets this is true for both, the transitions between the tunnel-split levels, Fig. 6.2, and the transitions between the adjacent $|m\rangle$ levels, Fig. 6.1.

In a typical experiment, one magnetizes the crystal and then sweeps the field in the opposite direction. We will be concerned with the situation when the electromagnetic transitions occur between tunnel-split levels, Fig. 6.2. These can be, e.g., transitions

between $m = -10$ and $m = 10$ levels shown in Fig. 6.1. The electromagnetic relaxation of that kind corresponds to the total magnetization reversal accompanied by the broad band superradiance. It is described by a rigorous model [7] which is reviewed in Section 6.1. In essence, if one neglects the electromagnetic radiation, the crossing of the (m, m') resonance by the magnetic field sweep, Fig. 6.2, is described by the Landau-Zener theory [110]. When the coupling between the spins and the electromagnetic radiation is taken into account, the magnetic state resulting from the LZ transition relaxes towards the lowest energy state via superradiance. The rate of the superradiant decay, as well as the time dependence of the relaxation, are sensitive to the parameters of the crystal and to the shape of the magnetic field pulse. Our goal is to compute the time dependence of the radiation power and the total radiated energy as functions of the field-sweep rate, the tunnel splitting, and the size of the crystal. This is done in Section 6.2 by analytical and numerical methods. Practical implications of our findings are discussed in Section 6.3.

6.1 Collective Landau-Zener relaxation

Consider a crystal of N magnetic molecules occupying an m magnetic state that is close to the resonance with the m' state, e.g. $m = -S, m' = S$ in Fig. 6.1. We shall assume that the molecules weakly interact with each other through the electromagnetic field. As has been shown in Ref. [7], the quantum magnetic relaxation of such a crystal satisfies the Landau-Lifshitz equation:

$$\dot{\mathbf{n}} = \gamma[\mathbf{n} \times \mathbf{H}_{\text{eff}}] - \alpha\gamma[\mathbf{n} \times [\mathbf{n} \times \mathbf{H}_{\text{eff}}]]. \quad (6.2)$$

Here \mathbf{n} is a unit vector of the pseudospin describing the two-state system, such that $n_z = -1$ corresponds to all molecules in the m -state, while $n_z = 1$ corresponds to all

molecules in the m' -state, $\gamma = g\mu_B/\hbar$ is the gyromagnetic ratio, the effective magnetic field is given by

$$g\mu_B\mathbf{H}_{\text{eff}} = \Delta\mathbf{e}_x + W\mathbf{e}_z, \quad (6.3)$$

with $\dot{W}(t) = \frac{1}{2}g\mu_B(m' - m)\dot{H}_z$ being the energy sweep rate (see Fig. 6.2), and $\alpha \ll 1$ is a dimensionless effective damping coefficient,

$$\alpha = \frac{1}{24}N(m' - m)^2g^2\alpha_o \left(\frac{\Delta}{m_e c^2} \right)^2, \quad (6.4)$$

with $\alpha_o = e^2/\hbar c \approx 1/137$ being the fine structure constant. Note that α is independent of the magnetic field.

The first term in Eq. (6.2) gives dissipationless Landau-Zener transitions when the field is swept through the resonance such that $W = W(t)$ satisfies $W(\pm\infty) = \pm\infty$, and the initial condition is $\mathbf{n}(-\infty) = -\mathbf{e}_z$. Indeed, at $\alpha = 0$ the Schrödinger equation for a two-level system is equivalent to the equation for a precessing spin. The probability $p(t)$ for the molecule to stay in the initial state is given by

$$p(t) = [1 - n_z(t)]/2. \quad (6.5)$$

For $W(t) = vt$, one obtains the famous Landau-Zener result [110]: $p(\infty) \equiv p_{LZ} = \exp(-\epsilon)$, where

$$\epsilon = \frac{\pi\Delta^2}{2\hbar v}. \quad (6.6)$$

The Landau-Zener effect corresponds to only partial magnetization reversal,

$$n_z^{LZ}(\infty) = 1 - 2\exp(-\epsilon), \quad (6.7)$$

see Fig. 6.3 at $\alpha = 0$. The value of $n_z^{LZ}(\infty)$ is close to -1 at $\epsilon \ll 1$, that is for the fast field sweep. In this case most of the molecules, after crossing the resonance, remain

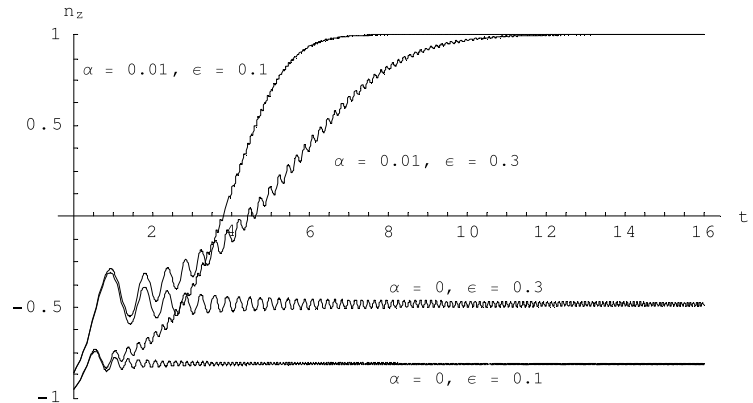


Figure 6.3: Time dependence of the magnetization reversal for two values of ϵ due to pure Landau-Zener relaxation of individual molecules ($\alpha = 0$) and due to collective relaxation via superradiance ($\alpha = 0.01$).

in the initial m -state by passing from the lower to the upper branch in Fig. 6.2. On the contrary, for a slow sweep, that is when $\epsilon \gg 1$, most of the molecules follow the lower branch in Fig. 6.2 and the final state of the crystal is exponentially close to $n_z^{LZ}(\infty) = 1$.

The second term in Eq. (6.2) describes collective magnetic relaxation via Dicke superradiance. Due to this term the magnetization of the entire crystal at long times reverses completely to $n_z(\infty) = 1$, as is shown in Fig. 6.3, for a finite α . The collective relaxation due to superradiance is significant for $\epsilon \lesssim 1$, that is, when $n_z^{LZ}(\infty)$ is not very close to 1. Thus, the observation of the superradiance requires a fast field sweep.

6.2 Radiation power

The power of the superradiance described by Eq. (6.2) can be obtained from the classical formula for the magnetic dipole radiation [7]:

$$P(t) = [2/(3c^3)]\ddot{m}_z^2(t), \quad (6.8)$$

where

$$m_z(t) = \frac{1}{2}N(m - m')g\mu_B n_z(t). \quad (6.9)$$

Close to the (m, m') resonance, nearly any field sweep of practical interest is linear in time, $W = vt$. It is convenient to use dimensionless variables:

$$t' = \frac{t\Delta}{\hbar}, \quad W'(t') = \frac{vt}{\Delta} = \frac{\hbar vt'}{\Delta^2} = \frac{\pi t'}{2\epsilon}. \quad (6.10)$$

In terms of these variables Eq. (6.2) and Eq. (6.8) become

$$\frac{d\mathbf{n}}{dt'} = [\mathbf{n} \times (\mathbf{e}_x + W'(t')\mathbf{e}_z)] - \alpha[\mathbf{n} \times [\mathbf{n} \times (\mathbf{e}_x + W'(t')\mathbf{e}_z)]] \quad (6.11)$$

and

$$P = \alpha N \hbar^{-1} \Delta^2 \left(\frac{d^2 n_z}{dt'^2} \right)^2. \quad (6.12)$$

The total emitted energy, $E = \int dt P(t)$, is given by

$$E = \alpha N \Delta E', \quad (6.13)$$

where we have introduced dimensionless

$$E' = \int dt' \left(\frac{d^2 n_z}{dt'^2} \right)^2. \quad (6.14)$$

6.2.1 Analytical

We shall start by developing an analytical approximation for the practical case of $\epsilon < 1$ and $\alpha \ll 1$. The time interval of interest is the one past the Landau-Zener transition: $W' \gg 1$. In this case, retaining the leading terms in Eq. (6.11), we get

$$\frac{dn_x}{dt'} = W' n_y \quad (6.15)$$

$$\frac{dn_y}{dt'} = -W' n_x \quad (6.16)$$

$$\frac{dn_z}{dt'} = -n_y + \alpha W'(t')(1 - n_z^2). \quad (6.17)$$

These equations show that n_x and n_y oscillate rapidly in time, while n_z , in accordance with Fig. 6.3, has a slowly varying average. Averaging Eq. (6.17) over the period of oscillations of n_y , one obtains:

$$\frac{d\bar{n}_z}{dt'} = \alpha W'(t')(1 - \bar{n}_z^2). \quad (6.18)$$

Eq. (6.18) describes the superradiant stage of the evolution of \bar{n}_z . Therefore, it must be solved with the initial condition $\bar{n}_z = n_z^{LZ}$ at $t = 0$. At small ϵ , Eq. (6.7) gives for that initial condition:

$$\bar{n}_z(0) = -1 + 2\epsilon. \quad (6.19)$$

The corresponding solution of Eq. (6.18) reads [109]

$$\bar{n}_z(t') = \tanh\left(\frac{\alpha\pi t'^2}{4\epsilon} - \frac{1}{2}\ln\frac{1}{\epsilon}\right). \quad (6.20)$$

It is shown by the solid line in Fig. 6.4. For $\epsilon = 0.1$ Eq. (6.18) is, clearly, a good approximation to the full solution averaged over oscillations. As ϵ increases, some discrepancy is observed. One can improve the analytical approximation by writing $n_z = \bar{n}_z + \delta n_z$ and solving Eq. (6.17) through iterations, but this, at the end, will require a numerical integration, so that the improvement obtained by this method does not give much advantage over the direct numerical solution of Eq. (6.11).

The approximate solution of Eqs. (6.15) and (6.16), satisfying $\mathbf{n}^2 = 1$, is given by

$$\begin{aligned} n_x &= \sqrt{1 - \bar{n}_z^2} \sin\left(\frac{\pi t'^2}{4\epsilon} + \phi_0\right) \\ n_y &= -\sqrt{1 - \bar{n}_z^2} \cos\left(\frac{\pi t'^2}{4\epsilon} + \phi_0\right), \end{aligned} \quad (6.21)$$

where ϕ_0 is a phase which we are not attempting to compute analytically. One can see from Eqs. (6.20) and (6.21) that \bar{n}_z , indeed, changes slowly with time, compared to the oscillations of $n_x(t')$ and $n_y(t')$, because of the condition $\alpha \ll 1$.

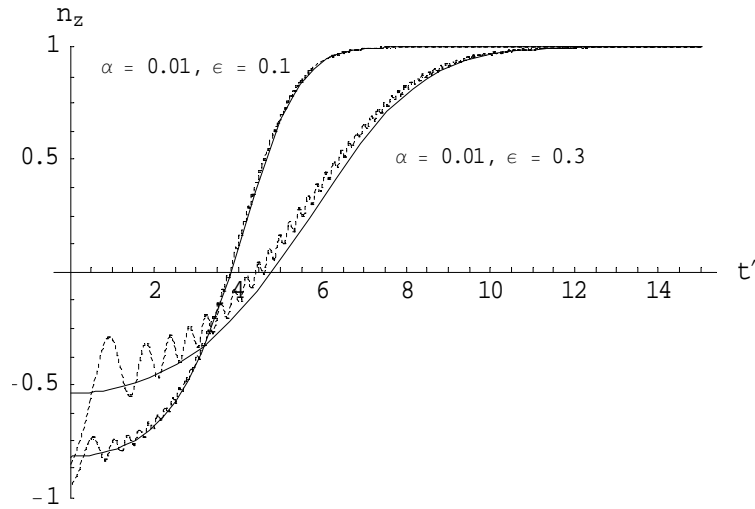


Figure 6.4: Approximate analytical solution for $n_z(t')$ averaged over oscillations, Eq. (6.20), for two values of ϵ and $\alpha = 0.01$ (solid line). The numerical solution of Eq. (6.11) is shown by the dash line.

Let us now turn to the analytical approximation for the power and the total radiated energy. It is easy to see from Eqs. (6.17)-(6.21) that the main contribution to d^2n_z/dt'^2 is determined by the rapidly oscillating n_y -term in the right-hand-side of Eq. (6.17):

$$\frac{d^2n_z}{dt'^2} = - \left(\frac{\pi t'}{2\epsilon} \right) \frac{\sin[(\pi t'^2/4\epsilon) + \phi_0]}{\cosh[(\alpha\pi t'^2/4\epsilon) + \frac{1}{2} \ln \epsilon]} . \quad (6.22)$$

Substituting this expression into Eq. (6.14) and replacing the rapidly oscillating $\sin^2(\pi t'^2/4\epsilon)$ under the integral by $1/2$, one finally obtains:

$$E' = \frac{\sqrt{\pi}}{\epsilon^{1/2}\alpha^{3/2}} \int_0^\infty \frac{x^2 dx}{\cosh^2(x^2 + \frac{1}{2} \ln \epsilon)} . \quad (6.23)$$

Equations (6.12), (6.13), (6.14), (6.22), and (6.23) give the dependence of the radiation power and the total emitted energy on the field sweep rate and on the parameters of the crystal.

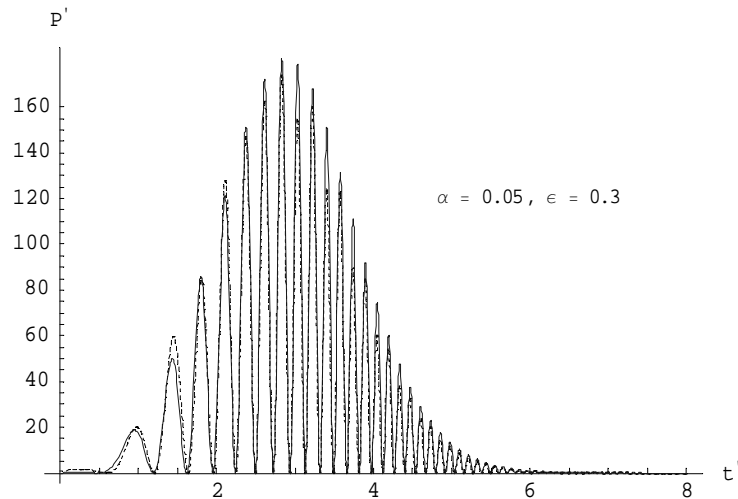


Figure 6.5: Time dependence of the reduced radiation power, $P' = (d^2n_z/dt'^2)^2$ at $\epsilon = 0.3$ and $\alpha = 0.05$. Solid line represents numerical results. Dash line corresponds to Eq. (6.22) at $\phi_0 = 2.576$.

6.2.2 Numerical

We shall now compute $P(t)$ and E by numerical integration of Eq. (6.11), and compare them with our analytical findings.

The time dependence of the reduced power, $P' = (d^2n_z/dt'^2)^2$, is shown in Fig. 6.5. The comparison with Eq. (6.22) is performed by fitting the value of ϕ_0 until the match with the numerical solution of Eq. (6.11) for $(d^2n_z/dt'^2)^2$ is obtained. Even for ϵ as large as 0.3 the agreement of the numerical results with the analytical formula is rather good. Note that the oscillation of the power in time is a quantum effect related to the oscillation of n_z .

Fig. 6.6 shows the dependence of the total emitted energy on the parameter ϵ , that is, on the inverse field sweep rate. Fig. 6.7 shows the dependence of E' on the parameter α .

The question of significant importance for experiment is the spectral composition

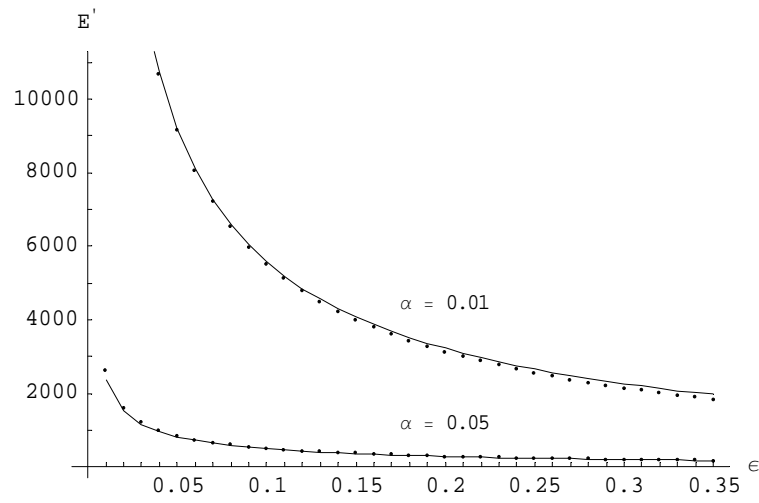


Figure 6.6: The ϵ dependence of the total emitted energy at two values of α . Points represent numerical results. Solid line corresponds to Eq. (6.23).

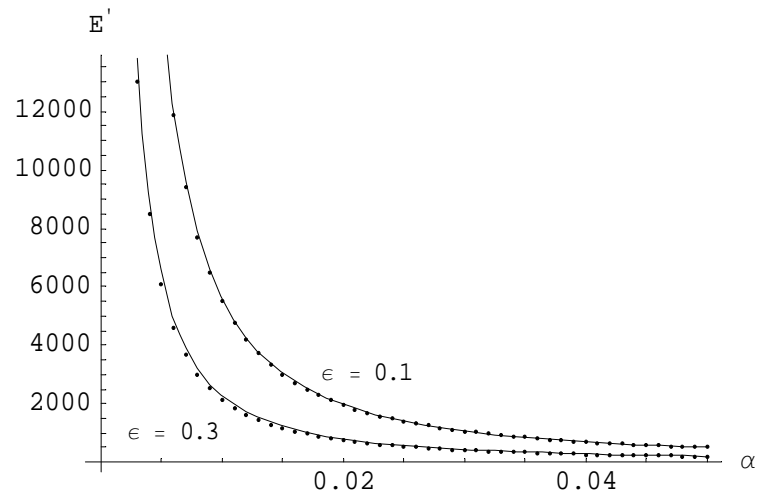


Figure 6.7: The α dependence of E' at two values of ϵ . Points represent numerical results. Solid line corresponds to Eq. (6.23).

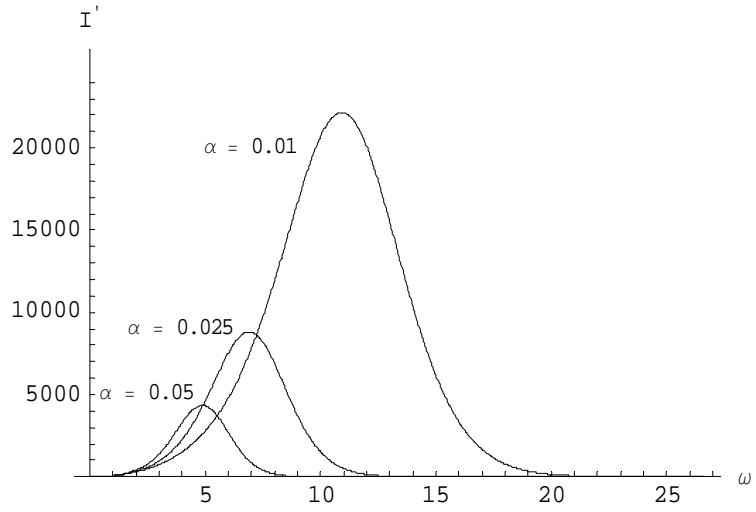


Figure 6.8: Spectral function $I'(\omega')$ for three values of alpha at $\epsilon = 0.1$.

of the radiation. The total emitted energy can be presented as

$$E = \int d\omega I(\omega) , \quad (6.24)$$

where

$$I(\omega) = \hbar \alpha N I'(\omega') \quad (6.25)$$

is the spectral power. Here $I'(\omega')$ is a dimensionless function of the dimensionless frequency, $\omega' = \hbar\omega/\Delta$. It must be computed via the Fourier transform of d^2n_z/dt'^2 :

$$I'(\omega') = \frac{1}{2\pi} \left| \int dt' e^{i\omega't'} \left(\frac{d^2n_z}{dt'^2} \right) \right|^2 . \quad (6.26)$$

This function is shown in Fig. 6.8. The peak of the power occurs at

$$\hbar\omega_{max} = \frac{\Delta}{\sqrt{\alpha}} f(\epsilon) . \quad (6.27)$$

This scaling of $\hbar\omega_{max}$ on α follows from Eq. (6.11). The function $f(\epsilon)$, computed numerically, is shown in Fig. 6.9.

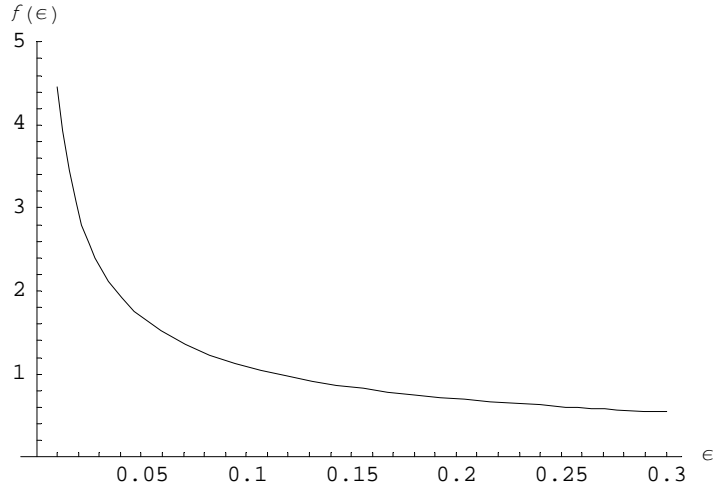


Figure 6.9: Dependence of f of Eq. (6.27) on ϵ .

6.3 Discussion

The formulas and the numerical results obtained above are valid if the energy distance between the resonant levels, W , is small compared to the distance between the adjacent m -levels. For numerical estimates, we shall stick to the $(-S, S)$ -resonance. The conclusions of this section, however, will apply to other resonances as well. For the model illustrated by Eq. (6.1) and Fig. 6.1, the distance between the $m = -S$ level and the $m = -S + 1$ level is $(2S - 1)D \approx 2SD$. The validity condition we are looking for is then $W(t) \ll 2SD$. For $W = vt$ one should verify this condition at $W_{max} = vt_{max}$, where $t_{max} = \hbar t'_{max}/\Delta$ is the time when the superradiance drops exponentially due to the hyperbolic cosine in Eq. (6.22). According to this equation and Eq. (6.10), $t'_{max} \sim \sqrt{\epsilon/\alpha}$ and $W_{max} \sim \Delta/\sqrt{\epsilon\alpha}$. Substituting this into $W_{max} \ll 2SD$ and using Eq. (6.4) for α , one obtains the validity condition in the form of the lower bound on the total number of molecules:

$$N \gg \frac{1}{\epsilon\alpha_o} \left(\frac{m_e c^2}{U_a} \right)^2, \quad (6.28)$$

where $U_a = DS^2$ is the energy barrier between $m = \pm S$ states due to magnetic anisotropy. Eq. (6.28) shows that a high magnetic anisotropy and a not very small ϵ are needed if the size of the system is to remain within reasonable limits. The optimal would be $\epsilon \sim 1$ since, according to Eq. (6.7), $\epsilon \lesssim 1$ (that is, a sufficiently high field-sweep rate) is needed to create an inverse population of spin levels. For Mn_{12} and Fe_8 , the anisotropy barrier is of order 60K and 30K respectively, and the lower bound on N , according to Eq. (6.28), must be between 10^{18} and 10^{19} molecules. With account of the unit cell volume (3.7 nm^3 and 2.0 nm^3 for Mn_{12} and Fe_8 , respectively) this translates into a volume of order or greater than 1 mm^3 . Remarkably, this agrees with the reported lower bound on the volume of the crystal (or crystal assembly) that shows evidence of electromagnetic radiation during magnetization reversal [105, 108, 109].

We shall now estimate the total emitted energy and the power of the radiation. According to Eq. (6.23), $E' \sim \epsilon^{-1/2} \alpha^{-3/2}$. This gives for E of Eq. (6.13): $E \sim N\Delta/\sqrt{\epsilon\alpha}$. With the help of Eq. (6.4) one obtains:

$$E \sim \epsilon^{-1/2} N^{1/2} m_e c^2 . \quad (6.29)$$

For the purpose of the order-of-magnitude estimate we have dropped the factor $gS\sqrt{\alpha_0}$ of order unity. Notice that the total emitted energy is proportional to the square root of the crystal volume. At $\epsilon \sim 1$ and $N \sim 10^{18}$, Eq. (6.29) provides $E \sim 0.1 \text{ mJ}$.

According to Eqs. (6.12) and (6.22) (see also Fig. 6.5) the power of the radiation oscillates in time. In most cases, observation of these oscillations must be impeded by the finite time resolution of the measuring equipment, so that only the envelope of the curve shown in Fig. 6.5 will be observed. The peak power can be estimated as $P_{max} \sim E/t_{max} \sim N\Delta^2/\hbar\epsilon$. Substituting here ϵ of Eq. (6.6), one obtains

$$P_{max} \sim Nv \sim \delta M \frac{dH}{dt} , \quad (6.30)$$

where we have introduced $\delta M = g\mu_B(m' - m)N$, the change in the total magnetic moment of the crystal due to collective electromagnetic relaxation. Note that the relations $E \propto \sqrt{N}$ and $P_{max} \propto N$ are specific to the radiation problem we have studied. For an assembly of a few mm-size crystals Eq. (6.30) gives $P_{max} \sim 10 \mu\text{W}$ at a typical laboratory field sweep rate of 0.01 T/s [105, 108] and $P_{max} \sim 1 \text{ W}$ for a fast field pulse, $dH/dt \sim 10^3 \text{ T/s}$ [109]. Note, however, that in the case of an ultrafast sweep the condition $\epsilon \sim 1$ can be satisfied only by a large tunnel splitting Δ , making the preparation of the initially magnetized state less simple than in the case of small Δ .

During the adiabatic sweep, the frequency of the radiation is determined by the distance between the spin levels, $\hbar\omega = \sqrt{\Delta^2 + W^2}$. For the most of the relaxation process, $W \gg \Delta$, and, thus, $\omega = W(t)/\hbar$. The peak of the spectral power, Fig. 6.8, corresponds to $\hbar\omega_{max} \sim W(t_{max}) \sim \Delta/\sqrt{\epsilon\alpha}$. Up to a factor of order unity, that depends logarithmically on ϵ , this coincides with Eq. (6.27). The logarithmic difference of $f(\epsilon)$ in Fig. 6.9 from $1/\sqrt{\epsilon}$ is due to $\ln \epsilon$ in Eq. (6.22). With the help of Eq. (6.4), we obtain that by order of magnitude

$$\omega_{max} \sim \frac{m_e c^2}{\hbar \sqrt{\epsilon N}}, \quad (6.31)$$

where we again omitted the factor $gS\sqrt{\alpha_0}$ of order unity. For $\epsilon \sim 1$ and $N \sim 10^{18}$, required to produce significant radiation (see above), this frequency is in the terahertz range.

For the radiation to be coherent, the inhomogeneous broadening of ϵ must be small throughout the crystal. This translates into narrow distribution of the tunnel splitting and narrow distribution of the magnetic field felt by the spins. Both conditions must be satisfied in Fe_3 because they are also the necessary conditions for the Berry phase

effect observed in that system [4]. In Mn_{12} the situation is less clear due to solvent disorder, large hyperfine interactions, dislocations, etc., which result in a distribution of Δ [111, 112, 113, 67, 114]. The suitability of Mn_{12} for the study of superradiance depends on whether the distribution of Δ is continuous or consists of a finite number of narrow lines due to, e.g., finite number of nuclear spin states, presence of isomers in the structure of the molecule [113], etc. Systems with narrow distribution of Δ probably exist among hundreds of new molecular magnets synthesized in recent years. In such systems, narrow distribution of the magnetic field should be achieved automatically when the spins of the initially saturated sample rotate coherently due to superradiance.

Papers and presentations by C. Calero

Published and submitted works

Articles

1. C. L. Joseph, C. Calero, and E. M. Chudnovsky. *Collective electromagnetic relaxation in crystals of molecular magnets*, Phys. Rev. B **70**, 174416 (2004).
2. C. Calero, E. M. Chudnovsky, and D. A. Garanin. *Quantum dynamics of a nanomagnet in a rotating field*, Phys. Rev. B **72**, 024409 (2005).
3. C. Calero, E. M. Chudnovsky, and D. A. Garanin. *Field dependence of the electron spin relaxation in quantum dots*, Phys. Rev. Lett. **95**, 166603 (2005).
4. C. Calero, E. M. Chudnovsky, and D. A. Garanin. *Relaxation of the electron spin in quantum dots via one- and two-phonon processes*, arXiv:cond-mat/0609108 (to be published in the Journal of Magnetism and Magnetic Materials).
5. C. Calero, E. M. Chudnovsky, and D. A. Garanin. *Two-phonon spin-phonon relaxation of rigid atomic clusters*, Phys. Rev. B **74**, 094428 (2006).

6. C. Calero and E. M. Chudnovsky. *Rabi oscillations from ultrasound in spin systems*, arXiv:cond-mat/0702116 (2007) (submitted to Phys. Rev. Lett.).
7. C. Calero, E. M. Chudnovsky, and D. A. Garanin. *Magneto-elastic waves in crystals of magnetic molecules*. arXiv:0705.0371 (2007) (submitted to Phys. Rev. B).

Books

Eugene M. Chudnovsky, Javier Tejada, Carlos Calero, Ferran Macià. *Problem Solutions to Lectures on Magnetism by Chudnovsky and Tejada*, Rinton Press (2007).

Presentations

1. *Conference on Single Molecule Magnets and Hybrid Magnetic Nanostructures*. International Center of Theoretical Physics. Trieste, Italy (June 2005). Presentation of the poster “Quantum dynamics of a nanomagnet in a rotating field”.
2. *III Joint European Magnetic Symposia* San Sebastián, Spain (June 2006). Presentation of the poster “Relaxation of the electron spin in quantum dots via one- and two-phonon processes”.
3. Talk at Lehman College of the City University of New York: “Rabi oscillations from ultrasound in spin systems ”, December 2006.
4. Talk at the Physics Department of the University of Barcelona: “Rabi oscillations from ultrasound in spin systems ”, January 2007.
5. *March Meeting of the American Physical Society*. Denver, USA (March 2007). Presentation of the contributed talk “Effects of surface waves on crystals of

molecular magnets: semi-classical approach”.

Bibliography

- [1] R. Sessoli, D. Gatteschi, A. Ganeschi, and M. A. Novak, *Nature (London)* **365**, 141 (1993).
- [2] J. R. Friedman, M. P. Sarachik, J. Tejada, and R. Ziolo, *Phys. Rev. Lett.* **76**, 3830 (1996).
- [3] J. M. Hernández, X. X. Zhang, F. Luis, J. Bartolomé, J. Tejada, and R. Ziolo, *Europhys. Lett.* **35**, 301 (1996); L. Thomas, F. Lioni, R. Ballou, D. Gatteschi, R. Sessoli, and B. Barbara, *Nature (London)* **383**, 145 (1996); C. Sangregorio, T. Ohm, C. Paulsen, R. Sessoli, and D. Gatteschi, *Phys. Rev. Lett.* **78**, 4645 (1997).
- [4] W. Wernsdorfer and R. Sessoli, *Science* **284**, 133 (1999).
- [5] E. del Barco, A. D. Kent, S. Hill, J. M. North, N. S. Dalal, E. M. Rumberger, D. N. Hendrickson, N. Chakov, and G. Christou, *Journal of Low Temperature Physics* **140**, 119-174 (2005).
- [6] P. Shor, *Proceedings of the 35th Annual Symposium on the Foundations of Computer Science* (IEEE Press, Los Alamitos, 1994).
- [7] E. M. Chudnovsky and D. A. Garanin. *Phys. Rev. Lett.* **89**, 157201 (2002).

- [8] C. L. Joseph, C. Calero, and E. M. Chudnovsky. *Phys. Rev. B* **70**, 174416 (2004).
- [9] I. Waller, *Z. Phys.* **79**, 370 (1932).
- [10] W. Heitler and E. Teller, *Proc. R. Soc. A* **155**, 629 (1936).
- [11] R. de L. Kronig, *Physica* **6**, 33 (1939).
- [12] J. H. Van Vleck, *Phys. Rev.* **57**, 426 (1940).
- [13] R. Orbach, *Proc. R. Soc. A* **264**, 458 (1961).
- [14] M. N. Leuenberger and D. Loss, *Nature* **410**, 789 (2001).
- [15] B. Lüthi, *Physical Acoustic in the Solid State*, Springer (2005).
- [16] A. Abragam and B. Bleaney, *Electron paramagnetic resonance of transition ions*, Clarendon Press (1970).
- [17] D. E. Eastman, *Phys. Rev.* **148**, 530 (1966).
- [18] R. L. Melcher, *Phys. Rev. Lett.* **25**, 1201 (1970).
- [19] W. F. Brown Jr., *Magnetoelastic Interactions*, Springer (1966).
- [20] H. F. Tiersten, *J. Math. Phys.* **5**, 1298 (1964).
- [21] B. W. Southern and D. A. Goodings, *Phys. Rev. B* **7**, 534 (1973).
- [22] R. L. Melcher, *Phys. Rev. Lett.* **28**, 165 (1972).
- [23] V. Dohm and P. Fulde, *Z. Physik B* **21**, 369 (1975).
- [24] Lynn Bonsall and R. L. Melcher, *Phys. Rev. B* **14**, 1128 (1976).

- [25] P. Fedders and R. L. Melcher, Phys. Rev. B **14**, 1142 (1976).
- [26] R. Camley and P. Fulde, Phys. Rev. B **23**, 2614 (1981).
- [27] P.S. Wand and B. Lüthi, Phys. Rev. B **15**, 2718 (1977).
- [28] J. Jensen, Phys. Rev. B **37**, 9495 (1988).
- [29] A. Einstein and W. J. de Haas, D. Ph. Ges **8** (1915).
- [30] O. W. Richardson, Phys. Rev. **26**, 248 (1908).
- [31] S. J. Barnett, Phys. Rev. **6**, 239 (1915).
- [32] R. N. Thurston, *Physical Acoustics* Vol. 1A, New York and London, ed. by W. P. Mason (1964).
- [33] E. M. Chudnovsky, Phys. Rev. Lett. **72**, 3433 (1994).
- [34] E. M. Chudnovsky, X. Martinez Hidalgo, Phys. Rev. B **66**, 054412 (2002).
- [35] E. M. Chudnovsky, D. A. Garanin. Phys. Rev. Lett. **93**, 257205 (2004).
- [36] E. M. Chudnovsky, D. A. Garanin, and R. Schilling, Phys. Rev. B **72**, 94426 (2005).
- [37] L. D. Landau and E. M. Lifshitz, *Theory of Elasticity* (Pergamon, New York, 1970).
- [38] F.W. Hehl and W.-T. Ni, Phys. Rev. D **42**, 2045 (1990).
- [39] R. Dicke. Phys. Rev. **93**, 99 (1954).

- [40] J. J. Sakurai, *Modern Quantum Mechanics*, Adison-Wesley Publishing Company (1994).
- [41] C. Calero, E. M. Chudnovsky, and D. A. Garanin, *Phys. Rev. B* **74**, 094428 (2006).
- [42] D.A. Garanin, *J. Phys. A* **24**, L61 (1991).
- [43] E. M. Chudnovsky and J. Tejada Palacios, *Magnetism in Solids*, Rinton Press (2006).
- [44] D. Zipse, J. M. North, N. S. Dalal, S. Hill, and R. S. Edwards, *Phys. Rev. B* **68**, 184408 (2003); K. Petukhov, S. Hill, N. E. Chakov, K. A. Abboud, and G. Christou, *Phys. Rev. B* **70**, 054426 (2004).
- [45] G. Dresselhaus, *Phys. Rev.* **100**, 580 (1955).
- [46] E. I. Rashba, *Sov. Phys. Solid State* **2**, 1109 (1960); Yu. A. Bychkov and E. I. Rashba, *JETP Lett.* **39**, 78 (1984).
- [47] H. Hasegawa, *Phys. Rev.* **118**, 1523 (1960).
- [48] L. M. Roth, *Phys. Rev.* **118**, 1534 (1960).
- [49] A. V. Khaetskii and Yu. V. Nazarov, *Phys. Rev.* **B61**, 12639 (2000); **B64**, 125316 (2001).
- [50] B. A. Glavin and K. W. Kim, *Phys. Rev.* **B68**, 045308 (2003).
- [51] E. I. Rashba, *Phys. Rev.* **B68**, 241315 (2003).
- [52] E. I. Rashba and A. I. Efros, *Phys. Rev. Lett.* **91**, 126405 (2003).

- [53] V. N. Golovach, A. Khaetskii, and D. Loss, Phys. Rev. Lett. **93**, 016601 (2004).
- [54] C. Tahan and R. Joynt, Phys. Rev. **B71**, 075315 (2005).
- [55] R. J. Elliot, Phys. Rev. **96**, 266 (1954).
- [56] Yu. A. Serebrennikov, Phys. Rev. Lett. **93**, 266601 (2004).
- [57] C. Calero, E. M. Chudnovsky, and D. A. Garanin, Phys. Rev. Lett. **95**, 166603 (2005).
- [58] R. Winkler, S.J. Papadakis, E. P. De Poortere, and M. Shayegan, Phys. Rev. Lett. **85**, 4574 (2000).
- [59] G. Salis, D. D. Awschalom, Y. Ohno, and H. Ohno, Phys. Rev. **B64**, 195304 (2001).
- [60] R. Hanson, B. Witkamp, L. M. K. Vandersypen, L. H. Willems van Beveren, J. M. Elzerman, and L. P. Kouwenhoven, Phys. Rev. Lett. **91**, 196802 (2003).
- [61] C. Calero, E. M. Chudnovsky, and D. A. Garanin Journal of Magnetism and Magnetic Materials.
- [62] C. Calero and E. M. Chudnovsky, arXiv:cond-mat/0702116 (2007).
- [63] A. Hernández Mínguez, J. M. Hernández, F. Maciá, A. García Santiago, J. Tejada, and P. V. Santos, Phys. Rev. Lett. **95**, 217205 (2005).
- [64] A. Hernández Mínguez, F. Maciá, J. M. Hernández, J. Tejada, and P. V. Santos, cond-mat/0609429 (unpublished).

- [65] K. Gottfried and T.-M. Yan, *Quantum Mechanics: Fundamentals* (Springer-Verlag, 2003).
- [66] L. Sorace, W. Wernsdorfer, C. Thirion, A.-L. Barra, M. Pacchioni, D. Mailly, and B. Barbara, Phys. Rev. B **68**, 220407 (2003); K. Petukhov, W. Wernsdorfer, A.-L. Barra, and V. Mosser, Phys. Rev. B **72**, 052401 (2005).
- [67] S. Hill, R. S. Edwards, S. I. Jones, N. S. Dalal, and J. M. North, Phys. Rev. Lett. **90**, 217204 (2003); S. Hill, R. S. Edwards, N. Aliaga-Alcalde, G. Christou, Science **303**, 1015 (2003).
- [68] E. del Barco, A. D. Kent, E. C. Yang, and D. N. Hendrickson, Phys. Rev. Lett. **93**, 157202 (2004)
- [69] M. Bal, J. R. Friedman, Y. Suzuki, K. M. Mertes, E. M. Rumberger, D. N. Hendrickson, Y. Myasoedov, H. Shtrikman, N. Avraham, and E. Zeldov Phys. Rev. B **70**, 100408 (2004).
- [70] M. M. de Lima, Jr. and P. V. Santos, Rep. Prog. Phys. **68**, 1639 (2005).
- [71] J. F. Fernandez and J. J. Alonso, Phys. Rev. B **62**, 53 (2000); X. Martinez-Hidalgo, E. M. Chudnovsky, and A. Aharony, Europhys. Lett. **55**, 273 (2001); A. Morello, E. L. Mettes, F. Luis, J. F. Fernandez, J. Krzystek, G. Aromi, G. Christou, and L. J. de Jongh, Phys. Rev. Lett. **90**, 017206 (2003); M. Evangelisti, F. Luis, E. L. Mettes, G. Aromi, J. J. Alonso, G. Christou, and L. J. de Jongh, Phys. Rev. Lett. **93**, 117202 (2004).
- [72] C. Calero, E. M. Chudnovsky, and D. A. Garanin, arXiv:0705.0371 (2007).

- [73] E. H. Jacobsen and K. W. H. Stevens, Phys. Rev. **129**, 2036 (1963).
- [74] F. Hartmann-Boutron, P. Politi, and J. Villain, Int. J. of Mod. Phys. **10**, 2577 (1996).
- [75] D. A. Garanin and E. M. Chudnovsky, Phys. Rev. **56**, 11102 (1997).
- [76] M. N. Leuenberger and D. Loss, Europhys. Lett. **46**, 692 (1999); Phys. Rev. B **61**, 1286 (2000).
- [77] E. M. Chudnovsky and D. A. Garanin, Europhys. Lett. **52**, 245 (2000); M. N. Leuenberger and D. Loss, Europhys. Lett. **52**, 247 (2000).
- [78] I. D. Tokman, G. A. Vugalter, and A. I. Grebeneva, Phys. Rev. B **71**, 094431 (2005).
- [79] X.-T. Xie, W. Li, J. Li, W.-X. Yang, A. Yuan, and X. Yang, Phys. Rev. B, to appear.
- [80] C. Calero, E. M. Chudnovsky, and D. A. Garanin, Phys. Rev. B **72**, 024409 (2005).
- [81] V.V. Dobrovitski and A. D. Zvezdin, Europhys. Lett. **38**, 377 (1997).
- [82] L. Gunther, Europhys. Lett. **39**, 1 (1997).
- [83] V.L. Pokrovsky and N. A. Sinitsyn, Phys. Rev. B **67**, 144303 (2003).
- [84] V.L. Pokrovsky and N. A. Sinitsyn, Phys. Rev. B **69**, 104414 (2004).
- [85] V.L. Pokrovsky and S. Scheidl, Phys. Rev. B **70**, 014416 (2004).

- [86] M. N. Leuenberger and D. Loss, Phys. Rev. B **61**, 12200 (2000)
- [87] N. A. Sinitsyn and V. V. Dobrovitski, Phys. Rev. B **70**, 174449 (2004).
- [88] See, e.g., Y. Kayanuma, Phys. Rev. B **47**, 9940 (1993), and references therein.
- [89] Y. Kayanuma and H. Nakayama, Phys. Rev. B **57**, 13099 (1998).
- [90] D. A. Garanin, Phys. Rev. B **68**, 014414 (2003).
- [91] N. A. Sinitsyn and N. Prokof'ev, Phys. Rev. B **67**, 134403(2003).
- [92] W. Wernsdorfer, S. Bhaduri, C. Boskovic, G. Christou and D. H. Hendrickson, Phys. Rev. B **65**, 180403 (2002).
- [93] E. del Barco, A. D. Kent, E. M. Rumberger, D. N. Hendrikson and G. Christou, Europhys. Lett. **60**, 768 (2002); E. del Barco, A. D. Kent, S. Hill, J. M. North, N. S. Dalal, E. M. Rumberger, D. N. Hendrikson, N. Chakov and G. Christou, arXiv:cond-mat/0404390 (2004).
- [94] J. L. van Hemmen and A. Suto, J. Phys.: Condens. Matter **9** 3089 (1997).
- [95] D. A. Garanin and R. Schilling, Phys. Rev. B **66**, 174438 (2002).
- [96] N. V. Prokof'ev and P. C. E. Stamp, Phys. Rev. Lett. **80**, 5794 (1998).
- [97] J. F. Fernandez and J. J. Alonso, Phys. Rev. Lett. **91**, 047202 (2003).
- [98] D. A. Garanin and R. Schilling, ArXiv:cond-mat/0501089 (2005).
- [99] D. A. Garanin, E. M. Chudnovsky, and R. Schilling, Phys. Rev. B **61**, 12204 (2000).

- [100] Yang et al., *Polyhedron* **22**, 1727 (2003).
- [101] E. M. Chudnovsky and D. A. Garanin, *Phys. Rev. Lett.* **79**, 4469 (1997); D. A. Garanin and E. M. Chudnovsky, *Phys. Rev. B* **56**, 11102 (1997)
- [102] A. D. Kent, Y. Zhong, L. Bokacheva, D. Ruiz, D. N. Henrickson, and M. P. Sarachik, *Europhys. Lett.* **49**, 521 (2000).
- [103] L. Bokacheva, A. D. Kent, and M. A. Walters, *Phys. Rev. Lett.* **85**, 4803 (2000); K. M. Mertes, Y. Suzuki, M. P. Sarachik, Y. Paltiel, H. Shtrikman, E. Zeldov, E. Rumberger, and D. N. Hendrickson, *Europhys. Lett.* **55**, 874 (2001).
- [104] L. Sorace, W. Wernsdorfer, C. Thirion, A.-L. Barra, M. Pacchioni, D. Mailly, and B. Barbara, *Phys. Rev.* **B68**, 220407 (2003).
- [105] J. Tejada, R. Amigo, J. M. Hernandez, and E. M. Chudnovsky, *Phys. Rev.* **68**, 014431 (2003).
- [106] V. K. Henner and I. V. Kaganov, *Phys. Rev.* **68**, 144420 (2003).
- [107] D. Mittleman, *Sensing with Terahertz Radiation*, Springer (2003).
- [108] J. Tejada, E. M. Chudnovsky, J. M. Hernandez, and T. Amigo, *Appl. Phys. Lett.* **84**, 2373 (2004).
- [109] J. Vanacken, S. Stroobants, M. Malfait, V. V. Moshchalkov, M. Jordi, J. Tejada, R. Amigo, E. M. Chudnovsky, and D. A. Garanin, arXiv:cond-mat/0404041.
- [110] L. D. Landau, *Phys. Z. Sowjetunion* **2**, 46 (1932); C. Zener, *Proc. R. Soc. London, Ser. A*, **137**, 696 (1932); E. C. G. Stueckelberg, *Helv. Phys. Acta* **5**, 369 (1932).

- [111] E. M. Chudnovsky and D. A. Garanin, Phys. Rev. Lett. **87**, 187203 (2001); D. A. Garanin and E. M. Chudnovsky, Phys. Rev. **B65**, 094423 (2002).
- [112] K. M. Mertes, Y. Suzuki, M. P. Sarachik, Y. Paltiel, H. Shtrikman, E. Zeldov, E. Rumberger, D. N. Hendrickson, and G. Christou, Phys. Rev. Lett. **87**, 227205 (2001).
- [113] A. Cornia, R. Sessoli, L. Sorace, D. Gatteschi, and A. L. Barra, Phys. Rev. Lett. **89**, 257201 (2002).
- [114] E. del Barco, A. D. Kent, E. M. Rumberger, D. N. Hendrickson, and G. Christou, Phys. Rev. Lett. **91**, 047203 (2003); E. del Barco, A. D. Kent, N. E. Chakov, L. N. Zakharov, A. L. Rheingold, D. N. Hendrickson, and G. Christou, Phys. Rev. **69**, 020411(R) (2004).